Herpetological Monographs, 33, 2019, 71–107

Phoxophrys After 60 Years: Review of Morphology, Phylogeny, Status of *Pelturagonia*, and a New Species from Southeastern Kalimantan

Michael B. Harvey[1,7], Thorton R. Larson[2], Justin L. Jacobs[2], Kyle Shaney[2,6], Jeffrey W. Streicher[3], Amir Hamidy[4], Nia Kurniawan[5], and Eric N. Smith[2]

[1] Department of Biological Sciences, Broward College, 3501 Southwest Davie Road, Davie, FL 33314, USA
[2] The Amphibian and Reptile Diversity Research Center and Department of Biology, University of Texas at Arlington, 501 South Nedderman Drive, Arlington, TX 76010, USA
[3] Department of Life Sciences, The Natural History Museum, London SW7 5BD, UK
[4] Laboratory of Herpetology, Museum Zoologicum Bogoriense, Research Center for Biology, Indonesian Institute of Sciences–LIPI, Jl Raya Jakarta Bogor km 46, Cibinong, West Java, 16911, Indonesia
[5] Department of Biology, Universitas Brawijaya, Jl Veteran, Malang, East Java, 65145, Indonesia

Abstract: We review morphology and systematics of *Phoxophrys* using new specimens of previously rare species. In addition to external characters, we relied heavily on skull morphology visualized using computed tomography data of all currently recognized species in this genus. Phylogenetic analysis of ND4, 12S, and 16S mDNA sequences reveal that *Ph. tuberculata* is sister to a clade containing *Dendragama*, *Lophocalotes*, and insular *Pseudocalotes*. *Phoxophrys tuberculata* is only distantly related to Bornean congeners. Phylogenetic analysis of 29 morphological characters scored for all the species of *Phoxophrys* and a diverse set of 22 outgroup taxa found four well-supported lineages: *Ph. tuberculata*, a clade of all Bornean congeners, *Ph. nigrilabris*, and a clade of the four large Bornean species. To resolve paraphyly of *Phoxophrys*, we revalidate *Pelturagonia* Mocquard for all Bornean species of this genus. As redefined, *Phoxophrys* contains a single species: *Ph. tuberculata* of Sumatra. We describe a new species of *Pelturagonia* from the Meratus Range of southeastern Kalimantan. The new species is the sister species of *Pe. spiniceps*. Like that species, it differs from congeners in having large, dorsally projecting scales between the dorsolateral caudal crests and a postorbital process of the frontal bone reaching the postciliary ornament.

Key words: Agamidae; Borneo; Computed tomography; Osteology; *Pelturagonia anolophium* sp. nov.; Skull; Sumatra; Systematics

Early in a long and prolific career studying systematics of Bornean reptiles and amphibians, Inger (1960) revised the small agamid genus *Phoxophrys* Hubrecht (Fig. 1). Prior to his research, most herpetologists referred Bornean species of these lizards to *Japalura* (e.g., Peters 1864; Boulenger 1885, 1891; De Rooij 1915), a genus now confined to mainland Asia (Wang et al. 2018). Four of the five species of *Phoxophrys* known to Inger occur only on Borneo, whereas *Ph. tuberculata* is endemic to Sumatra. Sixty years later these lizards remain poorly known, leading Manthey and Denzer (2019:9) to remark recently that "hardly any other draconine lizard genus has been studied less in recent decades than *Phoxophrys*." Monophyly of the genus has never been tested, and some characters thought to be diagnostic of *Phoxophrys* occur in only some of the species or are widespread in other draconines. In recent years, herpetologists obtained sizable series of *Ph. nigrilabris* (e.g., Lloyd et al. 1968). However, few additional specimens of the other species reached museum collections. At least on Borneo, these small- to medium-sized lizards (maximum snout-to-vent length [SVL] = 84 mm) can be readily distinguished from other agamids by distinctive dorso-lateral crests at the base of the tail, strongly heterogenous dorsal scalation, relatively wide heads, bluish buccal epithelia, and no visible tympana. No aspect of their ecology has been systematically studied. Nonetheless, they lay only 2–4 eggs, are cryptically colored, and occur in the understory of humid forests of Borneo and Sumatra (Malkmus et al. 2002; Das 2010). *Phoxophrys nigrilabris* appears to be restricted to the lowlands and foothills, whereas *Ph. borneensis* and *Ph. cephalum* reach 2,000 m on Mount Kinabalu (Malkmus et al. 2002).

In November 2016, T.R. Larson and M. Munir collected a small number of reptiles and amphibians on Gunung Lumut, a remote mountain of the Meratus Range in southern East Kalimantan Province. The samples included four specimens of *Phoxophrys*. Our attempts to identify and then properly diagnose these lizards required a review of external morphology of the genus. Our survey of morphology includes new data for the skull and raised questions about the monophyly of the genus. Herein, we present the results of our morphological review before evaluating relationships among species of *Phoxophrys* and formally describing the new lizards from Kalimantan.

Materials and Methods

Fieldwork

T.R. Larson and M. Munir surveyed reptiles and amphibians on Gunung (=Mountain) Lumut, Kalimantan Timur, Indonesia on 12–14 November 2016. They conducted most surveys at night and recorded GPS coordinates using the WGS-84 geodetic system. They photographed specimens in life, euthanized them with benzocaine, fixed the lizards in 10% formalin, and transferred them to 70% ethanol for permanent storage at the Museum Zoologicum Bogoriense (MZB) and Amphibian and Reptile Diversity Research Center, University of Texas at Arlington (UTA). We sexed the specimens by examination of the gonads. Before fixing, Larson and Munir weighed each specimen to the nearest 1 g using an electronic

[6] Present Address: Departamento de Ecología de la Biodiversidad, Instituto de Ecología, Universidad Nacional Autónoma de México, Apartado Postal 70-275, Ciudad Universitaria, Ciudad de México, 04510, México
[7] Correspondence: e-mail, mharvey@broward.edu

Fig. 1.—Female (A, UTA 21844, SVL = 44.5 mm) and male (B, MZB 14993, SVL = 42.8 mm, photos by T.R. Larson) paratypes of *Pelturagonia anolophium* from Mount Jumut, Kalimantan Timur, Indonesia, 1,090 m; male *Pe. cephalum* (C, not collected, photo by Elijah Wostl) from Mount Kinabalu, Sabah, Malaysia; male *Pe. nigrilabris* (D, not collected, photo by Chien C. Lee; http://www.chienclee.com) from Sarawak, Malaysia; male *Pe. spiniceps* from Mount Murud, Sarawak, Malaysia (E, not collected, photo by Andrej Masonzravky); and male *Phoxophrys tuberculata* (F, UTA 65254, SVL 36.5 mm, photo by E.N. Smith) from Batang Gadis, Sumatera Utara, Indonesia, 1,223 m.

balance. They placed each specimen on a flat surface next to a ruler and took photographs of the dorsal, lateral, and ventral sides. For selected specimens, they also made multiple photos of live animals in natural settings. We deposited photos of all specimens at UTA.

Collection of Morphological Data and Definition of Characters

We compared museum specimens of our new species to 62 specimens of all currently recognized congeners (Appendix I). Our comparative series includes type specimens of all species except *Phoxophrys nigrilabris*. We use the museum acronyms of Sabaj (2016). ZRC(IMG).2.187a-f are image vouchers deposited in the Lee Kong Chian Natural History Museum, Singapore. The specimen of *Ph. borneensis* appearing in these photos was not deposited at the museum (K. Lim Kok Peng, personal communication). Asad et al. (2015) misidentified this specimen as *Ph. spiniceps*. This female specimen lacks the various diagnostic spinose scales

of *Ph. spiniceps* and cannot be referred to *Ph. cephalum*, because it has 3/3 (count on left side/right side) sublabial tubercular scales, has a lorilabial separating the enlarged suprarictal scale from the scales of the rictal fold, and lacks a row of paired enlarged subcaudals. We assign ZMB 57237 and ZMB 57238 to *Ph. cephalum* (Malkmus et al. 2002 initially identified these specimens as *Ph. borneensis*; however, Manthey 2010:Fig. RA03421-2 later reidentified the larger specimen as *Phoxophrys* cf. *cephalum*), because they have two (vs. four) rows of enlarged subcaudals; a single large sublabial tubercular scale below the rictus without a row of tubercular or heavily keeled scales anterior to it; gulars with rounded low keels; 25 and 23 (respectively) gulars down the midline from the chin shields to the chest; and an enlarged suprarictal scale in broad contact with the first scale of the rictal fold.

We scored each specimen for a suite of meristic, mensural, and qualitative characters that have proven useful for diagnosing and describing lizards in other draconine genera (Harvey et al. 2014, 2017a,b, 2018). To the nearest 0.1 mm with a digital caliper, we measured SVL (from the tip of the snout to the anterior lip of the cloaca), body length (from the posterior insertion of the arm to the anterior insertion of the leg), pectoral width (axilla to axilla), length of the tail (from the posterior lip of the cloaca), head length (from the occiput to the center of the snout), head width (at rictus), maximum diameter of the orbit (bony edge to bony edge; we took this measurement along a line parallel to the ocular aperture, because the orbit is widest along this line), width of the snout (between the upper margins of the nostrils), greatest width and height of the medial rostral (if present), length of the shank (from the center of the knee to the preaxial base of Toe I), height of the longest nuchal crest scale (a straight-line measure from the anteriormost edge of the scale to its apex), and height of the longest dorsal crest scale (using the same technique as for nuchal crest scales). We measured Fingers III and IV and Toes IV and V by pressing the digits to a flexible ruler and measuring from the interdigital skin to the base of the claw.

For characters that could be scored on either side of the body (i.e., bilateral characters) such as length of the shank and counts of labials, we scored meristic characters on the left side and mensural characters on the right side of each specimen. When a bilateral character could not be scored on one side, we switched sides.

Our counts of labials differ from those of previous revisors of *Phoxophrys* (notably Inger 1960). Confusion may also arise when identifying the first supralabial, because Bornean *Phoxophrys* have vertically divided rostrals (Fig. 2). We consider the first supralabial to be the scale behind the lateralmost rostral. A postrostral separates the lateralmost rostral from the nasal, and the nasal either contacts the first supralabial or is separated from it by a lorilabial. As in *Lophocalotes* (Harvey et al. 2018), *Phoxophrys* has an enlarged lorilabial just below and behind the eye. This scale is positioned above the last supralabial. The last infralabial is the scale positioned directly below the last supralabial.

Herein, we use the term *supercilium* to refer to the flap of skin that roofs the orbit. We identified the last canthal as a scale ending directly above or extending beyond a straight vertical line at the anterior margin of the orbit. We counted circumorbitals using the method of Harvey et al. (2014) and transorbitals as the number of scales in a transverse line between, but not including, the last supraciliary scales. Our transorbital count is identical to the "Head Scales: HeadStr" character defined by Zug et al. (2006). Counts of subdigital lamellae include all scales from the interdigital skin to the claw and include the elongate ungual scale. We use some special terminology defined by Harvey et al. (2014, 2017a,b, 2018) for scales of the head, neck, and flanks. Names of scales and skin folds associated with the corner of the mouth frequently include the suffix "rictal." In our experience, a rictal fold (sensu Cadle 1991) is invariably present in draconines.

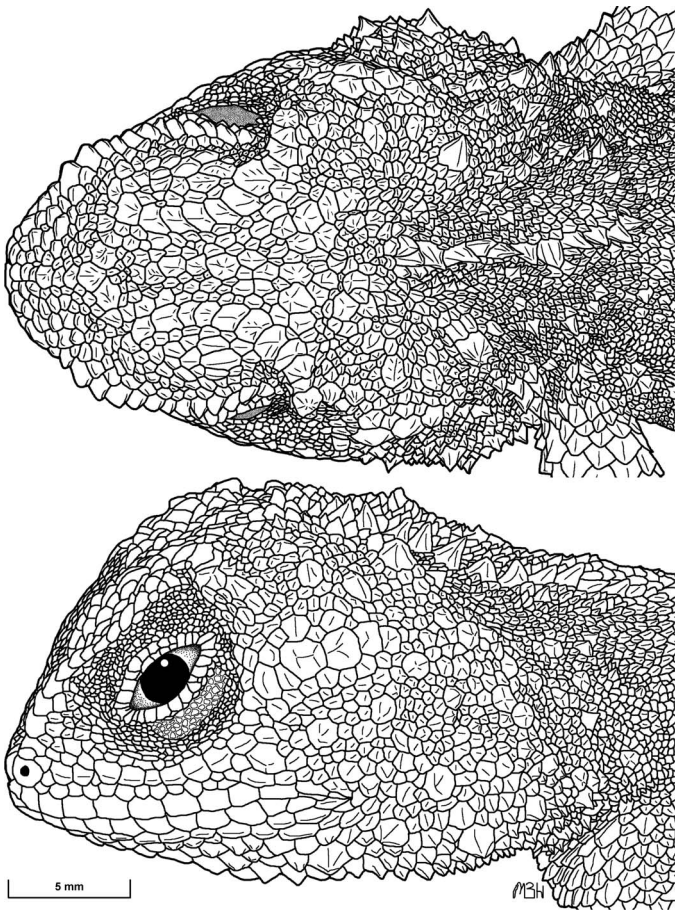

FIG. 2.—Cephalic morphology of *Pelturagonia anolophium* (adult female holotype, MZB 14992).

Vertebral crests of *Phoxophrys* often contain a complex mix of enlarged flat or projecting scales, small vertebrals, and paravertebral scales in medial contact with one another. When counting vertebral scales, we use the same methods as in our recent revisions of *Dendragama* and *Lophocalotes* (Harvey et al. 2017a, 2018). However, we could not confidently distinguish between tiny vertebrals and paravertebrals in medial contact within the dorsal crests of *Ph. anolophium*, *Ph. borneensis*, and *Ph. cephalum*. Thus, we caution readers that nuchal crest counts exclude paravertebrals in medial contact (as in Harvey et al. 2014, 2017a,b, 2018), but dorsal crest counts include these scales, unlike counts in our earlier studies. The nuchal crest counts and pectoral gap counts can be directly compared to similar

counts in other draconines described by us; however dorsal crest counts and total vertebral counts cannot.

We struggled to find a repeatable method of counting caudal dorsolateral crest scales. Distally on the tail, the degree to which these scales project laterally diminishes continuously. To count these scales, we viewed the tail in dorsal aspect and stopped the count with the last scale having a slightly pointed distal tip of the keel.

To study the skull and pectoral girdle, we collected computed tomography (CT) data from each of the six known species of *Phoxophrys* and 22 additional species in 16 draconine genera (Appendix I). We immobilized each specimen, then scanned it for 15–45 min per scan. We scanned the holotypes of *Ph. spiniceps* and *Japalura robinsoni* at the Natural History Museum, London (formerly BMNH) using a Nikon Metrology HMX ST 225 scanner at 80 kV and 80 μA. We scanned all other specimens at the UTA Shimadzu Center for Environmental Forensics and Material Sciences, using the Shimadzu inspeXio SMX-100 CT scanner at 65 kV and 40 μA. We used Shimadzu's inspeXio software to reconstruct raw X-ray data and exported them as stacks of 1,024 × 1,024 16-bit tif images. We then rotated and cropped each stack in ImageJ (National Institutes of Health, Bethesda, MD) and imported it into the open-source program Drishti 2.0 (available at http://sf.anu.edu.au/Vizlab/drishti/). We then generated one surface per skeletal structure and recorded characteristics from these three-dimensional surfaces.

With a few exceptions (defined on first use), we use the terminology of Evans (2008) in our description of the skull. In our description, we reference character states of Moody (1980) and Stilson et al. (2017) in brackets, and we developed a set of measurements and ratios that quantify some descriptive terms used by these authors. We measured width (between lateral margins of quadrates at their articular facets with the mandible) and length (from posterior edge of lateral articular surface of quadrate to middle of premaxilla) of the skull. For the dermal roofing bones, we measured the midline length (points placed at anterior tip of nasal where it curves laterally to surround premaxilla and a midpoint between posterior tips of nasals) and maximum width (from tip of lateral process to tip of lateral process of paired nasals divided by two) of the nasal, length (anterior tip where midline suture of nasal ends to frontoparietal suture) and width (at prefrontal–frontal suture) of the frontal, and midline length (from frontoparietal suture to bone's transverse ridge) and width (lateral edge of bone's orbital process) of the parietal.

For the circumorbital bones and temporal arcade, we measured the greatest length and width of the supratemporal fossa (from ridge or crest to ridge or crest. The measure captures the dimensions of the dorsolateral aperture. Length of this fossa is the longest diameter and width is the longest diameter perpendicular to the length.), width and greatest length of the suborbital fenestra (in orbital view), width and greatest height of the lacrimal canal, and length of the anterior process of the supratemporal extending along the medial edge of the supratemporal fossa (reported as a ratio to length of fossa and measured as a straight line from its anterior tip to top of squamosal at about the same point as that used for measuring length of fossa).

For the palatoquadrate derivatives, we measured height (from posterolateral edge of dorsal condyle immediately below shallow groove in squamosal to lateral edge of ventral condyle) and width (in posterior aspect, widest point just above ventral condyle) of the quadrate, width of the conch (from base of pillar to widest point of conch), width of the medial lamina of the quadrate (from base of pillar), widths of the lateral and medial portions of the ventral condyle (taken in posterior aspect when measuring width of quadrate. After recording width of the quadrate, we measured from the lateral point to the middle of a vertical groove separating the lateral and medial portions of the condyle. We then subtracted the width of the lateral portion from the quadrate width to obtain width of the medial portion of the condyle), length of the epipterygoid (from the fossa columella to its dorsal tip), and distance from the fossa columella to the pointed ventral process in line with the epipterygoid on the supratemporal process of the parietal.

For the palatal bones, we measured the length (from anterior tip to posterior tip of nasal process. We located this process in ventral aspect, because it is usually overlapped by the nasal dorsally) and alveolar width (widest point below premaxillary process of maxilla) of the premaxilla, greatest width of the nasal process of the premaxilla (usually just above premaxillary process of maxilla), angle of the maxilla–palatine suture to the maxillary teeth row (in lingual aspect, points placed at dorsal end of suture where it curves into lacrimal canal and at base of teeth with apex placed at base of teeth directly below posterior tip of suture), length of the maxilla (from just above first maxillary tooth to posterior tip of bone), length and width of the vomer in palatal view, length (from anterior tip of bone, usually on palatal ridge but sometimes in dorsal flange edging interpterygoid vacuity, to medial tip of its posterior process) and width (palatal ridge to infraorbital canal at point where palatine–pterygoid suture enters canal) of pterygoid, anterior separation of pterygoids in palatal view (at palatine–pterygoid suture from palatal ridge to palatal ridge), and separation of pterygoids at posterior inflection (from palatal ridge to palatal ridge at inflection point where posterior process begins, above anterior end of basipterygoid process).

In the otoccipital region, we measured the length (from foramen magnum to base of processus ascendens) and width (at dorsal constriction, lateral to common crus of anterior and posterior semicircular ducts) of the supraoccipital, midline distance from foramen magnum to dorsal constriction of supraoccipital, greatest diameter of the stapedial footplate, smallest diameter of the stapedial rod; length and smallest diameter of the basipterygoid process; greatest diameter of the articular facet of the basipterygoid; distance from the center of a tuber of the basioccipital to a point in the middle of the medial side of the facet of the basipterygoid process; midline distance from the midpoint between the tubera to the basisphenoid–basioccipital suture; distance between the ventral tips of tubera (points placed in center of distal surface of each tuber); length of the left tuber (base of tuber to its distal point. We established the base of the tuber when placing the apex of the angle measuring this process's orientation in sagittal view); greatest diameter of the foramen magnum; and distance between the articular facets (at their midpoints) of the paroccipital processes of the otoccipitals. To compare relative sizes of selected fenestrae,

we first measured the greatest diameter (a) of each opening and then measured a smaller diameter (b) perpendicular to this diameter. We then calculated the area of each opening using the formula for an ellipse (=abπ).

We measured the angle separating the supratemporal processes of the parietal (points placed at the posterior tips with apex above the fossa for the processus ascendens. For this process of the parietal, we prefer Oelrich's 1956 name "supratemporal process" to "postparietal process" as used by Evans 2008); the angle formed by the tubera of the basioccipital with one another (by placing points distally in center of each tuber then affixing apex at a point halfway between tubera on surface of basioccipital); the angle formed by a tuber in sagittal view (by affixing first point on alar process of sphenoid and second point distally in center of tuber, then affixing apex to center of base of tuber in line with first point); and the angle made by a paroccipital process to horizontal. (We established the horizonal plane by affixing the first point and apex of the angle to the bases of the process, at the margin of each recessus scali tympani. We placed the second point in the center of the articular face of the paroccipital process. Finally, we subtract the obtuse angle formed by the points from 180°.) In a parasagittal plane we measured the downward curve of the supratemporal process of the parietal to horizontal (skull positioned so that maxillary tooth row was horizontal).

For the teeth, in alveolar aspect, we measured the length (from edge of tooth's socket to its distal tip) of pleurodont teeth on the premaxilla, maxilla, and dentary. In lingual view, we measured height (from gutter to tip of tooth) and width (where tooth abuts its neighbors) of the second and penultimate acrodont maxillary and dental teeth.

Herein, we approximate Moody's (1980) measurements of the mandible by defining three measurements that abut one another. We measured the precoronoid length by affixing anchor points at the anteriormost tip of the mandible and on the labial side of the mandible in line with the tooth row and the dorsal tip of the coronoid process. From this point, we then measured the coronoid–articular length to the posterior margin of the lateral condyle of the quadrate (this position is close to the center of the articular, used as a landmark by Moody 1980) and length of the retroarticular process from the lateral condyle to the tip of the retroarticular process. Length of the posterolateral processes of the coronoid also abuts the precoronoid length, but ends at the distal tip of the posterolateral process. Additionally, we measured the total length of the mandible from its anterior tip to the posterior tip of the retroarticular process, greatest length of the exposed splenial in lingual view, greatest length of the adductor fossa in dorsal aspect, height of the dorsal process of the coronoid in labial view (minimal distance from its dorsal tip to the dentary), and height of the coronoid in lingual view (straight-line measurement from dorsal tip of dorsal process of coronoid to ventral tip of the posteromedial process of the coronoid. This measure is not usually vertical, but slightly angled forward, because the posteromedial process projects behind the dorsal process).

Inferring Species Boundaries

We view species as separately evolving metapopulations and agree with de Queiroz's (1998) observation that many, if not all, contemporary species concepts are special cases of the general lineage concept. Operationally, we recognize allopatric populations as species when they are diagnosable by concordance of multiple apparently independent characters (Avise and Ball 1990; Wiens and Penkrot 2002).

For interspecific comparisons of meristic data, we used Tukey's test to compare means when samples satisfied assumptions of normality (verified with the Shapiro–Wilk test) and homogeneity of variance (verified by Levene's test). We used the Mann–Whitney *U*-test as a nonparametric alternative to Tukey's test. To test for sexual size dimorphism in meristic characters, we verified that our meristic characters satisfied assumptions of homogeneity and normality, then compared sexes using a Student's *t*-test. We used Welch's nonparametric *t*-test when data violated assumptions. To compare species for mensural traits, we used analysis of covariance (ANCOVA), treating SVL as a covariate. For the ANCOVAs, we verified the assumption of parallel slopes with an *F*-test. We log-transformed characters that violated the assumption of parallel slopes. To avoid inflation of the Type I error rate, we adjusted probabilities of ANCOVAs using the Bonferroni method whenever the same set of measurements were used in more than one set of comparisons. We used the PAST 3.20 statistical software program (Hammer et al. 2001) for all statistical tests.

In this study, we compared means or size-adjusted means for 20 meristic and 8 mensural characters. Our comparisons of means serve two purposes: (1) to identify interspecific differences of potential diagnostic value and (2) to uncover evidence of interrupted gene flow. Tukey's test and the Bonferroni method avoid inflation of the Type 1 error rate when using the same data set in multiple comparisons. They are suitable for testing null hypotheses of the form: Means of character X are the same for the various species. However, one might argue that each test of whether a character differs among species is being used as a proxy for a different null hypothesis: Population A and population B are the same species. If the Type 1 error rate is set at 5%, then these tests become repeated trials with a fixed rate of success. Using the binomial equation, there is a 35.0% probability that at least 1 of our 28 tests will reject the null hypothesis even if it is true. This probability falls precipitously when multiple test have low probabilities. For 28 tests, the probability drops to 4.9% that four or more tests will be significant. Therefore, when comparing means, we accept four or more significant results as supporting the alternative hypothesis that two or more species are present. We also approached this problem in a way analogous to the Bonferroni correction. For individual characters, we multiplied each probability by the number of characters tested. When a probability is still less than 5% after making this calculation, we add an asterisk (*) immediately after the probability.

Phylogenetic Analysis

Based on our survey of morphology, we define 29 characters that we later use to estimate phylogeny of *Phoxophrys*. We surveyed each character across a diverse set of outgroup taxa (Table 4). Then, we polarized characters using parsimony (method of Maddison et al. 1984) by mapping the character states on a recent phylogenetic hypothesis of draconine relationships (Grismer et al. 2016, as further refined by Wang et al. 2018). These studies recovered a clade containing *Diploderma*, *Otocryptis*,

mainland *Pseudocalotes*, and *Sitana* as sister to *Phoxophrys* with *Acanthosaura* sister to this larger clade. We chose to use this phylogenetic hypothesis to polarize characters, because it is the most comprehensive to date, both in terms of number of species and genes sampled.

Our survey includes all known species of the Sunda Shelf genera *Dendragama* and *Lophocalotes*. Neither Grismer et al. (2016) nor Wang et al. (2018) include these two genera, however. To err on the side of caution, we treated *Dendragama* and *Lophocalotes* as potential sister groups to *Phoxophrys* when polarizing characters.

We analyzed our morphological data matrix with the branch-and-bound algorithm (Implicit Enumeration) with the program Tree Analysis Using New Technology (TNT; Goloboff et al. 2008). We evaluate branch support by (1) standard bootstrapping using 1,000 replicates and (2) the implicit enumeration setting in TNT and Bremer support on suboptimal trees up to five steps longer than our phylogeny.

To test the monophyly of *Phoxophrys*, we generated a data set of sequences from the 12S, 16S, and ND4 mitochondrial genes. This data set included 12S and 16S mitochondrial DNA sequences of *Ph. nigrilabris* downloaded from GenBank, new 16S and ND4 sequences from *Ph. anolophium*, sequences previously generated by Harvey et al. (2017b, 2018) and Shaney (2017) for *Ph. tuberculata* and 19 other draconines. We failed to amplify the 12S gene for *Ph. anolophium*, and, for *Ph. nigrilabris*, we lack the ND4 gene. In the description of *Ph. anolophium*, we provide GenBank accession numbers for new sequences generated in this study.

To sequence the 16S gene fragment of the new species, we used the forward primer 5′CGCCTGTT TAACAAAAA-CAT-3′ (16Sf) and reverse primer 5′CCGGTCTGAAC TCAGATCACGT (16Sr; Leaché et al. 2009). To sequence the ND4 fragment, we used the forward primer 5′CACCTATGACTACCAAAAGCTCATGTAGAAGC-3′(ND4) and reverse primer 5′CATTACTTTTACTT GGATTTGCACCA-3′(LEU), which targeted an 892–base pair (bp) region (Harvey et al. 2017b). For these genes, the thermal cycling profiles consisted of an initial denaturation at 94°C for 3 min, followed by 30 cycles of denaturation at 94°C for 30 s, a 50°C annealing phase for 45 s, and a 72°C extension for 1 min, followed by a 72°C extension for 7 min, then a holding phase at 4°C. We cleaned the products of amplification using Sera-Mag Speedbeads (Fisher Scientific), following the procedure outlined by Rohland and Reich (2012).

We sequenced PCR products in both directions with Sanger sequencing technology. To edit sequences, we used Geneious Prime v2019.2.1 (available at https://www.geneious.com; Kearse et al. 2012). We aligned all sequences using the MAFFT alignment setting (Katoh et al. 2002; Katoh and Standley 2013) implemented within Geneious Prime. We checked the ND4 alignment for stop codons by eye and trimmed them to equal lengths to remove missing data.

We conducted maximum-likelihood analyses using raxmlGUI (Stamatakis 2006). In this analysis, we utilized the thorough bootstrapping setting, sampling over 10 runs of 10,000 repetitions, and carried out 20 searches for the best tree. We selected the most likely model of evolution for each codon position using Bayesian information criteria implemented in jModelTest v2.1.10 (Darriba et al. 2012). Based on the results of jModelTest, we partitioned by each codon position using GTR + Γ + I. We carried out Bayesian phylogenetic analysis using MrBayes v3.2.6 (Ronquist et al. 2011), and used four independent runs (nruns = 4) and four chains for 10 million generations, sampling every 1,000 generations on the CIPRES Science Gateway (Miller et al. 2010). We used default temperatures for chains. We assessed the appropriate amount of burn-in and convergence by inspecting the log files in the program Tracer (v1.6; BEAST, Bayesian Evolutionary Analysis Sampling Trees) and discarded the first 25% of trees in TreeAnnotator (v2.4.6; BEAST, Bayesian Evolutionary Analysis Sampling Trees).

Review of External Morphology and List of Characters

In this section, we discuss characters found to vary among the six species of *Phoxophrys*. We number characters that we code for phylogenetic analysis and omit numbers from characters used for diagnostic and descriptive purposes only. Many of the excluded characters are continuous or polymorphic. Although methods for coding polymorphic and continuous data exist (e.g., Smith and Gutberlet 2001; Lawing et al. 2008), sample sizes of only *Ph. nigrilabris* are adequate, and three of the six species are known from four or fewer specimens. Small sample sizes would likely lead to spurious inferences about relationships and unnecessarily obscure relationships revealed by the various qualitative characters.

External Morphology

Lorilabial and infraorbital series.—Number and condition of scales below the eye have considerable diagnostic value among draconines (e.g., Wood et al. 2009; Mahony 2010; Harvey et al. 2017a,b). Between the orbital margin and supralabials, species of *Phoxophrys* invariably have an enlarged row of infraorbitals (Fig. 3). The infraorbitals may contact the supralabials or be separated from them by a row of small lorilabials. Like Inger (1960), we use the term *infraorbitals* for both types of scales and use the term *lorilabial* when we need to draw a distinction between these two types of scales. Inger's (1960) key uses variation in these scales at two places. First, in his Couplet 2, he distinguishes *Ph. nigrilabris* from congeners based on a lorilabial separating the nasal from the supralabials. Then, in Couplet 4, he uses a count of infraorbital rows to distinguish *Ph. borneensis* (one row) from *Ph. cephalum* (two rows). A continuous series of small lorilabials separates enlarged infraorbitals from the supralabials in his "two rows" character state, whereas one or more of the enlarged infraorbitals contacts the supralabials in his "one row" character state.

With larger samples than those available to Inger (1960), number of infraorbital rows proves to be polymorphic in *Phoxophrys cephalum*. Among our sample of *Ph. cephalum*, 40% have one row (Table 1) and this character should not be used to distinguish *Ph. cephalum* from *Ph. borneensis*. Inger (1960:224) also noted some variation in this character, when he remarked "a second syntype [i.e., referring to *Ph. cephalum*] has only one continuous row of infraorbitals."

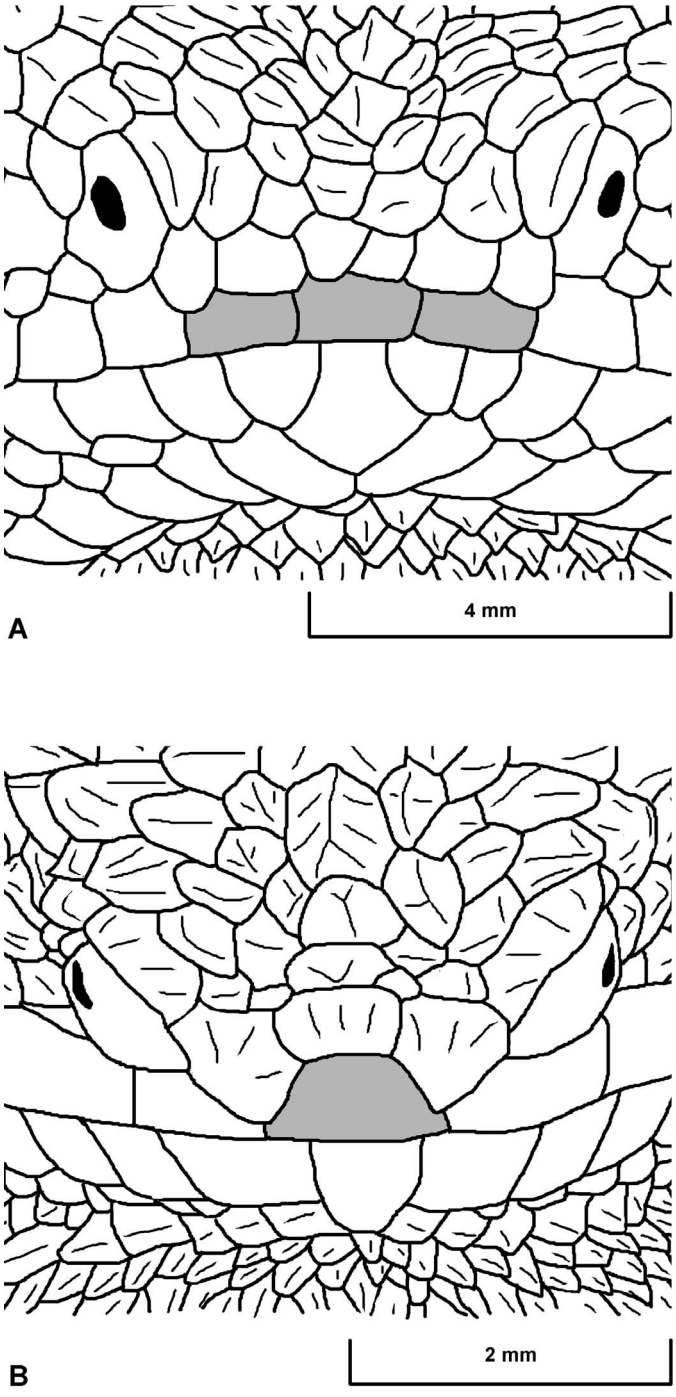

FIG. 3.—Snout morphology of *Pelturagonia anolophium* (female holotype, MZB 14992) and *Phoxophrys tuberculata* (UTA 65254). Rostral scales shaded gray.

Consequently, we do not use this character to distinguish between *Ph. cephalum* and *Ph. borneensis* in our revised key.

Polymorphism of a character in one species should not negate its usefulness as a diagnostic character in other species, because most multistate characters likely pass through a period of polymorphism during their evolution (Harvey 2008). Each of the four specimens of *Phoxophrys anolophium* has a continuous row of lorilabials separating the enlarged infraorbitals from the supralabials, whereas one or more infraorbitals contact the supralabials in the three types of *Ph. borneensis* (Inger 1960; this study) in ZRC(IMG).2.187, on both sides of the two MCZ specimens, and in all but one of the eight NMW specimens. Thus, this character will usually distinguish *Ph. anolophium* from *Ph. borneensis*. The holotype of *Ph. spiniceps* and a specimen illustrated in our Fig. 1 both lack continuous rows of lorilabials below the enlarged infraorbitals.

Nasal–supralabial contact.—The nasal usually contacts one supralabial in *Phoxophrys anolophium*, *Ph. borneensis*, *Ph. cephalum*, and *Ph. spiniceps*, whereas a lorilabial usually separates the nasal from the supralabials in *Ph. nigrilabris*. The nasal contacts a supralabial in only 1 of our 20 specimens (5%) of *Ph. nigrilabris*. Interestingly, the nasal contacts supralabials 1 and 2 on all eight sides of the four specimens of *Ph. tuberculata*. Among the other species, we found this character state in only one specimen of *Ph. borneensis* and one specimen of *Ph. cephalum* (Table 1).

Contact between suprarictal scale and first elongate scale above rictal fold.—Lorilabials of *Phoxophrys anolophium*, *Ph. borneensis*, and *Ph. nigrilabris* usually separate the enlarged suprarictal scale from the first elongate scale of the rictal fold (Table 1). In contrast, these two scales are in broad contact in *Ph. cephalum*. In *Ph. spiniceps* (both sides of all three specimens), the enlarged scale contacts the last supralabial, and a small scale behind and slightly below it separates the enlarged scale from the first scale of the rictal fold. Lorilabials separate the scales on both sides of the holotypes of *Ph. tuberculata* and *Japalura robinsoni*. However, a large projecting suprarictal scale broadly contacts scales of the rictal fold on both sides of the new male specimen of *Ph. tuberculata*.

1. Shape of supraciliaries.—The supraciliaries are subrectangular and juxtaposed to imbricating (0) or arched dorsally, producing a serrate edge to the supercilium (1).

Phoxophrys nigrilabris and *Ph. tuberculata* have distinctly arched supraciliaries forming a serrate series, whereas *Ph. anolophium*, *Ph. borneensis*, *Ph. cephalum*, and *Ph. spiniceps* have low, subrectangular supraciliaries.

Among outgroups, supraciliaries may be subrectangular to elongate and overlapping to varying degrees, but other draconines examined by us did not have arched supraciliaries like those in *Ph. nigrilabris* and *Ph. tuberculata*.

2. Supraciliary spine.—Subrectangular or serrate supraciliaries extend to the postciliary scale or ciliary notch (0) or they terminate in an elongate spine in the middle of the supracilium (1).

Phoxophrys spiniceps has a prominent superciliary spine, positioned above the center of the eye (Fig. 1). This scale is a modified scale of the supraciliary series. In front of the spine, the supraciliary scales are subrectangular. Interestingly, small granular scales extend from the spine to the postciliary scale. Several scales surrounding the base of the spine are somewhat elongate and project upward, evidently supporting the spinose scale.

Among other draconines, postciliary, temporal, and/or posttemporal scales may be elongated into spines. For example, the prominent spine at the corner of the eye of *Acanthosaura* is a modified postciliary scale. A single spinose scale above the center of the eye appears to be unique to *Phoxophrys spiniceps*. *Ceratophora karu* has several elongate scales in the center of the supercilium, but they are not long spines.

TABLE 1.—Frequencies of selected diagnostic characters among *Phoxophrys tuberculata* and five species of *Pelturagonia*. Data for *Pe. borneensis* includes ZRC(IMG) 2.187 for characters visible in the photos.

Diagnostic character	*Pe. anolophium*	*Pe. borneensis*	*Pe. cephalum*	*Pe. nigrilabris*	*Pe. spiniceps*	*Ph. tuberculata*
Infraorbital rows	1 (0%, $n = 4$) 2 (100%)	1 (92%, $n = 13$) 2 (8%)	1 (40%, $n = 15$) 2 (60%)	1 (10%, $n = 20$) 2 (90%)	1 (100%, $n = 3$) 2 (0%)	1 (50%, $n = 4$) 2 (50%)
Nasal–supralabial contact	0 (0%, $n = 4$) 1 (100%) 1–2 (0%)	0 (8%, $n = 13$) 1 (69%) 1–2 (8%) 2 only (15%)	0 (16%, $n = 19$) 1 (79%) 1–2 (5%)	0 (95%, $n = 20$) 1 (5%) 1–2 (0%)	0 (0%, $n = 3$) 1 (100%) 1–2 (0%)	0 (0%, $n = 4$) 1 (0%) 1–2 (100%)
Enlarged supraricta scale of rictal fold	Separated (100%, $n = 4$) In contact (0%)	Separated (92%, $n = 12$) In contact (8%)	Separated (0%, $n = 14$) In contact (100%)	Separated (100%, $n = 20$) In contact (0%)	Separated (100%, $n = 3$) In contact (0%)	Separated (67%, $n = 3$) In contact (33%)
Rostrals	– – 3 (100%, $n = 4$)	– 2 (8%, $n = 13$) 3 (53%) 4 (31%) 5 (8%)	– 2 (15%, $n = 13$) 3 (85%) – –	– – 3 (89%, $n = 18$) 4 (11%) –	– – 3 ($n = 3$) – –	1 (100%, $n = 3$) – – – –
Medial rostral compared to mental	Wider (100%, $n = 317$)	Wider (92%, $n = 13$) Subequal (8%)	Narrower (85%, $n = 13$) Subequal (15%)	Wider (100%, $n = 13$)	Wider (100%, $n = 3$)	Wider (100%, $n = 3$)
Chin shields contacting infralabials	1 (50%, $n = 4$) 2 (25%) 3 (25%)	1 (8%, $n = 13$) 2 (31%) 3 (61%)	– 2 (67%, $n = 15$) 3 or 4 (33%)	1 (74%, $n = 19$) 2 (26%) –	1 (33%, $n = 3$) 2 (67%) –	1 (25%, $n = 4$) 2 (25%) 3 (50%)
Tubercular sublabials	4–7 (5 ± 1, $n = 4$)	2–6 (4 ± 1, $n = 13$)	0 ($n = 14$)	2–6 (4 ± 1, $n = 19$)	2 ($n = 3$)	2 or 3 ($n = 3$)
Maximum snout-to-vent length of females (mm)	80	62	68 (74 mm, Inger 1960)	53	59 (60, Manthey 2010)	43

3. Projecting and triangular supracilium.—The supracilium is rounded laterally, unmodified, and roofs the orbit (0) or it projects upward and outward as a pointed, triangular flap (1; Fig. 4).

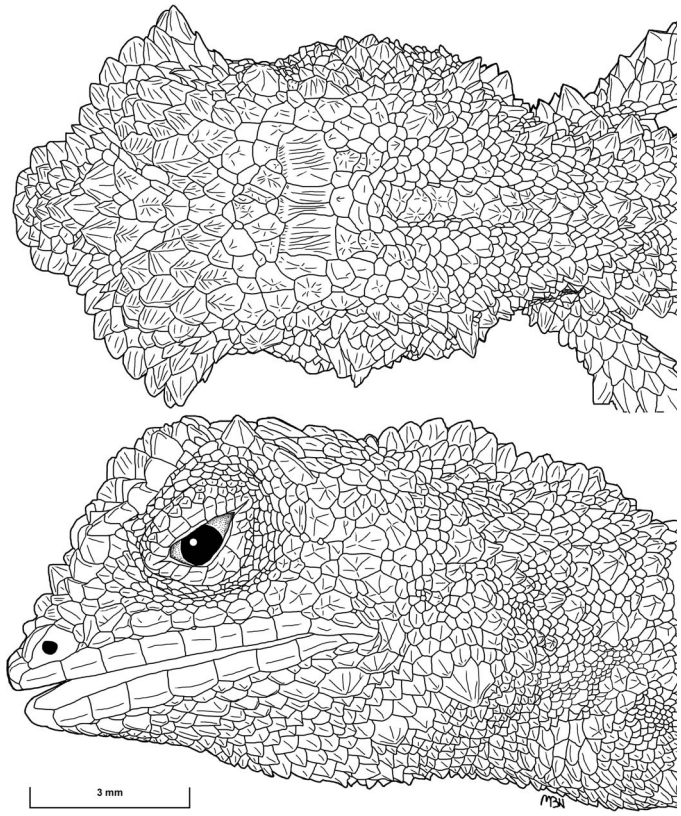

FIG. 4.—Cephalic morphology of *Phoxophrys tuberculata* (adult male, UTA 65254).

Several draconines have modified supercilia. For example, many species of *Gonocephalus* have vertically arched supercilia that are sometimes supported by bony pre- and postorbital processes. None of the draconines examined in this study have a distinctive triangular supracilium like *Phoxophrys tuberculata*. Nonetheless, the supercilium of *Ph. tuberculata* resembles that of *Ceratophora aspera* and *C. karu*. Like *Ph. tuberculata*, the supercilia of these Sri Lankan endemics projects upward and outward. In all three species a patch of distally attenuate, flattened, and multicarinate superciliary scales comprise a triangular patch above the center of the eye. Pethiyagoda and Manamendra-Arachchi (1998:Fig. 22) illustrate this structure.

4. Vertical division of rostral scale.—The rostral is entire (0) or divided into two or more scales (1).

The Bornean species of *Phoxophrys* usually have three rostrals (Table 1; Fig. 2) with a postrostral separating the nasal from the rostral series on each side. *Phoxophrys borneensis* exhibits more variation than congeners in the rostral series with 39% ($n = 13$) of specimens having four or five rostrals. In contrast, *Ph. tuberculata* has a single rostral.

Among outgroups, the three Sri Lankan endemics all have divided rostrals (four in *Ceratophora stoddartii*, three in *Cophotis ceylanica*, and five or six in *Lyriocephalus scutatus*). Like its congeners, *Bronchocoela hayeki* has a wide medial rostral. As defined here, we consider a small scale on either side of the medial rostral to be a rostral rather than the first supralabial, because the lateralmost postrostral separates this scale from the nasal.

Reduction of the mental scale and its width relative to the rostral.—Along with vertical division of the rostral, the mental also appears to have undergone vertical division in all Bornean *Phoxophrys*, except *Ph. cephalum*. In this species, the mental is wider than or of equal width to the medial rostral. This character is not applicable to specimens with even numbers of rostrals.

Reduction of the mental is particularly pronounced in *Phoxophrys nigrilabris*. Arrangement of the mental and chin shields resembles other draconines in most species of *Phoxophrys*. Because of the mental's large size, the first pair of chin shields have relatively short medial contact behind it or the pair may be separated by one or more gulars. In contrast, the mental of *Ph. nigrilabris* is substantially reduced in size relative to the first pair of chin shields, and the chin shields have a relatively long point of medial contact. Unlike any other *Phoxophrys*, 26% of *Ph. nigrilabris* ($n = 19$) have a single azygous postmental positioned behind the mental and between the first pair of chin shields. We refer to this scale as a postmental instead of a gular, because of its shape and because the first pair of chin shields usually contact one another behind it. In our sample of *Ph. nigrilabris*, a gular and an azygous postmental completely separate the first pair of chin shields in a single specimen (5%; $n = 20$). Finally, we note that a single chin shield contacts the infralabials in all but one specimen of *Ph. nigrilabris*, whereas two or more chin shields contact the infralabials in *Ph. cephalum* and all but one *Ph. borneensis* (Table 1).

Chin shields contacting infralabials.—In most Bornean *Phoxophrys* two or more chin shields contact the infralabials, whereas only the first chin shield contacts the infralabials in most *Ph. nigrilabris*.

5. Sublabial tubercular scales.—Sublabial scales are unmodified (A) or tubercular (B) anterior to a large tubercular scale below the rictal fold.

Harvey et al. (2017a) recently used counts of tubercular sublabial scales to diagnose species of *Dendragama*. These same scales have diagnostic value in *Phoxophrys*. All *Phoxophrys* have a prominent tubercular scale positioned below the rictal fold (Fig. 3). Most species also have 2–7 similar tubercular scales on sublabials anterior to this subrictal scale. However, *Ph. cephalum* lacks the additional scales and only has the single subrictal tubercular scale.

Tubercular sublabials may be related to condition of the gulars. Most *Phoxophrys* have spinose gulars with prominent keels and projecting mucrons. In contrast, *Ph. cephalum* lacks spinose gulars. Its gulars bear low rounded keels and lack mucrons.

Among outgroups, most species lack both enlarged subrictal and sublabial tubercular scales (Table 4). Nonetheless, presence of tubercular sublabials in *Dendragama* (Harvey et al. 2017a) makes it impossible to polarize this character without further resolution of draconine phylogeny. Each of the species of *Diploderma* examined in this study have swollen to tubercular sublabials; *Cristidorsa planidorsata*, *D. slowinskii*, *D. splendidum*, and *D. yunnanese* also have subrictal tubercular scales behind the tubercular sublabial scales. *Lyriocephalus* has a continuous row of enlarged, keeled scales in the same anatomical location as the sublabial and subrictal tubercles of *Phoxophrys*; however, its scales are not tubercular and not separated from one another by smaller, unmodified scales.

6. Dorsal crests.—A dorsal crest of continuous projecting scales extends from the pectoral gap to the base of the tail (0) or is replaced by widely spaced tubercular scales frequently in pairs or short transverse series (1).

All known *Phoxophrys* have a nuchal crest of relatively low triangular scales. *Phoxophrys anolophium*, *Ph. borneensis*, *Ph. cephalum*, and *Ph. spiniceps* lack a continuous dorsal crest and instead have widely spaced tubercular (spinose in *Ph. spiniceps*) scales along the vertebral midline, behind the pectoral gap. Inger (1960) noted that *Ph. nigrilabris* has a continuous dorsal crest and used this character in his key. With discovery of male specimens of *Ph. tuberculata*, we now know that condition of the dorsal crest is sexually dimorphic in this species. As Inger (1960) observed, females lack a crest or, at least, have a poorly defined one. Males have a continuous, projecting dorsal crest of small triangular scales extending from the pectoral gap to the base of the tail (Fig. 1; see also Manthey 2010:Fig. RA03453-4, who illustrates an additional male specimen from "near Solok" with a clearly visible dorsal crest extending onto the tail). Thus, when identifying male *Phoxophrys*, this character causes confusion at Couplet 2 of Inger's key, potentially leading some to misidentify *Ph. tuberculata* as *Ph. nigrilabris*.

Draco sumatranus lacks a dorsal crest, but also lacks the widely spaced tubercles forming a broken dorsal crest in *Phoxophrys*. Widely spaced projecting dorsals occur in *Ceratophora stoddarti* and *Lyriocephalus scutatus*. However, these species lack the distinctive paired or transverse rows of tubercles found in Bornean *Phoxophrys*.

7. Orientation of middorsal scales on the neck and in the pectoral gap.—Middorsal scales on the neck point dorsally and posteriorly (0) or they point anteriorly and undergo a 180° rotation across the pectoral gap (1).

Unusual orientation of scales on the neck and in the pectoral gap of *Phoxophrys nigrilabris* is arguably one of this species' most distinctive characteristics. With only two specimens at hand in 1960, Inger did not mention this character. In this species, middorsal scales on the neck point anteriorly, whereas they point posteriorly in all congeners. The middorsal scales then undergo an abrupt 180° counterclockwise rotation across the pectoral gap to point dorsally and posteriorly along the dorsal crest. In the center of the gap, some scales point transversely to the left in 58% of specimens ($n = 33$; Fig. 5), whereas in the remaining 42% of specimens the scales abruptly switch direction somewhere in the middle of the gap. In all other *Phoxophrys*, scales across the entire gap point backward.

Among outgroup species, scales on the sides of the neck point dorsally and anteriorly and undergo a 180° reorientation across the pectoral gap in *Acanthosaura armata*, *A. crucigera*, and *Gonocephalus grandis*.

8. Dorsolateral caudal crests.—The tail lacks dorsolateral crests (0) or a pair of enlarged, heavily keeled scales form dorsolateral crests at the base of the tail (1).

Bornean *Phoxophrys* have prominent dorsolateral crests (Figs. 1 and 6) at the base of their tails. A row of enlarged scales, thickened medially and projecting laterally, forms each of the crests. Inger (1960) illustrated this distinctive caudal morphology in males of *Ph. borneensis*, *Ph. cephalum*, and *Ph. nigrilabris*. In his diagnoses, he included counts of crest scales and used the counts to differentiate *Ph. borneensis* from *Ph. cephalum*. Inger (1960) described similar crests in *Diploderma flaviceps*. *Diploderma varcoae* and *Cristidorsa planidorsata* have dorsolateral caudal crests, but also have a vertebral crest at the base of the tail. All three crests in these two species are continuous with dorsolateral

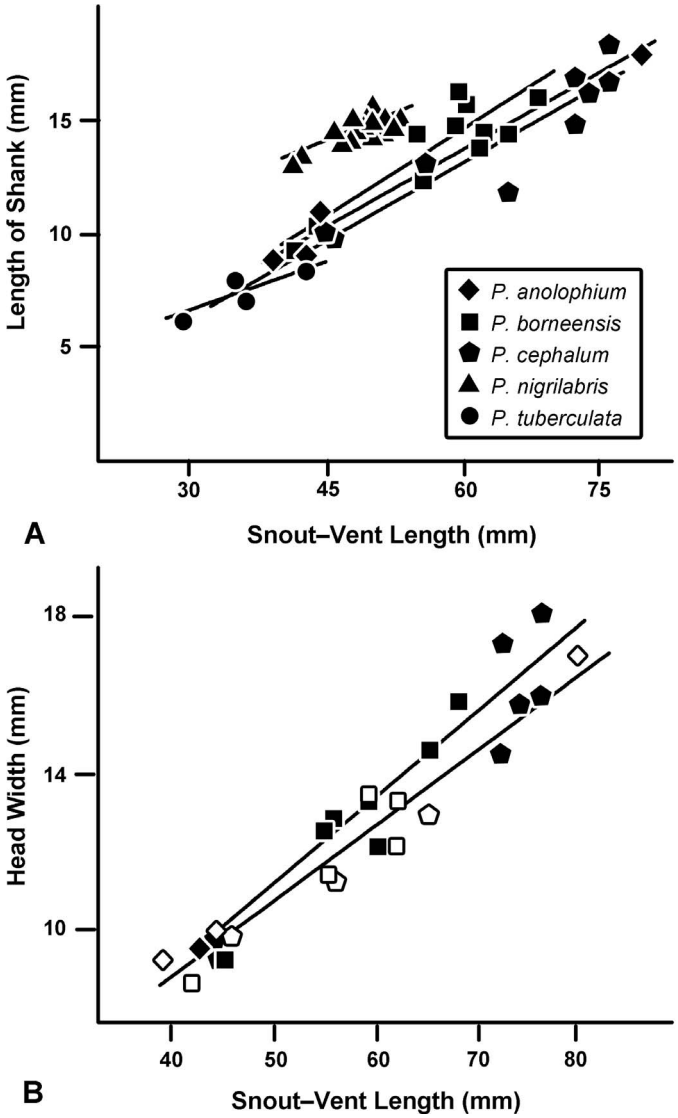

FIG. 5.—(A) Relative length of the shank in *Pelturagonia* and *Phoxophrys*. (B) Relative head width in males (solid symbols) and females (open symbols) of *Pelturagonia anolophium*, *Pe. borneensis*, and *Pe. cephalum* (key to symbols in A also applies to B).

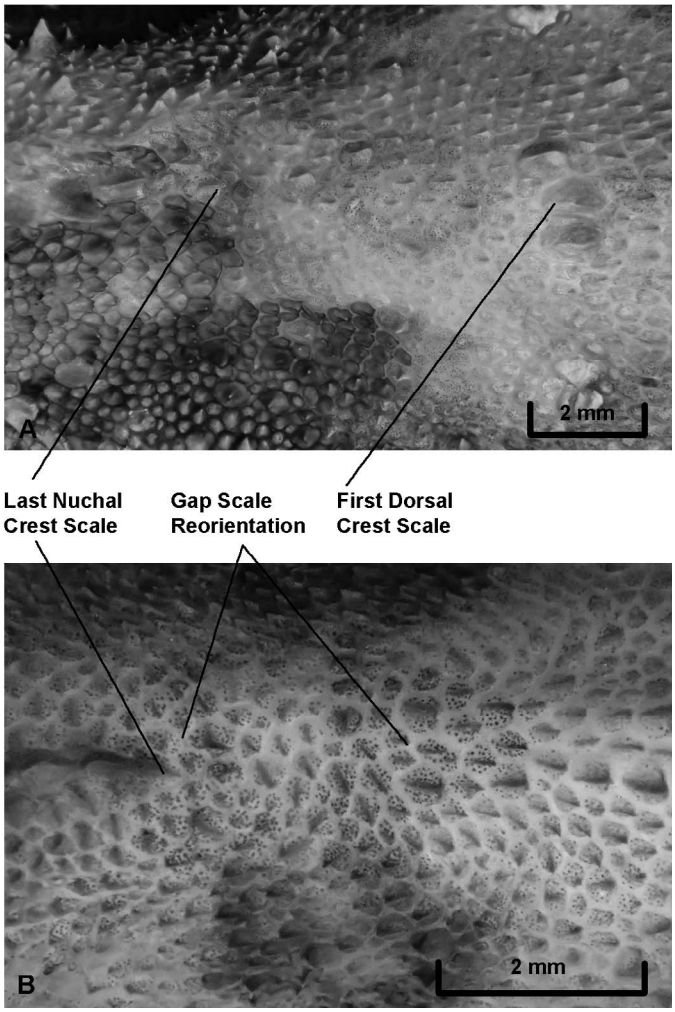

FIG. 6.—Pectoral gap of *Pelturagonia anolophium* (A, holotype, MBZ 14992) and *Pe. nigrilabris* (B, FMNH 138483), illustrating 180° counterclockwise rotation of vertebral scales in *Pe. nigrilabris*.

and vertebral crests on the body, whereas the bodies of Bornean *Phoxophrys* lack dorsolateral crests.

In *Phoxophrys*, sexual dimorphism in tail morphology has been overstated somewhat. Both sexes of all Bornean *Phoxophrys* have dorsolateral crests at the base of the tail, and we did not find intersexual differences in counts of crest scales for any of the species. Keratinized layers of the crests thicken substantially in larger male *Ph. borneensis* and *Ph. cephalum*, whereas thickness of the keratinized layers resembles that of adjacent scales in females.

Counts of crest scales prove more variable than originally thought (Table 1), and we did not find differences in counts among Bornean *Phoxophrys*.

Phoxophrys tuberculata lacks dorsolateral crests and its vertebral crest extends onto the base of the tail. Our male specimen has 2/2 multicarinate tubercular scales positioned dorsolaterally on the proximal tail. These scales are a continuation of the dorsolateral series of widely spaced multicarinate scales found on the body. Five/seven small scales laterally separate each pair of multicarinate scales. Dorsally, the tail of *Ph. tuberculata* is somewhat rounded rather than flat; medially, five scales separate the first pair of multicarinate scales and three scales separate the second pair.

9. Projecting scales between dorsolateral crests.—Dorsally, the tail is flat between the crests (A), or dorsally projecting scales separate the crests medially (B). This character is not applicable to any outgroups examined by us, all of which either lack dorsolateral caudal crests or have a vertebral crest between the caudal crests.

In *Phoxophrys borneensis*, *Ph. cephalum*, and *Ph. nigrilabris*, the area between the crests is flattened dorsally, so that the proximal tail is subtriangular in cross section. In these species, the area between the crests is flat and covered by scales that are mostly small and keeled, but not projecting. In contrast, *Ph. anolophium* and *Ph. spiniceps* have tubercular scales between the crests. These scales are larger than the crest scales in both species, pointed and projecting in *Ph. anolophium* and spinose in *Ph. spiniceps*. In the other species, a row of flat scales supports the crests medially; although enlarged, these supporting scales are

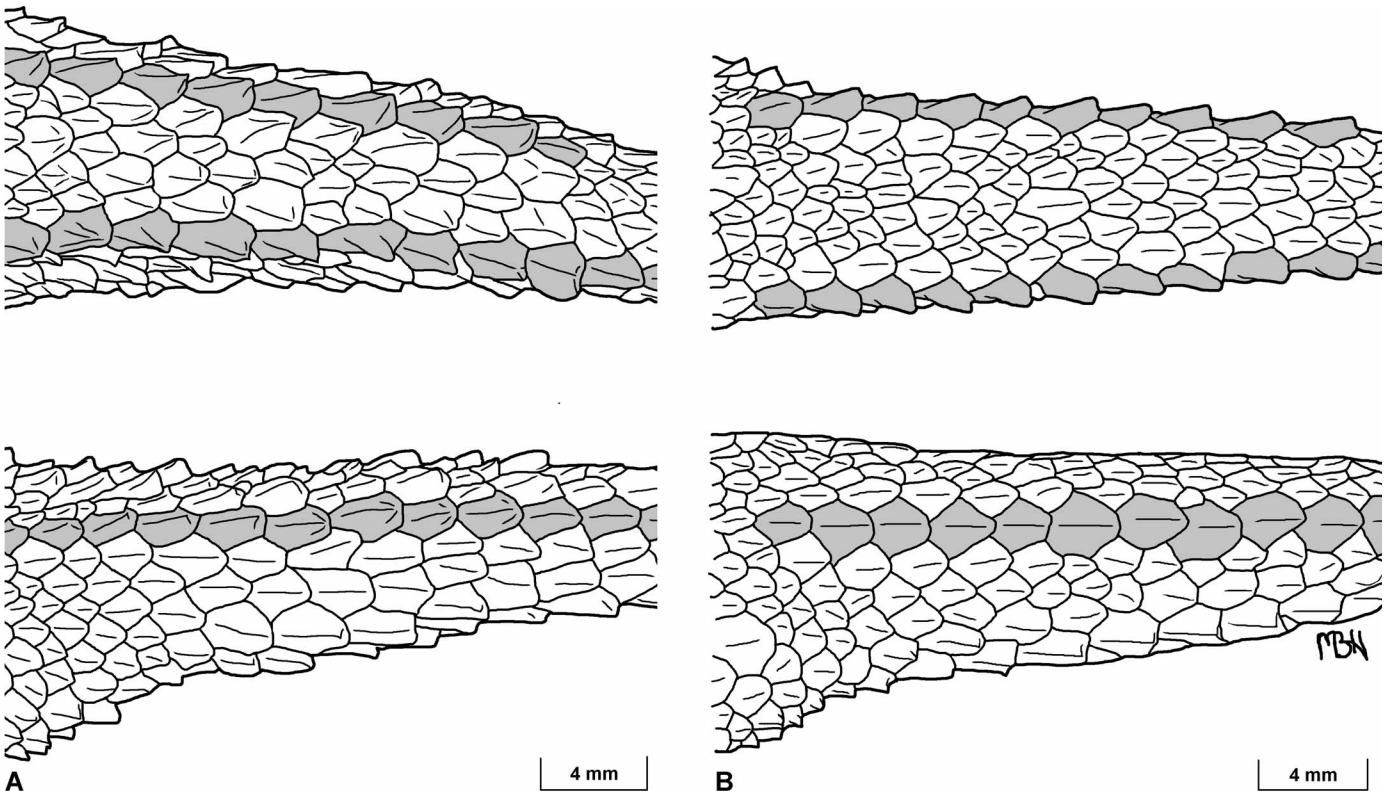

FIG. 7.—Proximal tails of female *Pelturagonia anolophium* (A, holotype, MZB 14992) and *Pe. borneensis* (B, MCZ 43487) in dorsal and lateral aspect. Dorsolateral crest scales shaded gray.

nonetheless smaller than scales of the crest. Scales separating the crests reduce from 4–10 at the beginning of the crests to 3–4 distally in *Ph. borneensis* and *Ph. cephalum*. In *Ph. anolophium* scales separating the crests reduce from 6 to 2 (75%, $n = 4$) or 3 (25%); they reduce to 2 large scales in the holotype of *Ph. spiniceps*.

10. Enlarged subcaudals.—Enlarged subcaudals are absent or in four rows (0) or in two rows (1) near the base of the tail.

In ventral aspect, the tail tapers distally to the end of the retracted hemipenis, then bears a subtle swelling extending about as far as the dorsolateral crests (Fig. 7). This swollen portion of the tail bears enlarged subcaudals in Bornean *Phoxophrys*. As noted by Inger (1960), *Ph. cephalum* has two enlarged subcaudals, whereas other Bornean species have four enlarged subcaudals. The scales are poorly differentiated in females of *Ph. anolophium*, but countable and evident in both sexes of the other Bornean species. Eight to thirteen scales separate the enlarged subcaudals from the vent. However, these scales increase in size distally and the last row is almost as large as the first row of enlarged subcaudals. *Phoxophrys tuberculata* lacks enlarged subcaudals.

Interestingly, in the six males of *Phoxophrys borneensis* in the NMW, a wash of greenish to greenish-orange pigment encircles the tail over the section with enlarged subcaudals (Fig. 7). We noted an identical band overlying enlarged subcaudals of *Lophocalotes ludekingi* in the same collection. We cannot explain the presence of these bands of pigment. They warrant histological study and likely represent an undescribed glandular product or chemical compound deposited in the stratum corneum of this portion of the tail.

The keys of Inger (1960) and Malkmus et al. (2002) do not mention the difference in subcaudals; instead, they distinguish *Phoxophrys borneensis* from *Ph. cephalum* based on keeling of scales on the sides of the tail. Use of keeling on sides of the tail is unfortunate for three reasons. First, enlarged supracloacal scales have heavy keels and these scales are on the sides of the tail in both species, potentially confusing some novice users of these keys. Second, distal to the supracloacal scales some small male (e.g., FMNH 152166, SVL = 56 mm) and female (e.g., FMNH 251007, SVL 45 mm) *Ph. cephalum* have low keels on scales covering sides of the tail. Possibly, thickening of the beta-keratin–containing layers obliterates the keels in adults, but this hypothesis requires further study. Third, the enlarged pair of subcaudals is by far the most distinctive caudal character of *Ph. cephalum*. Accordingly, we omit any mention of keeling on the sides of the tail in our revised key.

Among outgroups, we found two rows of enlarged, heavily keeled subcaudals only in *Gonocephalus grandis* and *Ceratophora stoddartii*, whereas four rows occur in several genera. *Bronchocoela hayeki* has eight rows of enlarged subcaudals at the base of its tail. In many *Diploderma* and mainland *Pseudocalotes*, scales on sides of the tail are relatively large and usually not or only slightly smaller than subcaudals. When distinguishable (e.g., in *D. slowinskii*, *D. splendidum*, *Ps. kakhienensis*, and *Ps. kingdonwardi*) four medial rows of subcaudals are present in these genera.

Scale organs.—Comparing *Phoxophrys* to *Japalura*, Inger (1960:221) wrote "all species of *Japalura* seen have

hair-like sense organs on the cephalic scales similar to those described and figured by Scortecci (1937, pl. 1) and Cherchi (1958) for species of *Agama*; this type of sense organ is absent in *Phoxophrys*." Later, Moody (1980:data matrix in his Appendix D) coded *Phoxophrys* as having hair-like sense organs. Nonetheless, Inger's remarks misled some subsequent authors (e.g., Ananjeva and Stuart 2001), who used absence of hairlike sense organs to distinguish *Phoxophrys* from all other Draconinae.

We confirm Moody's (1980) coding of this character: all species of *Phoxophrys* have hairlike sense organs like those of other Draconinae. In old specimens, the hairs may be lost along with patches of stratum corneum; however, we found at least some remaining sensillae on all specimens examined in this study.

External meristic characters.—*Phoxophrys tuberculata* can be described as a large-scaled species (Tables 2 and 3). It has fewer circumorbitals, transorbitals, subdigital lamellae, infralabials, ventrals, and scales around midbody than the Bornean species. Moreover, ranges for the last three of these characters do not even overlap ranges of the other species.

In contrast, *Phoxophrys nigrilabris* can be described as a small-scaled species. Compared to congeners, it has higher counts of circumorbitals, transorbitals, parietals, supralabials, infraorbitals from the nasal to the posterior orbital border, and scales between the nasal and postciliary scale. Ranges for each of these characters overlap those of at least one of the other species, but barely so.

Most meristic characters of *Phoxophrys cephalum*, *Ph. anolophium*, and *Ph. borneensis* overlap. Nonetheless, *Ph. cephalum* has fewer gulars than the other two species, more loreals and subdigital lamellae than *Ph. borneensis*, and more supralabials and fourth-toe lamellae within the span of Toe V than *Ph. anolophium*. *Phoxophrys anolophium* has more nuchal crest scales than either *Ph. cephalum* or *Ph. borneensis*, and more loreals than *Ph. borneensis*. This difference in nuchal crest scale count can be attributed to a higher number of paravertebrals and small vertebrals interrupting the nuchal crests of these latter two species. More scales comprise the dorsolateral crests of *Ph. borneensis* than in either *Ph. anolophium* or *Ph. cephalum*.

We did not find interspecific differences for counts of scales separating the circumorbital series, total vertebrals, postrostrals, and combined canthals and supraciliaries ($P > 0.10$).

External mensural characters.—Treating SVL as a covariate, *Phoxophrys nigrilabris* has a relatively longer shank than the other Bornean species ($F_{3,39} = 39.28$, $P < 0.001$*; Table 2). Excluding *Ph. nigrilabris*, the shank of *Ph. tuberculata* is relatively shorter than the large Bornean species ($F_{3,24} = 3.10$, $P = 0.046$) but not after correcting the probability value for multiple tests. *Phoxophrys nigrilabris* has a relatively wider head ($F_{4,42} = 3.73$, $P = 0.01$) and larger eye (orbital length; $F_{4,42} = 11.24$, $P < 0.001$*) than congeners. Both *Ph. nigrilabris* and *Ph. tuberculata* have relatively narrower snouts (log-transformed character, $F_{4,42} = 3.819$, $P = 0.010$) and shorter fifth toes ($F_{3,38} = 7.02$, $P = 0.001$*. We excluded *Ph. tuberculata* from this analysis but our conclusion is supported by the low ratios presented in Table 2) than *Ph. borneensis* and *Ph. cephalum*. We did not find interspecific differences in head length, length of Finger IV, or length of Toe IV.

11. Maximum size.—Adults attain SVL greater than 52 mm (0) or do not exceed SVL of 43 mm (1).

The six species of *Phoxophrys* can be categorized into three groups based on maximum SVL. *Phoxophrys anolophium*, *Ph. borneensis*, *Ph. cephalum*, and *Ph. spiniceps* have SVLs exceeding 59 mm, *Ph. tuberculata* does not exceed 43 mm SVL, and *Ph. nigrilabris* is intermediate in size, attaining a SVL of 53 mm. With a SVL of 80 mm, the holotype of *Phoxophrys anolophium* is the largest known female *Phoxophrys* exceeding by 5 mm the maximum known SVL of female *Ph. cephalum* (Inger 1960; Malkmus et al. 2002). At least in *Ph. borneensis* and *Ph. cephalum*, males reach larger sizes than females. Some adult male *Ph. cephalum* are the longest specimens of *Phoxophrys*, reaching a SVL of 84 mm and total length of 140 mm (Inger 1960; Malkmus et al. 2002). Apparent sexual dimorphism of maximum size may be an artifact of inadequate sampling: adult female (up to 53.3 mm, $n = 9$) and male (up to 52.2, $n = 11$) *Ph. nigrilabris* have similar maximum SVLs and the largest male *Ph. borneensis* is only 6 mm longer than the longest female.

Although still known from very few specimens, *Phoxophrys tuberculata* appears to be a tiny species. MZB 9454 with a SVL of only 29.2 mm is gravid, containing a single shelled egg in its right oviduct. Similarly, the male specimen (SVL 36.5 mm) has convoluted vasa efferentia and appears to be sexually mature. The holotype (RMNH 4140) is the largest known specimen of *Ph. tuberculata* and has a SVL of 43 mm and total length of 101 mm.

Among near outgroups, species of *Acanthosaura*, *Dendragama*, *Diploderma*, *Lophocalotes*, *Pseudocalotes*, and *Sitana* all attain maximum SVLs greater than *Ph. tuberculata*. Nonetheless, the SVLs of some *Sitana* such as *S. bahiri* (45 mm), *S. devakai* (46 mm), and *S. ponticeriana* (49 mm) only just exceed those of *Ph. tuberculata* (43 mm; Amarasinghe et al. 2015; Deepak et al. 2016). The Sri Lankan endemics *Ceratophora aspera* and *C. karu* do not exceed SVLs of 35 mm (Pethiyagoda and Manamendra-Arachchi 1998) and may be the only other draconines that are smaller than *Ph. tuberculata*.

Sexual dimorphism.—Large males of *Phoxophrys cephalum*, with their robust, pale heads, at first appear to have proportionally wider heads than females. For example, in his description of the type series of *Ph. cephalum*, Mocquard (1890:130) remarked "la tête est proportionnellement très grosse chez les màles" and Malkmus et al. (2002:247, their key to *Phoxophrys*) described the heads of male *Ph. cephalum* as "conspicuously large" and the heads of male *Ph. borneensis* as "'normal' in size." However, these assertions have never been tested, and available data suggest that they may well be illusory (Table 2; Fig. 8).

The holotype of *Phoxophrys anolophium* has a relatively wide head, 21.3% as wide as SVL. This value falls within our range for adult male *Ph. cephalum* (20.1–24.0%, 21.9 ± 1.8%, $n = 5$), leading us to question past assertions of sexual dimorphism in head width. Constrained by small sample sizes, this hypothesis can only be tested rigorously for *Ph. nigrilabris* and *Ph. borneensis*. Nonetheless, we also combined our samples of *Ph. anolophium*, *Ph. borneensis*, and *Ph. cephalum* because of phenotypic similarity among these three species.

Table 2.—Variation in selected meristic and mensural characters among four species of *Pelturagonia* and *Phoxophrys tuberculata*.

Character	*Pe. anolophium*	*Pe. borneensis*	*Pe. cephalum*	*Pe. nigrilabris*	*Ph. tuberculata*
Circumorbitals	12 or 13 ($n = 4$)	11–14 (13 ± 1, $n = 11$)	10–13 (12 ± 1, $n = 16$)	14–19 (16 ± 1, $n = 18$)	8–10 (9 ± 1, $n = 4$)
Transorbitals	17–22 (20 ± 1, $n = 4$)	15–20 (17 ± 2, $n = 12$)	15–18 (16 ± 1, $n = 15$)	20–26 (23 ± 2, $n = 20$)	13–15 (14 ± 1, $n = 4$)
Parietals	7–9 (8 ± 1, $n = 4$)	7–11 (9 ± 1, $n = 12$)	6–12 (9 ± 2, $n = 12$)	8–13 (11 ± 2, $n = 19$)	7 in male
Palpebrals	12–14 (14 ± 1, $n = 4$)	12–15 (13 ± 1, $n = 12$)	8–14 (12 ± 2, $n = 12$)	12–15 (13 ± 1, $n = 20$)	9–11 (10 ± 1, $n = 4$)
Loreals between last canthal and supralabials	6–9 (7 ± 1, $n = 4$)	4–6 (5 ± 1, $n = 13$)	5–8 (6 ± 1, $n = 16$)	4–7 (8 ± 1, $n = 20$)	4–7 (6 ± 1, $n = 4$)
Supranasals	1 (100%, $n = 4$)	1 (58%, $n = 12$) 2 or 3 (42%)	1 (86%, $n = 14$) 2 (14%)	1 (100%, $n = 19$)	1/1 in male
Nasal to postciliary	16 or 17 (16 ± 1, $n = 4$)	13–18 (15 ± 1, $n = 12$)	12–19 (15 ± 2, $n = 14$)	15–20 (17 ± 2, $n = 19$)	14/14 in male
Infraorbital series	10–12 (11 ± 1, $n = 4$)	10–12 (11 ± 1, $n = 13$)	9–13 (11 ± 1, $n = 13$)	12–16 (15 ± 1, $n = 19$)	10/11 in male
Supralabials	8 or 9 (8 ± 1, $n = 4$)	7–11 (9 ± 1, $n = 13$)	9–12 (10 ± 1, $n = 1$, $n = 15$)	9–12 (11 ± 1, $n = 20$)	8–10 (9 ± 1, $n = 4$)
Infralabials	11 or 12 (12 ± 1, $n = 4$)	10–13 (11 ± 1, $n = 13$)	10–13 (11 ± 1, $n = 15$)	10–13 (12 ± 1, $n = 20$)	8 ($n = 4$)
Gulars	31–36 (33 ± 2, $n = 4$)	26–36 (31 ± 3, $n = 12$)	23–30 (26 ± 2, $n = 15$)	29–40 (35 ± 3, $n = 20$)	25–30 (28 ± 2, $n = 4$)
Ventrals	51–58 (56 ± 3, $n = 4$)	48–63 (57 ± 5, $n = 12$)	52–62 (57 ± 3, $n = 13$)	56–68 (62 ± 4, $n = 20$)	40–49 (45 ± 4, $n = 4$)
Scales around midbody	92–109 (100 ± 8, $n = 4$)	80–113 (96 ± 9, $n = 11$)	81–115 (94 ± 8, $n = 11$)	87–107 (97 ± 6, $n = 20$)	56–67 (62 ± 5, $n = 4$)
Nuchal crest	10–12 (11 ± 1,$n = 4$)	3–8 (5 ± 2, $n = 13$)	4–8 (5 ± 1, $n = 14$)	10–17 (13 ± 2, $n = 19$)	6 ($n = 2$)
Total vertebrals	73–90 (81 ± 9, $n = 4$)	61–85 (73 ± 7, $n = 10$)	60–78 (70 ± 6, $n = 9$)	60–75 (69 ± 4, $n = 19$)	61 in male
Lamellae under Finger IV	18 or 19 ($n = 4$)	15–19 (18 ± 1, $n = 4$)	17–21 (20 ± 1, $n = 13$)	16–19 (17 ± 1, $n = 20$)	13–17 (16 ± 2, $n = 4$)
Lamellae under Toe IV	18–24 (22 ± 3, $n = 4$)	19–26 (22 ± 2, $n = 12$)	23–29 (26 ± 2, $n = 14$)	19–23 (21 ± 1, $n = 20$)	17–19 (18 ± 1, $n = 4$)
Fourth-toe lamellae within span of Toe V	1–4 (3 ± 1, $n = 4$)	2–5 (4 ± 1, $n = 12$)	3–7 (4 ± 1, $n = 14$)	1 or 2 (1 ± 0, $n = 19$)	0–2 ($n = 4$)
Maximum snout-to-vent length (SVL; mm)	Males: 42.9 Females: 79.5	Males: 68 Females: 62	Males: 76 (84, Inger 1960) Females 68	Males: 41.5 Females: 41.5	Males: 36.5 Females: 43
Head width/SVL	Male: 22.3% Females: 21.3–23.6% ($n = 3$)	Male: 20.3–23.3% (22.3 ± 1.0, $n = 7$) Females: 19.6–22.7% (21.0 ± 1.2, $n = 5$)	Males: 20.1–24.0% (21.9 ± 1.8, $n = 5$) Females: 20.0–21.4% ($n = 3$)	Males: 22.0–25.0% (23.4 ± 0.9, $n = 10$) Females: 21.7–24.2% (23.1 ± 0.7, $n = 9$)	Male: 22.8% Females: 20.6–22.5% ($n = 3$)
Head length/SVL	Male: 25.4% Females: 22.5–27.3% ($n = 3$)	Males: 24.3–27.1% (25.7 ± 1.0, $n = 7$) Females: 23.1–25.5% (24.0 ± 0.9, $n = 5$)	Males: 23.7–26.9% (25.6 ± 1.1, $n = 5$) Females: 23.0–24.8% ($n = 3$)	Males: 24.6–27.6% (25.9 ± 0.9, $n = 10$) Females: 24.6–28.4% (25.9 ± 1.1, $n = 9$)	Male: 27.8% Females: 27.4–28.5% ($n = 3$)
Tail length/total length	Male: 60.3% Females: 58.7–61.6% ($n = 3$)	Males: 58.3–63.1% (60.1 ± 1.7, $n = 7$) Females: 54.5–63.8% (59.4 ± 3.4, $n = 5$)	Males: 62.9–65.5% (64.2 ± 1.1, $n = 4$) Females: 61.1–64.6% ($n = 3$)	Males: 59.0–63.5% (61.8 ± 1.3, $n = 10$) Females: 60.0–63.5% (62.1 ± 1.3, $n = 9$)	Male: 58.8% Females: 57.4–61.5% ($n = 3$)
Body length/SVL	Male: 46.2% Females 47.2–48.9% ($n = 3$)	Males: 36.5–52.0% (45.5 ± 6.3, $n = 6$) Females: 47.6–52.0% (49.7 ± 2.0, $n = 4$)	Males: 38.5–49.6% (46.5 ± 5.3, $n = 4$) Females: 48.8–53.0 ($n = 3$)	Males: 41.8–57.4% (48.4 ± 4.2, $n = 10$) Females: 40.5–54.6% (46.8 ± 4.6, $n = 9$)	Males: 52.1% Females: 47.7–51.4% ($n = 2$)
Length of shank/SVL	Male: 21.4% Females: 22.4–24.3% ($n = 3$)	Males: 22.2–26.1% (24.3 ± 1.4, $n = 7$) Females: 21.7–27.4% (23.4 ± 2.3, $n = 5$)	Males: 20.6–24.2% (22.6 ± 1.4, $n = 5$) Females: 18.3–23.3 ($n = 3$)	Males: 27.8–31.3% ($n = 29.6 \pm 1.2$, $n = 10$) Females: 27.8–31.6% (29.6 ± 1.5, $n = 9$)	Male: 19.4% Females: 19.4–23.1% ($n = 10$
Length of orbit/SVL	10.3–13.7% (12.3 ± 1.4, $n = 4$)	10.5–13.1% (11.5 ± 1.0, $n = 12$)	9.6–12.9% (11.4 ± 1.0, $n = 9$)	10.8–15.7% (13.3 ± 1.1, $n = 20$)	9.7–11.7% (10.8 ± 0.9, $n = 4$)
Width of snout/SVL	6.8–8.8% (8.2 ± 1.0, $n = 4$)	7.5–9.6 (8.8 ± 0.6, $n = 12$)	8.3–9.7% (8.8 ± 0.4, $n = 9$)	7.3–9.1% (8.3 ± 0.5, $n = 20$)	7.4–8.7% (7.8 ± 0.6, $n = 4$)
Toe V/SVL	10.3–13.0 (12.0 ± 1.2, $n = 4$)	9.9–13.0% (11.5 ± 1.0, $n = 12$)	9.7–13.3 (11.6 ± 1.1, $n = 9$)	9.6–12.0% (10.8 ± 7.8, $n = 18$)	10.3–10.5% ($n = 3$)

TABLE 3.—Summary of all possible comparisons among samples of four species of *Pelturagonia* and *Phoxophrys tuberculata*. In the upper half of the table, we report Tukey statistics and probabilities for comparisons that satisfied assumptions of normality and homoscedasticity. In the lower half, we report nonparametric comparisons: a Mann–Whitney *U* statistic and Bonferroni-corrected probabilities for samples of each species. Sample sizes of each test appear in Table 2. NS = not significant. For emphasis, we set significant results in bold font, and we add an asterisk to probabilities that are still significant when multiplied by 28, the number of mensural and meristic characters used in this study.

	Results of Tukey's test (*Q*, *P*)			
Character	*Pe. anolophium*	*Pe. borneensis*	*Pe. cephalum*	*Pe. nigrilabris*
Infraorbitals				
Pe. borneensis	0.57, NS			
Pe. cephalum	0.76, NS	1.93, NS		
Pe. nigrilabris	**9.45, 0.000***	**13.54, 0.000***	**15.65, 0.000***	
Supralabials				
Pe. borneensis	2.92, NS			
Pe. cephalum	**4.35, 0.03**	2.05, NS		
Pe. nigrilabris	**7.79, 0.000***	**7.28, 0.000***	**5.32, 0.004**	
Ph. tuberculata	1.68, NS	0.85, NS	2.25, NS	**5.62, 0.002**
Nasal to postciliary				
Pe. borneensis	2.20, NS			
Pe. cephalum	4.52, NS	0.40, NS		
Pe. nigrilabris	0.95, NS	**4.86, 0.007**	**5.54, 0.002**	
Gulars				
Pe. borneensis	2.06, NS			
Pe. cephalum	**6.22, 0.001***	**5.97, 0.001***		
Pe. nigrilabris	1.44, NS	**5.41, 0.003**	**12.55, 0.000***	
Ph. tuberculata	4.00, NS	2.84, NS	1.19, NS	**6.60, 0.000***
Ventrals				
Pe. borneensis	1.12, NS			
Pe. cephalum	1.07, NS	0.09, NS		
Pe. nigrilabris	**4.53, 0.019**	**5.03, 0.007**	**5.26, 0.005**	
Ph. tuberculata	**5.36, 0.004**	**7.68, 0.000***	**7.67, 0.000***	**11.45, 0.000***
Nuchal crest				
Pe. borneensis	**9.08, 0.000***			
Pe. cephalum	**9.44, 0.000***	0.409, NS		
Pe. nigrilabris	2.83, NS	**18.76, 0.000***	**19.62, 0.000***	
Scales around midbody				
Pe. borneensis	1.35, NS			
Pe. cephalum	2.28 NS	1.32, NS		
Pe. nigrilabris	1.07, NS	0.54, NS	1.91, NS	
Ph. tuberculata	**11.59, 0.000***	**12.69, 0.000***	**10.8, 0.000***	**13.89, 0.000***
Dorsolateral caudal crests				
Pe. borneensis	**4.09, 0.029**			
Pe. cephalum	0.77, NS	**6.99, 0.000***		
Pe. nigrilabris	1.98, NS	3.45, NS	**4.24, 0.022**	
Lamellae under Finger IV				
Pe. borneensis	1.88, NS			
Pe. cephalum	2.69 NS	**6.63, 0.000***		
Pe. nigrilabris	2.92, NS	1.41, NS	**8.96, 0.000***	
Ph. tuberculata	**5.03, 0.007**	**4.28, 0.031**	**8.96, 0.000***	3.57, NS
Fourth-toe lamellae within span of Toe V				
Pe. borneensis	2.21, NS			
Pe. cephalum	**4.18, 0.025**	2.78, NS		
Pe. nigrilabris	**4.59, 0.011**	**10.31, 0.000***	**13.9, 0.000***	
	Results of Mann–Whitney test (*U*, Bonferroni-corrected *P*)			
Character	*Pe. anolophium*	*Pe. borneensis*	*Pe. cephalum*	*Pe. nigrilabris*
Transorbitals				
Pe. borneensis	9.5, NS			
Pe. cephalum	4.5, NS	49, NS		
Pe. nigrilabris	14, NS	**0.5, 0.000***	**0, 0.000***	
Ph. tuberculata	0, NS	1, NS	**2.5, 0.048**	**0, 0.020**
Circumorbitals				
Pe. borneensis	21.5, NS			
Pe. cephalum	20, NS	60.5, NS		
Pe. nigrilabris	**0, 0.022**	**4, 0.000***	**0, 0.000***	
Ph. tuberculata	0, NS	**0, 0.032**	**1, 0.038**	**0, 0.021**
Parietals				
Pe. borneensis	15, NS			
Pe. cephalum	21.5, NS	64.5, NS		
Pe. nigrilabris	**4.5, 0.040**	**34.5, 0.007**	**44.5, 0.028**	
Loreals (last canthal–supralabial)				
Pe. borneensis	**1, 0.018**			
Pe. cephalum	22, NS	**32, 0.006**		
Pe. nigrilabris	26.5, NS	**1.5, 0.000***	**58, 0.008**	
Ph. tuberculata	4.5, NS	13, NS	26, NS	9.5, NS

TABLE 3.—Continued.

Character	Results of Mann–Whitney test (*U*, Bonferroni-corrected *P*)			
	Pe. anolophium	*Pe. borneensis*	*Pe. cephalum*	*Pe. nigrilabris*
Palpebrals				
Pe. borneensis	16, NS			
Pe. cephalum	6.5, NS	28.5, NS		
Pe. nigrilabris	27.5, NS	113.5, NS	54.5, NS	
Ph. tuberculata	0, NS	**0, 0.035**	7.5, NS	**0, 0.015**
Lamellae under Toe IV				
Pe. borneensis	21, NS			
Pe. cephalum	5, NS	**21.5, 0.013**		
Pe. nigrilabris	31.5, NS	89, NS	**3, 0.000***	
Ph. tuberculata	2.5, NS	1, NS	**0, 0.032**	**1, 0.023**

We did not find head-width sexual dimorphism in *Ph. nigrilabris* ($F_{1,17} = 0.69$, $P = 0.421$), *Ph. borneensis* ($F_{1,9} = 3.08$, $P = 0.113$), or in our combined samples of *Ph. anolophium*, *Ph. borneensis*, and *Ph. cephalum* ($F_{1,23} = 2.98$, $P = 0.098$). As for head width, we did not detect sexual dimorphism in tail length, body length, or length of the shank (ANCOVA $P > 0.20$), when treating SVL as a covariate in *Ph. borneensis* or *Ph. nigrilabris*. Male *Ph. borneensis* have proportionately longer heads ($F_{1,9} = 14.24$, $P = 0.004$) than females, but we did not find a similar difference in *Ph. nigrilabris*.

Male ($n = 7$) *Phoxophrys borneensis* appear to have more ventrals than females ($n = 5$), although our comparison was just nonsignificant ($t = 2.15$, $P = 0.057$). We did not detect intersexual differences in counts of nuchal crest scales or total vertebrals in this species ($P > 0.12$). Comparing males ($n = 10$) to females ($n = 9$) of *Ph. nigrilabris*, we did not find intersexual differences in numbers of ventrals, nuchal crest scales, dorsal crest scales, or total vertebrals ($P > 0.2$).

Coloration.—The species of *Phoxophrys* are cryptically colored: primarily brown and green with transverse bands on the body, limbs, and tail (Fig. 1). Usually, the most prominent band crosses the neck, is widest paravertebrally, and extends ventrally behind the antehumeral fold. Facial pattern invariably includes a white, yellow, or pale saffron subocular stripe or blotch, extending from the eye to the first elongate scale edging the rictal fold. This subocular stripe and scales of the orbito-tympanic series usually abut a darkly pigmented area on the lower side of the head. However, this region is pale green like the rest of the head in adult male *Ph. cephalum*. All species have pale blue buccal epithelia and lack the bright yellow or orange buccal pigment diagnostic of some species of *Dendragama*, *Lophocalotes*, and *Pseudocalotes* (Harvey et al. 2014, 2017a, 2018). *Phoxophrys* also lacks the extensive black peritoneal pigmentation characteristic of most draconines (Harvey et al. 2014, 2017a, 2018).

Both sexes of *Phoxophrys borneensis* have prominent charcoal stripes extending posteriorly and medially across the throat (Fig. 7). In contrast, the holotype and one

TABLE 4.—Matrix of character states for five species of *Pelturagonia*, *Phoxophrys tuberculata*, and outgroup species. "Near Outgroups" appear in first half of table. na = not applicable.

Species	Characters																											
	1	2	3	4	5	6	7	8	9	10	11	12	13	14	15	16	17	18	19	20	21	22	23	24	25	26	27	28	29
Pe. anolophium	0	0	0	1	B	1	0	1	B	0	0	1	0	B	B	B	A	1	1	0	0	0	1	1	1	1	B	1	1
Pe. borneensis	0	0	0	1	B	1	0	1	A	0	0	1	0	B	A	A	A	1	0	0	0	0	0	1	1	1	B	1	1
Pe. cephalum	0	0	0	1	A	1	0	1	A	1	0	1	0	B	B	A	A	1	0	0	0	0	1	1	1	1	B	1	1
Pe. nigrilabris	1	0	0	1	B	0	1	1	A	0	0	1	0	B	B	A	A	2	0	1	1	1	0	1	1	0	A	1	1
Pe. spiniceps	0	1	0	1	B	1	0	1	B	0	0	1	0	B	B	B	A	1	0	0	0	0	1	1	B	1	B	1	1
Ph. tuberculata	1	0	1	0	B	0	0	0	na	0	1	1	1	B	1	A	B	2	0	0	0	0	0	1	A	0	A	0	A
Outgroup Node	0	0	0	0	?	0	0	0	?	0	0	0	0	?	?	?	?	0	0	0	0	0	0	0	?	0	?	0	0
Lophocalotes	0	0	0	0	A	0	0	0	na	0	0	0	0	A	A	A	B	0	0	0	0	0	0	0	B	0	B	0	B
Dendragama	0	0	0	0	B	0	0	0	na	0	0	0/1	0	A	B	B	B	0/1	0/1	0	0	0	0	0	B	0	A	0	A
Diploderma splendidum	0	0	0	0	B	0	0	0	na	0	0	0	0	B	B	B	A	1	0	0	0	0	1	0	A	0	A	1	B
Pseudocalotes floweri	0	0	0	0	A	0	0	0	na	0	0	0	0	A	B	A	A	0	0	0	0	0	0	0	A	0	A	0	B
Pseudocalotes kingdonwardi	0	0	0	0	A	0	0	0	na	0	0	0	0	A	B	A	A	0	0	0	0	0	0	0	B	0	A	0	1
Sitana	0	0	0	0	0	0	0	0	na	0	0	0	0	B	B	A	A	0	0	0	0	0	0	0	A	1	A	0	B
Acanthosaura armata	0	0	0	0	A	0	1	0	na	0	0	0	0	A	B	na	A	0	0	0	0	0	0	1	A	0	A	0	B
Acanthosaura crucigera	0	0	0	0	A	0	1	0	na	0	0	0	0	A	1	na	A	0	0	0	0	0	0	1	B	0	A	0	B
Calotes mystaceus	0	0	0	0	A	0	0	0	na	0	0	0	1	B	B	na	A	0	0	0	0	0	0	0	B	0	A	0	B
Aphaniotis acutirostris	0	0	0	0	A	0	0	0	na	0	0	0	0	A	B	A	A	0	0	0	1	0	0	0	A	0	A	0	1
Draco sumatranus	0	0	0	0	A	1	0	0	na	0	0	0	0	A	A	A	A	0	0	0	0	1	1	0	A	0	A	1	B
Bronchocoela hayeki	0	0	0	1	A	0	0	0	na	0	0	0	0	A	A	B	A	0	0	0	0	0	1	0	B	0	A	0	B
Gonocephalus grandis	0	0	0	0	A	0	1	0	na	1	0	0	0	A	B	A	A	1	0	0	2	0	1	0	B	0	A	0	B
Ptyctolaemus collicristatus	0	0	0	0	A	0	0	0	na	0	0	0	0	B	B	A	A	0	0	0	0	0	0	0	A	0	B	0	B
Salea anamallayana	0	0	0	0	A	0	0	0	na	0	0	1	0	B	B	A	A	0	0	0	0	0	0	0	B	0	A	0	B
Lyriocephalus scutatus	0	0	0	1	A	1	0	0	na	0	0	0	0	A	B	B	A	1	0	0	0	0	1	0	B	0	A	1	1
Ceratophora stoddartii	0	0	0	1	A	1	0	0	na	1	0	1	0	B	B	B	A	2	0	0	0	0	0	0	B	0	A	1	B
Cophotis ceylanica	0	0	0	1	A	0	0	0	na	0	0	1	0	B	B	B	A	0	0	0	0	0	0	0	A	0	A	1	B

FIG. 8.—Ventral coloration of adult male *Pelturagonia borneensis*, illustrating black lines in gular region and greenish coloration of enlarged subcaudals. From left to right, specimens are NMW 20854-3, 20854-1, 20854-7, and 20854-5 (SVL of NMW 20854-5 is 59 mm). A color version of this figure is available online.

paratype of *Ph. anolophium* (MZB 14993) have some pale saffron tubercles laterally, but their throats are otherwise immaculate. Throats of the other two paratypes have heavy charcoal mottling, but the dark pigment does not form regular stripes.

Dorsal coloration will immediately distinguish adult male *Phoxophrys borneensis* from male *Ph. cephalum*. Male *Ph. borneensis* are very dark green (dark blue in preservative) with narrow yellow bands (white in preservative; 1–2 dorsals long and including enlarged tubercles), whereas male *Ph. cephalum* are light green (pale blue or gray in preservative) with narrow, dark brown chevrons (black edged, dark blue, or brown scales in preservative). Male *Ph. cephalum* have pale green or pale gray heads, immaculate except for few scattered dark green spots and lacking obvious lines radiating across the palpebrals. In contrast, male *Ph. borneensis* have dark green heads with large yellow blotches and bands edged in black (white in preservative) and black-edged bands radiating out from the ocular aperture across the palpebrals and sides of the head. We have not seen enough female specimens in life to propose color characters to distinguish these two species.

All *Phoxophrys* have a distinct stripe extending from an outward bulge produced by the epiphyseal tuberosity of the ilium down to the insertion of the leg. This stripe is white, yellow, or pale saffron and edged in black in all species except *Ph. tuberculata*, where it is entirely black or absent altogether. The stripe covers enlarged scales that armor the ilium.

Dermatocranial Roofing Bones

12. Pineal foramen.—The pineal foramen is present (0) or completely absent (1).

The species of *Phoxophrys* lack a pineal foramen and have extensive sculpturing of the frontal and parietal bones, including along their sutures. Among other Sunda Shelf draconines, we observed loss of the pineal foramen in *Dendragama* where this character varies within the genus. *Dendragama schneideri* has a small foramen, whereas *D. australis*, *D. boulengeri*, and *D. dioidema* lack a pineal foramen.

Our coding of this character differs from that of Moody (1980). For his Character 16, Moody (1980) assigned State 1 to both *Dendragama* and *Phoxophrys*; however, he defined this state as "tiny pinhole or occluded." Thus, defined more broadly, Moody (1980) also reported a pinhole or occluded pineal foramen in *Ceratophora*, *Cophotis*, *Coryphophylax*, *Draco volans*, *Gonocephalus chamaeleontinus*, *Lophocalotes*, *Lyriocephalus*, and *Pseudocalotes*. Our specimens of *Ceratophora*, *Cophotis*, and *Salea* lack a pineal foramen. Our female specimen of *Lyriocephalus* has a tiny foramen and the male has a relatively large foramen. All remaining outgroup taxa have a pineal foramen.

13. Transverse shortening of the prefrontal and frontal–nasal contact.—In dorsal aspect, the prefrontal bone separates the nasal and frontal (0) or a narrow anterior process of the frontal extends medial to the prefrontal to contact the nasal (1).

The prefrontal of *Phoxophrys tuberculata* is modified in two ways relative to congeners. It forms a prominent triangular projection dorsolaterally, evidently to support the modified supercilium of this species. In congeners, a small knoblike process of the prefrontal extends the canthus for a short distance into the orbit. Medially, the prefrontal appears to be somewhat shortened relative to congeners. In our two skulls of *Ph. tuberculata*, a narrow process of the frontal separates the nasal from the prefrontal and contacts the facial process of the maxilla, whereas the nasal and prefrontal contact one another in all other congeners. Among other Draconinae examined, the frontal separates the nasal and prefrontal only in *Calotes mystaceus*.

The frontal of *Phoxophrys* resembles that of most draconines. Compared to congeners, *Ph. nigrilabris* has a narrower frontal, as reflected by its low frontal width/length ratio (34.3–34.5% vs. 45.0–57.8% in other *Phoxophrys*). We cannot say whether the narrow frontal of this species is apomorphic, however, because relative frontal width varies widely among draconines (26.5–61.1%). *Acanthosaura*, *Diploderma*, *Gonocephalus*, *Pseudocalotes*, and *Sitana* all contain species with frontals as narrow as or narrower than that of *Ph. nigrilabris*. Bony extensions of the frontal along the ocular margin support the highly modified supercilium of this species, and presence of these extensions makes the frontal of *Ph. tuberculata* substantially more concave than the frontals of congeners.

Circumorbital Bones and Temporal Arcade

Relative width of supratemporal fossa.—Compared to other agamids, the species of *Phoxophrys* have relatively narrow supratemporal fossae (ANCOVA of width vs. length of fossa $F_{33} = 9.06$, $P = 0.005$), although relative dimensions of the fossa overlap substantially with species in other draconine genera. Width of the supratemporal fossa is 51.2–70.9% of its length in *Phoxophrys* compared to 53.5–84.3% in other genera examined.

14. Erosion of the prefrontal below the lacrimal canal.—The prefrontal forms the ventral border of the lacrimal canal (A) or it is eroded below the canal so that the palatal shelf of the maxilla forms the canal's ventral border (B).

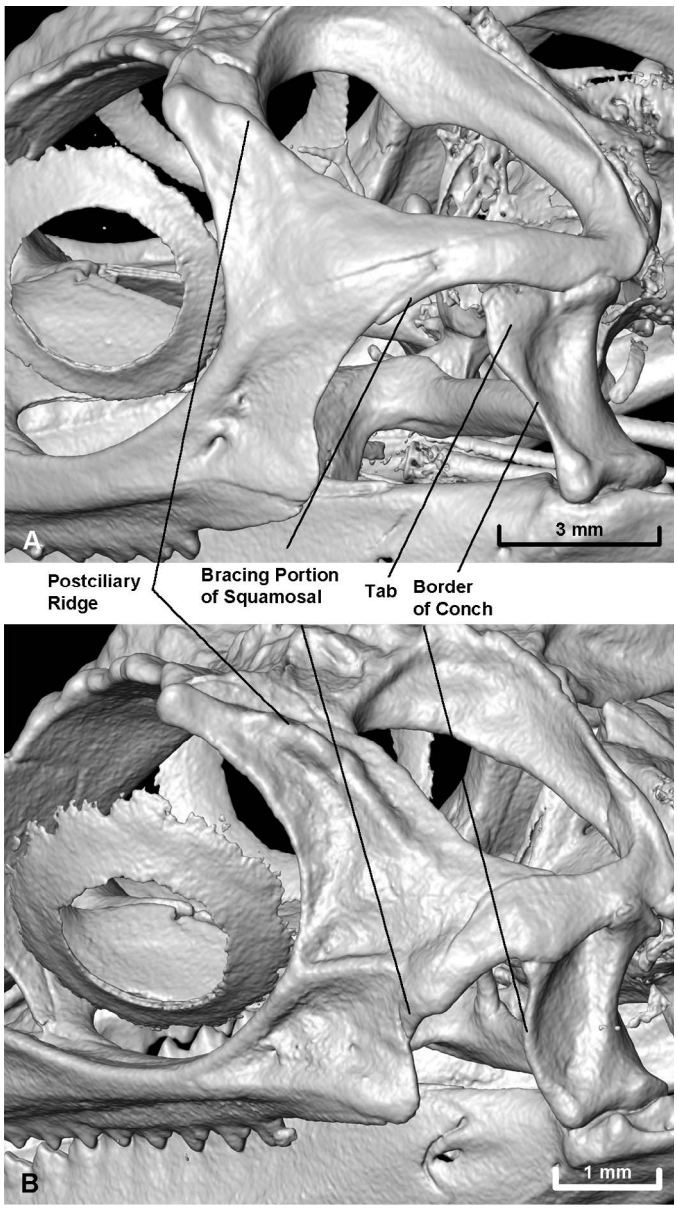

FIG. 9.—Morphology of the temporal arcade and conch of the quadrate in *Pelturagonia anolophium* (A, MZB 14992) and *Phoxophrys tuberculata* (B, UTA 65254). Skulls illustrated in lateral aspect and rotated slightly ventrally.

Like many agamids (Siebenrock 1895; Moody 1980), the species of *Phoxophrys* lack a lacrimal bone and have a relatively large lacrimal canal. Moody (1980) included this character in his study of agamid relationships. Complete erosion of the prefrontal further enlarges the lacrimal canal in *Phoxophrys*, so that the canal extends to the palatal shelf of the maxilla. Among outgroups, we observed this condition in *Calotes*, *Cophotis*, *Ceratophora*, *Diplodema*, *Ptycholaemus*, *Salea*, and *Sitana*, whereas the prefrontal forms the ventral portion of the canal in other genera examined in this study. Notably, the prefrontal forms the ventral border of the lacrimal canal in Sunda Shelf species other than *Phoxophrys* and *Calotes*. Although this character may contain phylogenetic signal within the Draconinae, it is invariate within *Phoxophrys* and both states occur in near outgroups of the genus.

15. Anterior extent of squamosal in lateral aspect.—In lateral aspect, the squamosal abuts the jugal (A), extends for a short distance horizontally below the jugal (B) or the squamosal extends anteriorly below the jugal and curves ventrally to brace against the vertical posterior margin of the jugal (1).

Posteriorly, the jugal is nearly vertical before it curves backward to contribute to the temporal arch (Fig. 9). In the temporal arch, this bone laterally overlaps the anterior end of the squamosal. The squamosal extends furthest anteriorly on the medial side of the jugal; nonetheless, a portion of the squamosal braces the jugal ventrally in most draconines (Fig. 9). This bracing portion is short, narrow, and horizontal in *Phoxophrys anolophium*, *Ph. cephalum*, *Ph. nigrilabris*, and *Ph. spiniceps*. *Phoxophrys tuberculata* has a substantially broader and longer bracing portion, extending below the jugal and curving ventrally to brace against the vertical posterior margin of the jugal. At the other extreme, *Ph. borneensis* lacks a bracing portion of the squamosal below the jugal, and the squamosal and jugal abut one another in lateral aspect.

Most outgroup species have short, narrow bracing portions, resembling those of most Bornean *Phoxophrys*. Like *Ph. borneensis*, *Bronchocoela hayeki*, *Draco sumatranus*, and both species of *Lophocalotes* lack bracing portions, and the jugal and squamosal abut one another in these species. *Phoxophrys tuberculata* has the most robust bracing portion of any draconine. Among the various outgroup species, only the bracing portion of *Acanthosaura crucigera* is comparable. As in *Ph. tuberculata* the bracing portion of this species reaches the vertical portion of the jugal.

16. Postorbital process of frontal and postciliary ornament.—A lateral process of the frontal is separated from the postciliary ornament (A) or reaches the postciliary ornament (B).

A rounded knob on the postorbital bone, hereafter referred to as the postciliary ornament, lies at the dorsoposterior border of the orbit in all *Phoxophrys* (Fig. 10). The postciliary scale named by Harvey et al. (2017a) overlays this ornament. In *Ph. anolophium*, *Ph. spiniceps*, and *Ph. tuberculata* a postorbital process of the frontal reaches this ornament laterally, whereas a sizable gap separates the process and ornament in *Ph. borneensis*, *Ph. cephalum*, and *Ph. nigrilabris*.

Among outgroups, the postorbital process of the frontal reaches the postciliary ornament in *Bronchocoela*, *Dendragama*, *Diploderma*, and the Sri Lankan endemics, whereas a gap separates the distal end of the process from the postciliary ornament in the remaining species (this character is not applicable to *Acanthosaura armata*, *A. crucigera*, and *Calotes mystaceus*, all of which lack postciliary ornaments).

17. Orientation of postorbital process of frontal.—The postorbital process of the frontal is oriented transversely (A) or angled antero-laterally because of substantial expansion of the postorbital above the orbit (B).

The postorbital extends substantially above the orbit in *Phoxophrys tuberculata* so that the postorbital process of the frontal is angled antero-laterally, whereas this process is transversely oriented in the remaining species and the postorbital does not extend above the orbit. Like *Ph. tuberculata*, the two species of *Lophocalotes* and five species

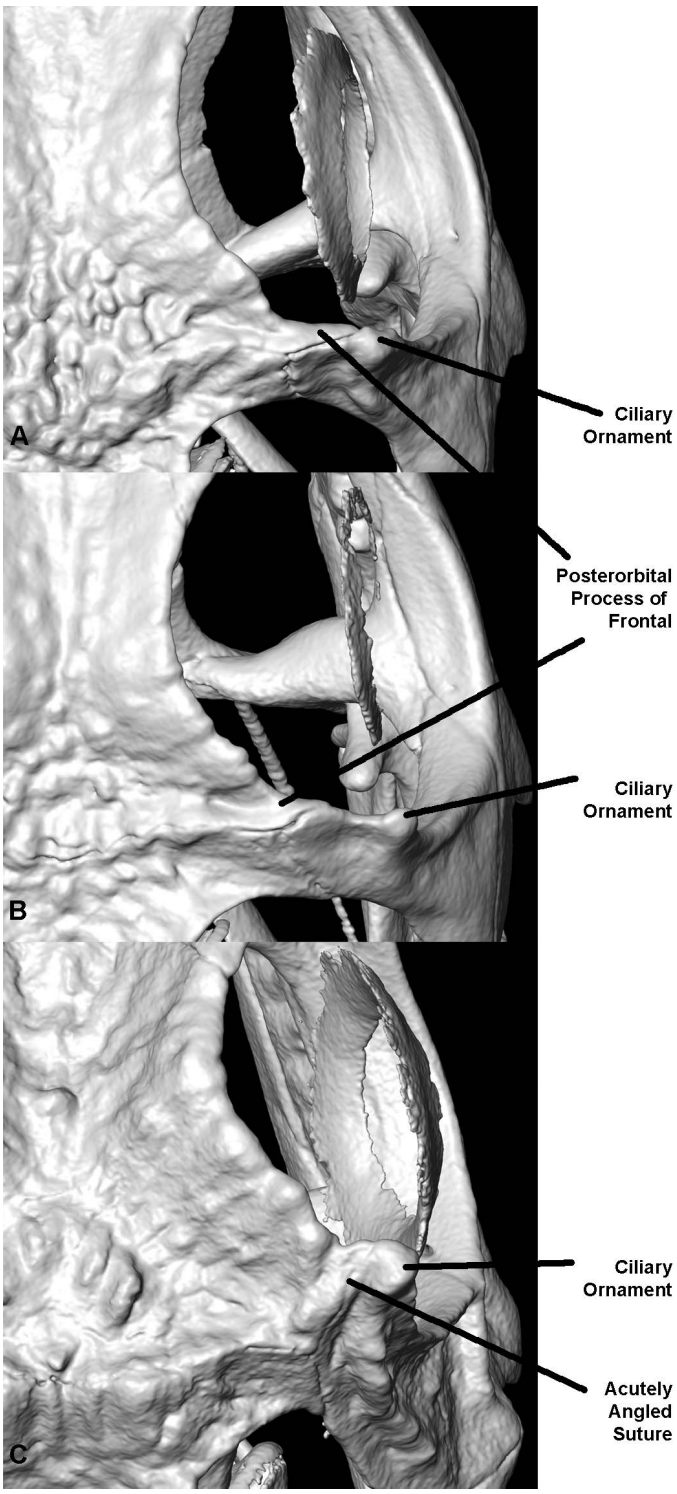

FIG. 10.—Shape of the postorbital process of the frontal and morphology of the postciliary ornament in *Pelturagonia anolophium* (A, MZB 14992), *Pe. borneensis* (B, FMNH 71856), and *Phoxophrys tuberculata* (C, UTA 65254). Skulls shown in dorsal aspect.

of *Dendragama* have antero-laterally angled postero-lateral processes of the frontal, whereas this process is straight in the remaining outgroups.

18. Postciliary bony ridge.—A bony ridge on the postorbital is absent, inconspicuous, or very short (0); extends from the postciliary ornament to the ventral margin of the supratemporal fossa (1); or curves ventrad to extend vertically down the postorbital (2).

Phoxophrys anolophium, *Ph. borneensis*, *Ph. cephalum*, and *Ph. spiniceps* have a relatively short ridge of bone, extending from the postciliary ornament to the temporal fossa and contributing to the ventral border of this fossa. In contrast, the ridge curves ventrad and is relatively long in *Ph. nigrilabris* and *Ph. tuberculata*. In these two species, the ridge does not reach the temporal fossa, although it closely approximates the fossa in the holotype of *Japalura robinsoni*.

Most draconines either lack postciliary ridges or have ridges that reach the temporal fossa. Among our outgroups, only *Ceratophora* has a prominent postciliary ridge that curves ventrad like the ridges of *Ph. nigrilabris* and *Ph. tuberculata*.

Otoccipital Region of Braincase

19. Ossification of parasphenoid.—The parasphenoid is ossified (0) or the floor and cultriform process of the parasphenoid are membranous (1).

The large holotype of *Phoxophrys anolophium* has ossified trabeculae communis but a membranous hypophyseal floor and cultriform process of the parasphenoid, whereas all three elements are ossified in congeners. Among outgroups, we observed this trait in both specimens of *Dendragama australis* and in the male of *D. boulengeri*. All four specimens with this character are large adults, and the membranous portions of the parasphenoid cannot simply be ascribed to ontogenetic variation.

20. Reduction of lateral aperture of recessus scali tympani.—The area of the lateral aperture of the recessus scali tympani is more than 21% as large as the fenestra ovalis (0) or it is less than 19% as large (1).

Phoxophrys nigrilabris (Fig. 11) has a noticeably reduced lateral aperture to the recessus scali tympani. In congeners, the lateral aperture is 42–94% as large as the fenestra ovalis, whereas it is only 17–18% as large in *Ph. nigrilabris*. On the other hand, the medial aperture of the recessus has a size comparable to other agamids. Consequently, the ratio of the area of the medial to the lateral aperture is 74–75% in *Ph. nigrilabris*, but only 11–27% in congeners and 22–63% in other agamid genera.

21. Erosion of crista interfenestralis and base of tuber of the otoccipital.—The crista interfenestralis is eroded below the recessus scali tympani and does not extend onto the base of the tuber of the otoccipital (0), or it extends onto the tuber to merge with the crista tuberalis (1).

In all *Phoxophrys*, the crista tuberalis extends onto to the posterolateral face of the tuber. However, the crista interfenestralis does not extend to the tuber in any *Phoxophrys* except *Ph. nigrilabris*. In *Ph. nigrilabris*, the crista interfenestralis extends as a narrow lamina to the anterior base of the tuber, and the crista tuberalis crosses the lateral face of the tuber to merge with the crista interfenestralis. Between the confluence of these two cristae and the ventral margin of the aperture of the recessus scali tympani, the basioccipital is excavated in *Ph. nigrilabris*, leaving an elongate depression extending from the aperture of the recessus antero-ventrally to the base of the tuber.

Among outgroups, the crista interfenestralis extends onto the tuber in *Aphaniotis acutirostris*; however, this species has a relatively large lateral aperture of the recessus scali

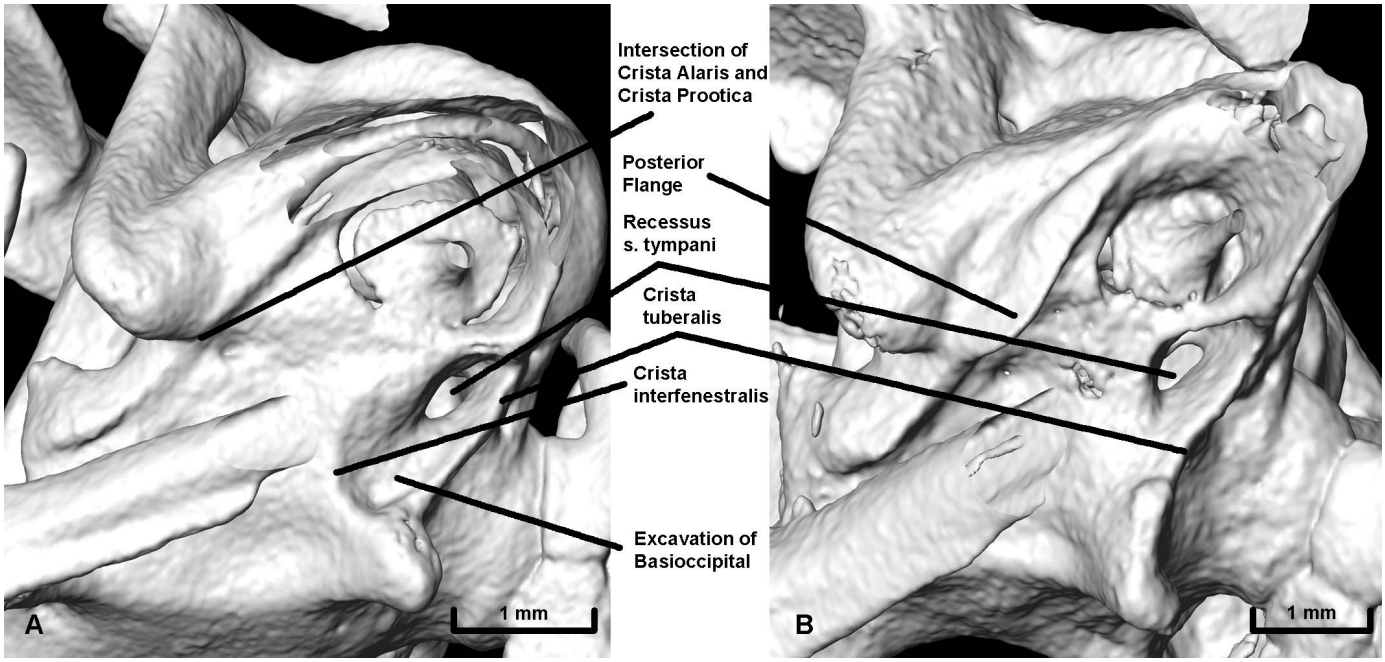

FIG. 11.—Several characters of the otoccipital region of the braincase of *Pelturagonia nigrilabris* (A, FMNH 269084) and *Pe. anolophium* (B, MZB 14992). Skulls oriented slightly ventro-posterior to lateral with bones of maxillary arcade removed.

tympani and lacks the distinctive excavation of the basioccipital. In *Lyriocephalus scutatus*, the crista interfenestralis extends to the crista tuberalis, but these cristae join just below the recessus scali tympani rather than at the base of the tuber as in *Ph. nigrilabris*. As for *A. acutirostris*, this species also lacks the excavation of the basioccipital. Below a relatively elongate recessus in *Gonocephalus grandis*, shallow excavation of the basioccipital extends onto the tuber proximally; however, the crista interfenestralis is eroded in this species as in *Phoxophrys* other than *Ph. nigrilabris*.

22. Merger of crista alaris and crista prootica.—A distinct gap separates the cristae alaris and prootica (0) or these two cristae merge with one another (1).

In *Phoxophrys nigrilabris*, the crista alaris merges seamlessly with the crista prootica (Fig. 11), whereas in most other agamids, the crista alaris approaches the crista prootica, but does not merge with it. Among outgroups examined in this study, the cristae alaris and prootica merge only in *Draco sumatranus*.

23. Lateral flaring of crista prootica behind crista alaris.—Except for a broad excavation below the crista alaris, the crista prootica is straight (0) or flared behind the crista alaris (1).

The crista prootica of *Phoxophrys nigrilabris* is noticeably reduced relative to other agamids, consisting of merely a low, straight ridge. The crista prootica is shelflike and roofs a distinct groove (i.e., the recessus vena jugularis, *sensu* Oehrich 1956) in all other agamids examined by us. Below the crista alaris, the crista prootica bears a broad excavation in most agamids. All *Phoxophrys* except *Ph. nigrilabris* have the excavation below the crista alaris, but development of the shelf varies somewhat among specimens. The holotype of *Ph. anolophium*, male specimen of *Ph. cephalum*, and holotype of *Ph. spiniceps* have conspicuous latero-ventral flaring (i.e., expansion) of the crista prootica both behind and in front of the excavation, whereas the female *Ph. cephalum* only has conspicuous flaring behind the crista alaris. The males of *Ph. borneensis* and *Ph. tuberculata* lack conspicuous expansions and their cristae prootica are straight except for the excavation.

Among outgroups, the crista prootica flares outward behind the crista alaris in *Diploderma spendidum*, *Draco sumatranus*, *Bronchocoela hayeki*, *Gonocephalus grandis*, and *Lyriocephalus scutatus*.

Palatal Bones and Teeth

Maxillary foramina.—The Bornean *Phoxophrys* have three maxillary foramina in the facial process, whereas *Ph. tuberculata* has only two. Nonetheless, we chose not to code this character for the following reasons. Among other draconines, our counts of these foramina range from one to five and show considerable variation both among and within genera. Counts are also polymorphic in some species. For example, our specimens of *Dendragama australis* have one foramen, whereas *D. boulengeri* and *D. schneideri* have three foramina. The trait is polymorphic in *D. dioidema*: the male specimen has two foramina and the female has one. Finally, small foramina are not always well resolved in CT scans, and some counts in our data may be artifacts of poor scan quality.

Elongation and narrowing of pterygoid.—Compared to other draconines, the species of *Phoxophrys* have relatively long and narrow pterygoids ($F_{1,31} = 28.11$, $P = 0.000$*; Fig. 12). In *Phoxophrys* the pterygoids are 56.1–64.7% of skull length (the female *Ph. cephalum* is the only specimen with pterygoids less than 60% as long as the skull). Among the various species we examined, relative pterygoid lengths of four species fell within the range of *Phoxophrys*: *Acanthosaura crucigera* (56.3%), *Draco sumatranus* (58.0%), *Sitana ponticeriana* (58.6%), and *Lyriocephalus scutatus*

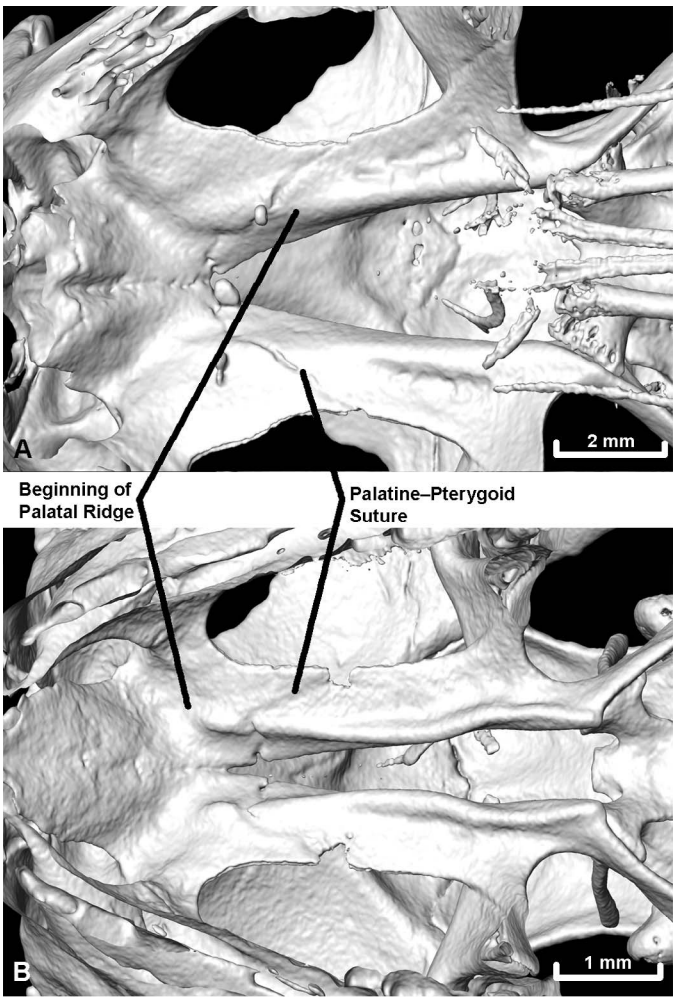

FIG. 12.—Palatal morphology of *Pelturagonia anolophium* (A, MZB 14992) and *Phoxophrys tuberculata* (UTA 65254) illustrating anterior extent of the palatal ridge relative to the palatine–pterygoid suture. Skulls shown in ventral aspect with mandible and hyoid apparatus removed.

(61.6%), whereas the remaining draconines had pterygoids 47.1–55.8% as long as head length.

24. Narrowing of alveolar portion of premaxilla.—The premaxilla is more than 11% of head width and bears three or more teeth (0), or it is less than 10% of head width and bears a single tooth or a large single tooth flanked by a pair of much smaller teeth (1).

In *Phoxophrys*, the alveolar portion of the premaxilla is reduced relative to other draconines. Measured in alveolar view, the premaxilla is 2.8–9.6% of head width. *Acanthosaura* has a comparable ratio of 7.8–11.0%, whereas remaining draconines have premaxillae 11.1–21.7% of skull width.

The narrow premaxillae of *Phoxophrys* frequently have a single large pleurodont tooth. Nonetheless, the holotypes of both *Ph. spiniceps* and *Japalura robinsoni* have a very small tooth on either side of the large medial tooth. The female of *Ph. cephalum* has two small teeth on its premaxilla, but lacks a large medial pleurodont tooth.

After returning most specimens to museums, we attempted to count premaxillary teeth on whole specimens. Many of the FMNH specimens of *Ph. nigrilabris* were preserved with their mouths open and the premaxilla could be examined by gently pressing on the upper lip of others. Among 12 of these *Ph. nigrilabris*, the premaxillae of 10 have three teeth, one has a single large pleurodont tooth, and one has two very small teeth separated by a gap where the large medial tooth would normally be. Of the 10 with three teeth, all except 1 (FMNH 147657) resemble the holotypes of *Ph. spiniceps* and *Japalura robinsoni* in having a large medial pleurodont tooth flanked on either side by a single tiny tooth. FMNH 147657 has three premaxillary teeth that are subequal in size but somewhat smaller than the medial pleurodont tooth of other specimens of this species. In all of these *Ph. nigrilabris* the medial pleurodont tooth of the premaxilla is substantially smaller than the largest pleurodont tooth on the premaxilla.

Among other draconines examined, *Acanthosaura armata* and *A. crucigera* have single pleurodont teeth and all other species examined have 3–5. Counts of acrodont and pleurodont teeth on other bones of *Phoxophrys* are comparable to the draconines examined.

25. Suturing and fusion of premaxillary processes of maxillae.—The premaxillary process of the mandible abuts or barely extend onto the premaxilla (A), extends onto the premaxilla to closely approximate the contralateral element (B), or sutures or fuses medially with the contralateral element (1).

The premaxillary processes of the maxillae abut the premaxilla in *Phoxophrys tuberculata*; whereas, in most Bornean congeners, the premaxillary process of the maxilla extends onto the face of the premaxilla to suture (female specimen of *Ph. cephalum*) or fuse with the contralateral element. In the holotype of *Ph. spiniceps*, the premaxillary processes closely approximate one another, but do not form a suture. Moody (1980:Character 43.2, Appendix D) found suturing or fusion of the premaxillary processes to be relatively rare in agamids, observing this character state only in *Phoxophrys*, *Bronchocoela*, *Ceratophora*, *Gonocephalus interruptus*, and *Lyriocephalus*. Except for *Phoxophrys*, a gap separates the premaxillary processes [Moody's Character 43.1] in specimens of these genera examined by us. We have not examined skulls of *G. interruptus*. Nonetheless, the processes only partially overlap the premaxilla in our large male *G. grandis* [43.1]. The processes almost meet in *Ceratophora stoddartii* [43.1].

26. Absence of palatal ridge from palatine bone.—The palatal ridges extend anteriorly beyond the palatine–pterygoid suture and terminate on the palatine (0), or they terminate posterior to the suture on the pterygoid (1).

The palatal ridges of *Phoxophrys tuberculata* and *Ph. nigrilabris* cross the pterygoid–palatine suture as in all other draconines examined except *Sitana*, whereas these ridges stop short of the suture in *Ph. anolophium*, *Ph. borneensis*, *Ph. cephalum*, and *Ph. spiniceps* (Fig. 12).

27. Condition of ventral flange on posterior pterygoid.—Near its posterior end, the pterygoid bears a distinct, high ventral flange (A) or lacks a flange (B).

Stilson et al. (2017) defined two character states for the ventral flange of the posterior process of the pterygoid. Near the pterygoid–quadrate articulation, the flange may be hooked (their Character 14.1) or not (14.0). Referring to illustrations provided in their supplementary material, skulls with either state have a high ventral flange that abruptly stops near the quadrate.

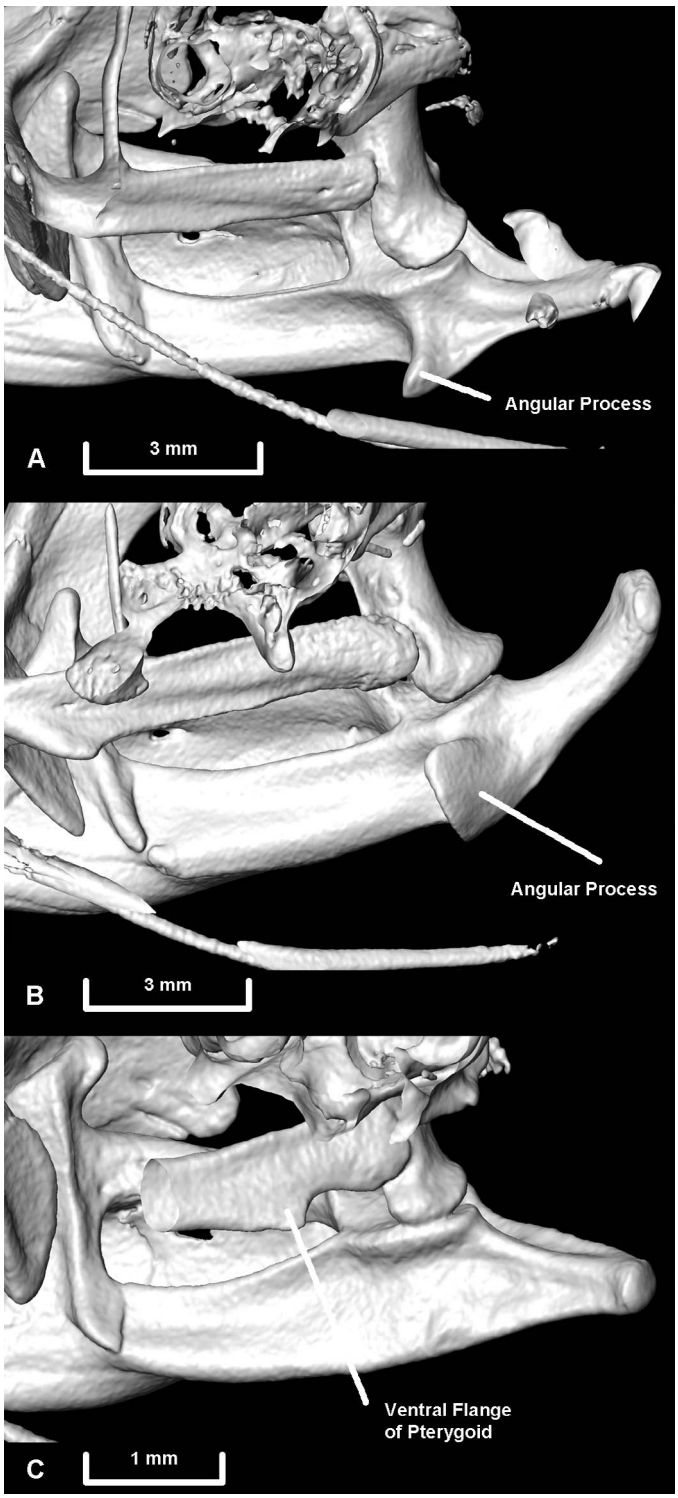

FIG. 13.—Medial aspect of mandible and pterygoid of *Pelturagonia anolophium* (A, MZB 14992), *Pe. borneensis* (FMNH 71856), and *Phoxophrys tuberculata* (UTA 65254).

The pterygoids of *Phoxophrys anolophium*, *Ph. borneensis*, *Ph. cephalum*, and *Ph. spiniceps* lack the flange or have a low ridge that ends in an inconspicuous, shallow dip near the quadrate (Fig. 13). In a broader analysis of agamids, the new character defined here could be treated as a third character state for Character 14 of Stilson et al. (2017). Among other Draconinae, the pterygoids of only *Lophocalotes* and *Ptycholaemus* lack the ventral flange. Pterygoids of *Phoxophrys nigrilabris* and *Ph. tuberculata* have well-developed ventral flanges, but lack terminal hooks.

Palatoquadrate Derivatives

Shape of quadrate.—Ventrally, the quadrate of *Phoxophrys* is relatively wider than that of other draconines ($F_{1,33} = 4.46$, $P = 0.043$), treating height of the quadrate as a covariate. Nonetheless, relative widths overlap substantially, especially for smaller species. Treating quadrate height as a covariate, we did not find a difference in width of the conch or medial lamina between *Phoxophrys* and other draconines. Moreover, we did not find substantial intrageneric differences in width of these structures. Though divergent in other aspects of quadrate morphology, our specimen of *Ph. tuberculata* actually fell on the regression line for width of the conch versus quadrate length and was very close to the line for width of the medial lamina versus quadrate length.

28. Lateral edge of conch of quadrate.—The conch is ovoid and its antero-lateral edge is outwardly convex, lacking a wide dorsolateral triangular portion (0), or the conch is rudimentary (=subtriangular, not too weakly concave, its antero-lateral edge straight) with a wide dorsolateral triangular portion (1).

Quadrates of the Bornean *Phoxophrys* are relatively similar to one another and differ in three ways from the quadrate of *Ph. tuberculata*. (1) The conchs of Bornean *Phoxophrys* are subtriangular and weakly to not concave with straight antero-lateral borders, sloping obliquely to the lateral condyle of the quadrate. In contrast, *Ph. tuberculata* has a concave conch with an outwardly bowed border (Fig. 9). (2) All members of the genus have a thickened tab of bone at the dorsolateral border of the conch for articulation with the squamosal. The tab is large and subtriangular in Bornean *Phoxophrys*, and less pronounced and positioned slightly lower along the lateral border of the conch in *Ph. tuberculata*. (3) On the medial face of the quadrate, a shallow facet for the pterygoid lies just posterior to the medial lamina and the posterior tip of the pterygoid articulates with the medial lamina and column of the quadrate. Above this articulation, the medial lamina of Bornean *Phoxophrys* is flat and subrectangular. In posteromedial aspect, the medial lamina merges seamlessly with the column of the quadrate. However, in anterior aspect, a rectangular patch of conspicuous and thick bony reinforcement demarcates the merger of the medial lamina and column in each of the Bornean species. *Phoxophrys tuberculata* lacks this bony reinforcement and the medial lamina of *Ph. tuberculata* is triangular and weakly concave posteromedially. This species has a rounded thickening of the medial lamina about one-third of its length down from the top of the quadrate, but based on its position and shape, we do not consider this thickening to be homologous with the rectangular reinforcement of Bornean species.

We have no reason to believe that the three differences are functionally linked and note that they do not always cooccur in outgroups. Nonetheless, we choose to err on the side of caution and code only one of these traits for phylogenetic analysis.

Moody (1980) coded *Phoxophrys* as having a rudimentary conch (his Character 24.2), describing this character state as

"conch rudimentary, only a small flat flange or absent" (Moody 1980:100). He also recognized an intermediate condition [24.1] described as "concave conch present but lateral margin straight and without a beaded edge." In his matrix, Moody reported rudimentary conchs only for *Phoxophrys* and the Sri Lankan endemics *Ceratophora*, *Cophotis*, and *Lyriocephalus*. We confirm his observations for the Sri Lankan endemics and note that the conch is even "more rudimentary" in these genera than in Bornean *Phoxophrys*. Nonetheless, the Sri Lankan genera have triangular medial laminae, shaped more like the lamina of *Ph. tuberculata* than the laminae of the Bornean species. The conchs of the female specimen of *Ph. cephalum* and holotype of *Ph. anolophium* are slightly concave, though not as concave as various species coded as 24.1 by Moody.

Among outgroups, the quadrate only *Diploderma splendidum* has all three characters found in Bornean *Phoxophrys. Draco sumatranus* has a rudimentary conch with a wide triangular portion dorsally. Though rectangular and relatively narrow, the medial lamina of this species lacks rectangular bony reinforcement on its anterior face.

Mandible

Mensural characters of the mandible.—Treating length of the mandible as a covariate, *Phoxophrys* has a shorter precoronoid length ($F_{1,32} = 10.01$, $P_{\text{Bonferroni}} = 0.009$) and longer retroarticular process ($F_{1,32} = 29.19$, $P_{\text{Bonferroni}} = 0.000$*) than other draconines. Treating height of the coronoid as a covariate, the species of *Phoxophrys* have shorter dorsal processes of the coronoid than other draconines ($F_{1,32} = 8.55$, $P = 0.006$). Nonetheless, in bivariate plots we found considerable overlap for each character and do not consider any of the three traits to be diagnostic of the genus or of the Bornean group.

29. Angular process of mandible.—The angular process is absent (A), developed horizontally (B), or developed vertically in a transverse plane (1).

The Bornean *Phoxophrys* have large tablike angular processes, with high vertical development in a transverse plane. In these species, the anterior face of the process is concave. In sharp contrast, *Ph. tuberculata* lacks an angular process (Fig. 13). Neither of these character states is common among other draconines. Among the species we examined, only the four species of *Dendragama* entirely lack angular processes, whereas only *Aphaniotis acutirostris*, *Pseudocalotes kingdonwardi*, and *Lyriocephalus scutatus* have transverse, vertical processes. The remaining species have horizontal processes that widen anteriorly. In *Ceratophora* and *Lophocalotes*, the angular processes have some vertical development anteromedially, but in a plane slightly oblique to longitudinal. Our interpretation of this character differs from that of Moody (1980), who assigned his State 2 (= process "tuberculate shaped or absent") to *Aphaniotis*, *Bronchocoela*, *Ceratophora*, *Cophotis*, *Lophocalotes*, and *Sitana*. Species of these genera examined by us have horizontal processes; however, development of the angular process appears to exhibit sexual dimorphism in some species. The process is horizontal and well developed in our male specimens of *Ceratophora stoddartii*, *Lophocalotes achlios*, and *L. ludekingi*, but reduced to a rounded mound in the female of *C. stoddartii* and a low thickening of the prearticular in the female of *L. achlios*.

Systematics

Phylogeny

Our Bayesian and maximum-likelihood analyses of mitochondrial DNA sequences recovered trees with near-identical topologies and with strong nodal support (Fig. 14). The maximum-likelihood and Bayesian trees differed only in placement of *Calotes versicolor*. With a posterior probability of 100%, the Bayesian analysis recovered *C. versicolor* as sister to all other draconines except for *Draco* and Bornean *Phoxophrys*, whereas the maximum-likelihood analysis placed *C. versicolor* above mainland *Pseudocalotes*, albeit with a bootstrap value of 65. Figure 13 does not show intergeneric relationships among the various species of *Dendragama*, *Lophocalotes*, and *Pseudocalotes*. With the exception of the three species of *Dendragama*, Harvey et al. (2017b, 2018) published these intergeneric relationships. Interested readers may also consult our supplementary material to view the unedited maximum-likelihood and Bayesian trees used to construct the simplified phylogeny in Fig. 13.

Molecular data did not support monophyly of *Phoxophrys* as defined by Inger (1960). Although we lack DNA sequences for half of the species of *Phoxophrys*, we found *Ph. tuberculata* to be more closely related to *Dendragama*, *Lophocalotes*, and insular *Pseudocalotes* than to the Bornean species *Ph. anolophium and Ph. nigrilabris* (Fig. 14). The two Bornean species form a clade that is sister to all other draconines except *Draco* in our analysis.

Phylogenetic analysis of our morphological characters found a single tree (Fig. 14) with strong support for *Phoxophrys tuberculata*, a clade containing the five Bornean species, *Ph. nigrilabris*, and a clade containing the four large Bornean species. Our survey of morphology found only one potential synapomorphy of *Phoxophrys* sensu lato: narrowing of the alveolar portion of the premaxilla (24.1), a trait that also occurs in *Acanthosaura*. Although *Ph. tuberculata* and the Bornean species have narrow premaxillae, the Bornean species brace the premaxilla with premaxillary processes of the mandible that fuse or suture over the premaxilla dorsally, whereas the premaxilla abuts short premaxillary processes in *Ph. tuberculata*.

This single putative synapomorphy of *Phoxophrys tuberculata* + the Bornean species stands in sharp contrast to the numerous differences between these lineages. Autapomorphies of *Ph. tuberculata* are a supercilium projecting upward and outward as a pointed, triangular flap (Character 3.1), small size with SVLs not exceeding 43 mm (11.1), transverse shorting of the prefrontal allowing nasal–frontal contact (13.1), and the squamosal extending anteriorly below the jugal to curve ventrally and brace against the vertical posterior margin of the jugal (15.1). Unlike the Bornean species, *Ph. tuberculata* lacks characters 4.1, 8.1, 25.1, 28.1, and 29.1. Unlike *Ph. tuberculata*, the Bornean species share a pale ischial stripe, nasals contacting one or no supralabials rather than broadly contacting two supralabials, multiple high scale counts with ranges not overlapping those of *Ph. tuberculata*, rectangular bony reinforcement on the anterior face of the quadrate, and a rectangular medial lamina of the quadrate. Finally, evolution of an antero-laterally angled postorbital process of the frontal (17.B, found only in *Ph. tuberculata*, *Dendragama*, and *Lophocalotes*) and loss of the

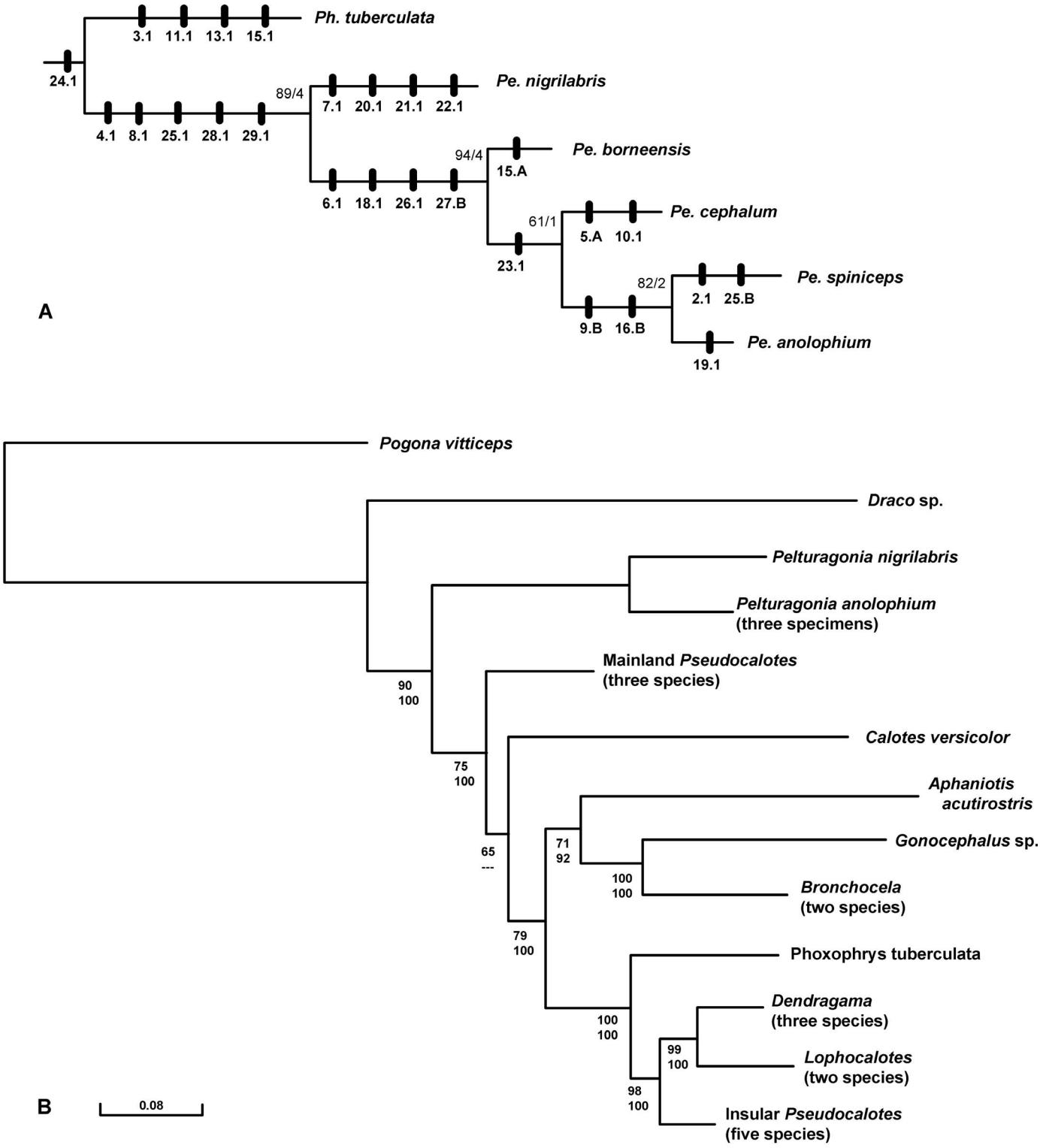

FIG. 14.—(A) Phylogeny of *Phoxophrys* and *Pelturagonia* based on morphology. Apomorphies identified by the TNT program are mapped on branches in bold font. Numbers in regular font immediately above and behind each node are bootstrap/Bremer support values. (B) Intergeneric relationships of Draconinae recovered by maximum-likelihood analysis of 16S and ND4 genes. Numbers below branches are bootstrap support values above percent posterior probabilities of clades in the Bayesian tree. (Supplementary data for this publication includes intrageneric topologies in both the maximum-likelihood and Bayesian trees.)

angular process of the mandible (29.A, found only in *Ph. tuberculata* and *Dendragama*) are consistent with the molecular phylogeny, since the Bornean species lack these characters.

Diagnostic characters proposed by Hubrecht (1881) and Inger (1960:221) are not synapomorphies of *Phoxophrys* + the Bornean species, because they do not occur in both clades or they are either plesiomorphic or have equivocal

polarity in the ancestor to *Phoxophrys*. Inger's (1960) study provided good reasons for removing Bornean *Phoxophrys* from *Japalura*, but did not make a strong case for placing the Bornean species in *Phoxophrys*. With only weak and contradictory evidence that the Bornean species share common ancestry with *Ph. tuberculata*, we remove *Pelturagonia* Mocquard from the synonymy of *Phoxophrys* Hubrecht.

Synapomorphies of *Pelturagonia* are vertical division of the rostral into two or more scales (4.1), presence of dorsolateral caudal crests (8.1), premaxillary processes of the mandible suturing or fusing with one another (25.1), a rudimentary conch of the quadrate with a wide dorsolateral triangular portion (28.1), and a vertical angular process of the mandible (29.1). Synapomorphies of the clade of large *Pelturagonia* are loss of a continuous dorsal crest on the body (6.1), a bony ridge extending from the postciliary ornament of the postorbital bone to the ventral margin of the supratemporal fossa (18.1), palatal ridges ending behind the palatine–pterygoid suture (26.1), and loss of the ventral flange from the posterior end of the pterygoid (27.B).

Relationships among the four large Bornean species require further study. Based on available data, *Pelturagonia anolophium* is the sister species of *Pe. spiniceps*. Synapomorphies of this clade are enlarged dorsally, projecting scales between the caudal crests (Character 9.B) and the postorbital process of the frontal reaching the postciliary ornament of the postorbital bone (16.B). Evolution of lateral flaring of the crista prootica behind the crista alaris (23.1) supports a sister relationship between *Pe. cephalum* and the *Pe. anolophium* + *Pe. spiniceps* clade; however, this group is only weakly supported by resampling values.

Special similarity between *Phoxophrys tuberculata* and *Pelturagonia nigrilabris* contradicts our phylogenetic hypotheses. In addition to both being relatively small species, they share two derived characters not found in the large species of *Pelturagonia*: arched supraciliaries producing a serrate edge to the supercilium (1.1) and a bony ridge that curves ventrad from the postciliary ornament to extend vertically down the postorbital bone (18.2). *Pelturagonia nigrilabris* is the most distinctive member of *Pelturagonia* and has evolved two to four times as many apomorphic characters as its congeners (Fig. 13).

Revised Taxonomy and Description of New Species

Phoxophrys Hubrecht

Phoxophrys Hubrecht 1881:51. Type species *Phoxophrys tuberculata* Hubrecht, by monotypy.

Diagnosis.—Small draconine agamids reaching a SVL of at least 43 mm and distinguished from all other Agamidae by the following combination of characters: (1) tympanum and external auditory meatus absent, extrastapes attaching to skin; (2) head robust, 77.4–92.1% as wide as long, comprising 27.4–28.5% of SVL; (3) rostral single; (4) prominent tubercular scale positioned below corner of jaw; (5) supercilium projecting upward and outward as pointed, triangular flap; (6) dorsal scales heterogenous with larger tubercular scales interspersed among smaller keeled scales, 56–67 scales around midbody; (7) premaxillary processes of mandible abutting premaxilla; (8) frontal and parietal extensively sculptured, not containing pineal foramen; (9) transverse shorting of prefrontal bone allowing nasal–frontal contact; (10) squamosal extending anteriorly below jugal to curve ventrally and brace against vertical posterior margin of jugal; (11) angular process of mandible absent.

Content.—*Phoxophrys tuberculata* Hubrecht (1881).

Etymology.—Hubrecht (1881) did not discuss the derivation of the name *Phoxophrys*. This feminine Latin noun in the nominative singular contains the Greek prefix *phoxos* meaning pointed or peaked and noun *ophrys* meaning eyebrow. The name likely refers to the arched, triangular supercilium of *Ph. tuberculata* and inspired coining of the common English name "eyebrow lizard," as frequently used by various websites and in some recent treatments of the Agamidae (Murphy and Hanken 2018).

Distribution.—*Phoxophrys* occurs only on Sumatra in Jambi, Sumatera Barat, and Sumatera Utara Provinces.

Remarks.—Although we currently consider *Phoxophrys* to be monotypic, differences among our male specimen and the two female types give us pause. The male has a vertebral crest, whereas females only have widely separated vertebral tubercles. The male was collected in lowlands near Medan on the eastern side of Sumatra's Bukit Barisan Range, whereas the female types were collected west of this range. Nonetheless, male specimens from west of the range have continuous vertebral crests, as illustrated by a specimen obtained near Solok and illustrated by Manthey (2010). Species boundaries should be investigated within *Phoxophrys* once series of both sexes can be obtained from both the eastern and western populations.

Pelturagonia Mocquard

Pelturagonia Mocquard 1890:130. Type species *Pelturagonia cephalum* Mocquard, by monotypy.

Diagnosis.—Medium-sized draconine agamids reaching a SVL of at least 84 mm and distinguished from all other Agamidae by the following combination of characters: (1) tympanum and external auditory meatus absent, extrastapes attaching to skin; (2) head robust, 77.5–98.3% as wide as long, comprising 22.5–28.4% of SVL; (3) rostral vertically divided into two or more scales; (4) prominent tubercular scale positioned below corner of jaw; (5) pair of dorsolateral caudal crests, not separated medially by vertebral crest; (6) dorsal scales heterogenous with larger tubercular scales interspersed among smaller-keeled scales, 81–115 scales around midbody; (7) alveolar portion of premaxilla relatively narrow, usually with single tooth and with premaxillary processes of mandible suturing or fusing over top of it; (8) frontal and parietal extensively sculptured, not containing pineal foramen; (9) conch of quadrate rudimentary, with wide dorsolateral triangular portion; (10) angular process of mandible large, tab-like, and vertically developed.

Content.—*Pelturagonia anolophium* Harvey et al. (this study), *Pelturagonia borneensis* (Inger 1960) comb. nov., *Pelturagonia cephalum* Mocquard (1890), *Pelturagonia nigrilabris* (Peters 1864) comb. nov., *Pelturagonia spiniceps* (Smith 1925) comb. nov.

Etymology.—Explaining the derivation of his new name, Mocquard (1890:130) described the distinctive angled aspect of the caudal crests and remarked "pour cette raison, nous imposons le nom générique de *Pelturagonia*." *Pelturagonia*

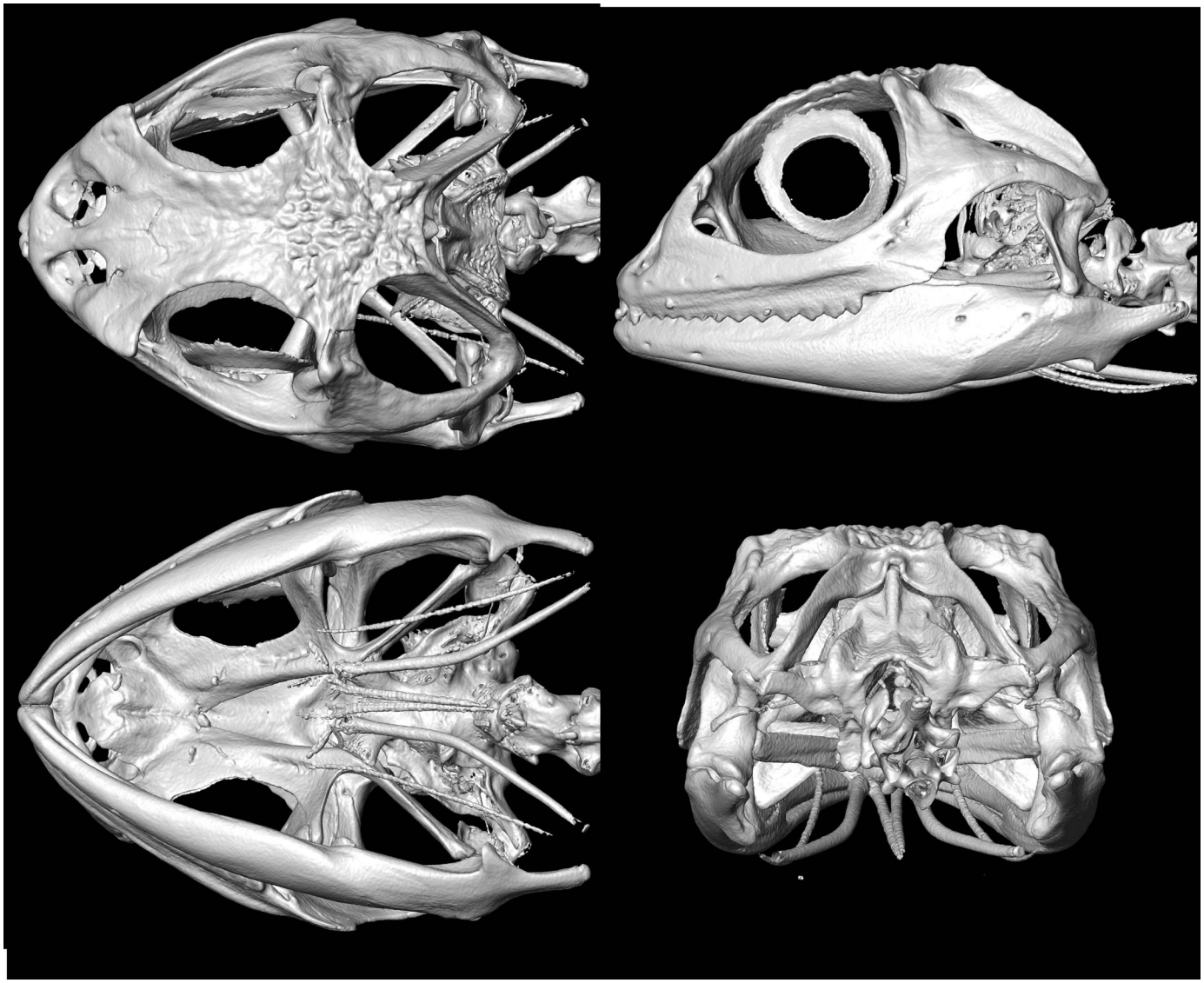

FIG. 15.—Skull of *Pelturagonia anolophium* (holotype, MZB 14992, skull width 15.9 mm) in dorsal, lateral, ventral, and posterior views.

is a feminine Latin noun in the nominative singular derived from the feminine Greek words *pelte* meaning shield and *gonia* meaning angle.

Distribution.—The genus occurs throughout Borneo and in the Natuna Achipelago (Fig. 15; Das 2010; Manthey 2010).

Remarks.—When Mocquard (1890) erected *Pelturagonia* for *Pe. cephalum*, he did not comment on *Pe. nigrilabris*, the only other member of the genus described at that time. Peters (1864) assigned *Pe. nigrilabris* to subgenus *Japalura* within *Otocryptis* as *Otocryptis (Japalura) nigrilabris*. Boulenger (1885) retained *nigrilabris* in *Japalura*, which he recognized as a genus. Later (1891), Boulenger referred *Pelturagonia cephalum* to the synonymy of *Japalura nigrilabris*. De Rooij (1915) accepted Boulenger's synonymy, and her description of *Japalura nigrilabris* is actually based on *Pe. cephalum* as previously pointed out by Inger (1960). Smith (1925) thought *Pe. spiniceps* was more closely related to *Phoxophrys tuberculata* and referred this species to *Phoxophrys*. Finally, Inger (1960) revalidated *Pe. cephalum* and transferred this species and *Pe. nigrilabris* to *Phoxophrys*.

Pelturagonia ***anolophium*** sp. nov.

Holotype.—An adult female (MZB 14992, Field tag 21838) collected by Thorton R. Larson and M. Munir on Gunung Lumut, Paser, Kalimantan Timur, Indonesia, 832 m elevation, 1.41078°S, 115.97771°E at 21:01 h. ND4 GenBank accession number MN548383; 16S GenBank accession number MN537800.

Paratypes (3).—Two subadult females (UTA 65255, 65256) and one subadult male (MZB 14993), collected by T.R. Larson and M. Munir from 19:10 to 19:34 h at the type locality, 1,090 m elevation, 1.40274°S, 115.98591°E. ND4 GenBank accession number MN548384 for UTA 65255 and MN548385 for UTA 65256; 16S GenBank accession number MN537801 for UTA 65255 and MN537802 for UTA 65256.

Diagnosis.—A large species of *Pelturagonia* reaching at least 193 mm (80 mm SVL) in length, distinguished from all congeners by the following combination of characters: (1)

supracilium lacking long spinose scale; (2) tubercular sublabials 4–7 anterior to enlarged subrictal tubercle; (3) enlarged middorsal scales widely spaced, not forming continuous dorsal crest; (4) nuchal crest consisting of 10–12 triangular scales mostly in continuous series; (5) paravertebrals on neck and scales of pectoral gap pointing backward; (6) base of tail with dorsolateral crest of 7–10 enlarged scales; (7) area between caudal dorsolateral crests not flat, with enlarged projecting scales; (8) four rows of enlarged subcaudals near base of tail (poorly differentiated in females); (9) gulars sharply keeled and mucronate, 31–36; (10) scales around midbody 92–109; (11) dorsum green with contrasting pale, saffron tubercles and reddish brown to brick red bands (at least in females and juvenile males; adult male unknown); (12) gular region without black pigment or with black reticulation but lacking sharp black lines extending postero-medially from labials.

Comparisons.—*Pelturagonia anolophium* is most likely to be confused with *Pe. borneensis* and *Pe. cephalum* (characters in parentheses). Unlike these species, *Pe. anolophium* attains a larger size (80 mm SVL in females compared to 62–74 mm in the other two species) and has enlarged projecting, tubercular scales dorsal to the caudal crests (area between crests flat with small keeled scales), 10–12 nuchal crest scales (4–8), nuchal crest mostly not interrupted by much smaller scales (2–5 small scales interrupting crests of *Pe. borneensis* and 3–13 small scales interrupting crests of *Pe. cephalum*), 2–3 enlarged posttemporal modified scales (single in all specimens except one *Pe. cephalum*, FMNH 152165), and the postorbital process of the frontal reaching the postciliary ornament (process and ornament separated by a large gap). All three species have strongly heterogeneous dorsal scales, but *Pe. anolophium* has scales that are distinctly more spinose. Additionally, unlike *Pe. borneensis*, *Pe. anolophium* has a continuous row of small lorilabials between the infraorbitals and supralabials (usually one or more large infraorbitals usually contacting supralabials) and lateral flaring of the crista prootica behind the crista alaris (crista prootica straight behind crista alaris); *Pe. anolophium* lacks oblique lines across the throat (prominent black to charcoal lines extend posteriorly and medially). Unlike *Pe. cephalum*, *Pe. anolophium* has spinose gulars (bluntly keeled), 4–7 tubercular sublabial scales anterior the subrictal tubercle (0 tubercular sublabials anterior to the subrictal tubercle), and four rows of enlarged subcaudals (two).

External morphology.—Characters of the female holotype appear in brackets after ranges of all the females. Females reaching 193 mm (SVL 80 mm) in length; two female paratypes 102 and 111 mm (SVL 63 and 66 mm); one male paratype 108 mm (SVL 65 mm); SVL 39.7% and tail length 60.3% of total length in male; SVL 38.4–41.3% [41.3%] and tail length 58.7–61.6% [58.7%] of total length in females; tail length 152 times as long as SVL in males and 142–161 [142] times as long as SVL in females; distance from axilla to groin accounting for 46.2–48.9% [48.9%] of SVL; distance between axillae 18.0–19.3% [19.3%] of SVL; head robust, 85.9–95.1% [95.1%] as wide as long, its length accounting for 22.5–27.3% [22.5%] of SVL; snout round in dorsal view, subacuminate in profile, sloping upward at about 80° to horizontal (Fig. 16); dorsal head scales weakly imbricate, keeled; rostrals three (100%); small medial rostral squarish but somewhat wider than tall [21.1% as wide as internarial distance], wider than mental; postrostrals 5–7 [6]; lateral postrostral contacting nasal (100%); noticeably enlarged azygous scales on snout arranged as inverted Y; each arm of Y consisting of one or two [2/2] large scales contacting base; arms of Y separated from orbital margin by one small scale with heavy keels directed postero-laterally; base of Y consisting of three or four [4] enlarged azygous scales in medial row with keels oriented longitudinally; slightly depressed prefrontal, frontal, and parietal regions bound by arms of Y, medial borders of orbit, and transverse parietal ridge; scales between orbits similar in size to supraoculars, distinctly smaller than circumorbitals, 5–7 [7] scales minimally separating circumorbital series; low, obtuse V-shaped parietal ridge covered by 7–9 [8] somewhat elongate parietals with low keels; discrete interparietal absent; no visible parietal eye; area in front of nuchal crest depressed, flanked on either side by elevated, rounded supratemporal areas.

One (100%) [1/1] supranasal scale separating postrostral series from first canthal; circumorbitals enlarged, angulate, 12 or 13 [13/13] from last canthal to postciliary scale; supraoculars somewhat heterogenous in size (=1–4 supraoculars in center of posterior half of supraocular region larger than rest), smaller than circumorbitals; transorbitals 17–22 [19]; canthals four or five [4/4]; supraciliaries 7–10 [10/10], resembling canthals and first best identified by probing orbital margin; supraciliaries subrectangular and not projecting, imbricating slightly (almost juxtaposed); combined count of canthals and supraciliaries 12–14 [14/14]; supraciliary notch prominent, containing three or four [3/3] small scales between last supraciliary and postciliary scale; 16 or 17 [17/17] scales between nasal and postciliary scale; postciliary scale prominent, enlarged, swollen and subpyramidal, abutting slightly smaller though still noticeably enlarged scale of temporal region; scalation of temporal region heterogenous, consisting of large angulate scales with heavier keels separated by small angulate keeled scales; 2–4 [4/3] noticeably enlarged scales between postciliary and posttemporal modified scales, with 2–4 scales [3/3] separating last enlarged temporal from largest posttemporal modified scale; posttemporal modified scales two or three [2/3] positioned on raised skin overlying posterior margin of skull; lower posttemporal modified scale as large as largest scales of nuchal crest, spinose and projecting dorsolaterally, surrounded by 7–10 [10/9] scales (including an enlarged spinose to pyramidal posttemporal dorsal to it, but somewhat smaller).

Nasal oval to trapezoidal, its dorsal border contributing to canthus; nasal contacting lateral rostral and first supralabial; nostril oval, directed laterally, occupying about one-fourth to one-third of nasal; scales of loreal region smooth to feebly keeled, 6–9 [7/6] scales in vertical row between last canthal and supralabials, 4–6 [4/4] scales in horizontal row from anterior border of orbit to nasal; orbit 45.8–50.0% [45.8%] of head length; palpebrals mostly granular; anterior and posterior scales of first row of palpebrals above eye evidently fused to second; heavily keeled palpebrals in center of eye not fused to first row; 12–15 [14/15] palpebrals between ocular angles; row of enlarged suboculars separated from supralabials by continuous row of lorilabials; distinctly enlarged scale positioned above first elongate scale of rictal

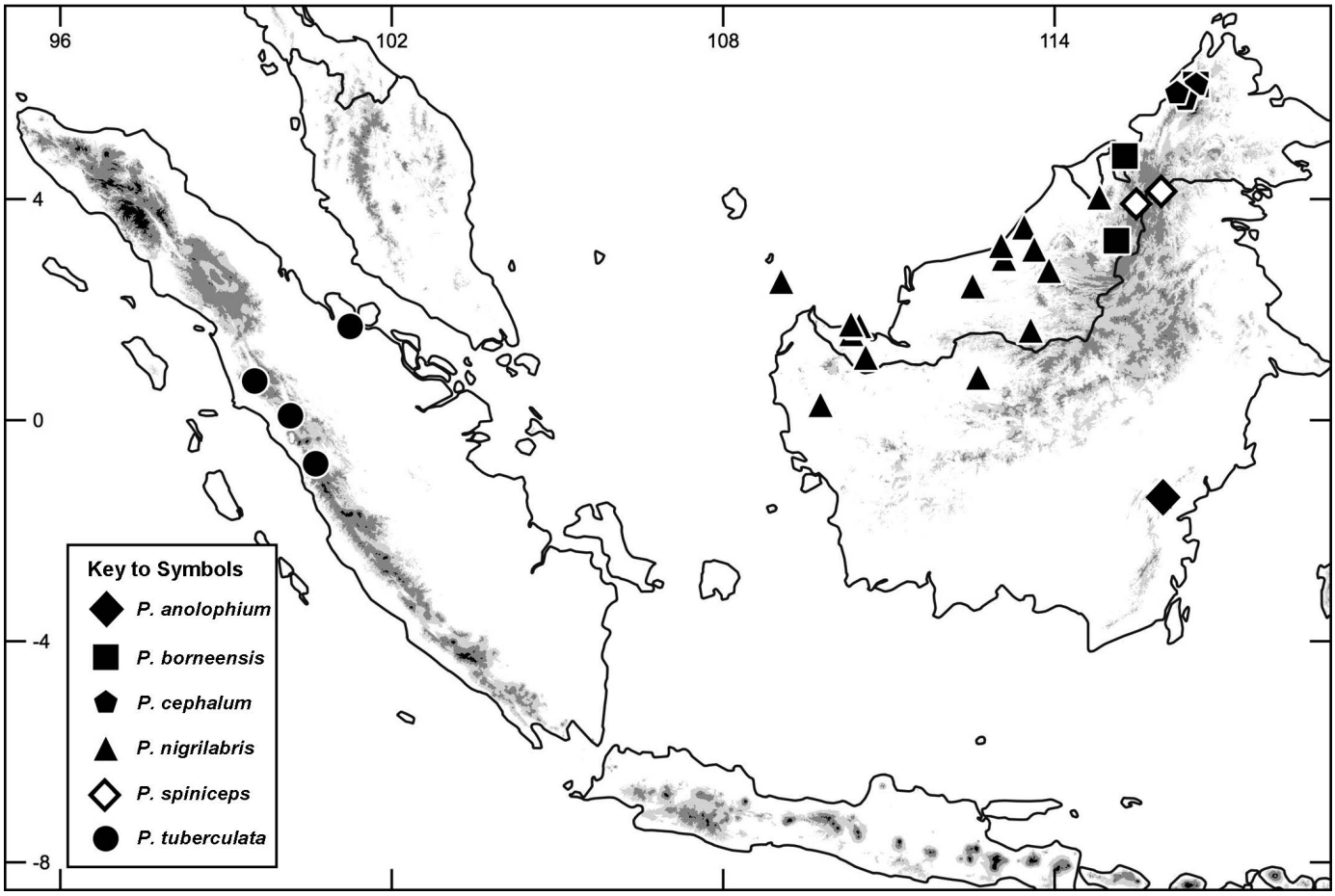

FIG. 16.—Distribution of *Pelturagonia* and *Phoxophrys* (areas above 500 m shaded gray).

fold (except in UTA 65255) and separated from it by small lorilabial; when enlarged scale present, scale in front of it divided longitudinally 100% of time; 10–12 [11/10] enlarged infraorbital scales from nasal to posterior border of orbit; tympanum and external auditory meatus absent; however, auditory region recognizable as subcircular, depressed area; 4–6 [5/6] scales comprising orbito-tympanic series, three or four [3/4] of them enlarged and somewhat rugose; distance from anterior border of auditory region to orbit 29.8–34.8% [34.8%] of head length; scales below and behind orbito-tympanic series heterogenous in size with numerous tubercular scales scattered among much smaller keeled to spinose scales.

Supralabials smooth, eight or nine [8/9]; rictal fold short, bordered dorsally by two or three [2] elongate scales; first scale bordering rictal fold longer than supralabial abutting it; infralabials smooth to feebly keeled, 11 or 12 [12/11]; mental entire, pentagonal; first pair of chin shields in medial contact behind mental and first 1–3 [2/3] contacting infralabials; sublabial tubercular scales 5–8 [5/6]; last sublabial tubercular scale much larger than rest, subpyrimidal and positioned below rictus; large spinose tubercular scales separated from one another by much smaller spinose scales in area behind rictus, below auditory region, and extending onto postero-lateral throat; gulars heavily keeled and terminating in downward-pointing mucrons, 31–36 [31] from point of medial contact between first pair of chin shields to preaxial margin of arm; 8–12 [9] enlarged and more pointed gular scales down midline in front of gular pouch, but these scales not forming obvious crest; transverse gular fold incomplete medially.

Nuchal crest prominent, consisting of 10–12 [11] triangular scales contacting one another except for single instance of paravertebrals in medial contact in MZB 14993; nuchal crest beginning immediately behind last occipital scale (50%, $n = 4$) or separated from it by single flat scale (50%) [in contact]; pectoral gap of 11–16 [12] small-keeled scales separating nuchal crest from transverse band of three or four [3] enlarged, heavily keeled and projecting scales; dorsal crest of widely spaced, single, enlarged, heavily keeled, projecting scales or short transverse bands of 2–4 similarly enlarged scales; 10–17 [17] enlarged scales from pectoral gap to posterior border of leg (count including single enlarged vertebrals, pairs of enlarged paravertebrals, and short transverse bands of enlarged vertebrals and paravertebrals), 50–62 [50] scales total in dorsal crest (count includes all scales along vertebral midline of dorsal crest, because we could not confidently distinguish between paravertebrals in medial contact and small vertebrals); total number of scales along vertebral line from posterior border of leg to occiput 73–90 [73].

Imbrication pattern on neck complex: wide band of paravertebrals pointing upward and backward anteriorly then reorienting to point backward by level of pectoral gap;

scales on lateral surface of neck pointing forward above antehumeral fold, then reorienting to point upward and backward at level of scapula; scales also reorienting below antehumeral fold to point downward and backward; paravertebrals on neck not enlarged relative to dorsals below them.

Dorsals much smaller than ventrals, weakly imbricate, strongly heterogenous with enlarged, heavily keeled spinose to pyramidal tubercles interspersed among smaller scales; 4–6 [5/5] irregular oblique lines one tubercular scale wide, directed anteriorly and ventrally on flanks; tubercles in oblique lines mostly separated from one another; smaller dorsals mostly with upturned tips and usually projecting somewhat but not as strongly as dorsal tubercles; dorsal tubercles extending onto ventro-lateral regions from posterior throat to groin; wide band of paravertebral scales pointing backward; sharp transition from backward-pointing paravertebrals to dorsals that point upward and backward below dorsolateral series of 11–14 [13/14] large tubercular scales (the abrupt reorientation is particularly evident in a few places where a backward pointing dorsolateral tubercle abuts a dorsal flank tubercle); first scale of dorsolateral series separated from first scale of dorsal crest by 6–8 [6] small paravertebrals; first scale of dorsolateral series spinose, larger than other enlarged scales of series and somewhat larger than other tubercular scales on flanks, directed laterally, whereas other tubercular scales of series directed posteriorly; scales around midbody 92–109 (100 ± 8, $n = 4$) [109]; four enlarged and heavily keeled scales in vertical line over ilium (uppermost positioned just above epiphyseal tuberosity), upper two of these as large as femoral armor and much larger than scales on flank, lower two of these about as large as tubercular scales on flank; ventrals imbricate, heavily keeled, 51–58 (56 ± 3, $n = 4$) [51] from preaxial edge of arm to vent, in 21–23 [22] longitudinal rows at midbody.

Base of tail rounded in cross-section; dorsolateral crest of 7–10 (8 ± 1, $n = 8$ sides of four specimens) [10/8] enlarged, heavily keeled scales; dorsally, scales between crests somewhat heterogenous in size, heavily keeled, projecting; minimally two scales between crests (100%, $n = 4$), maximally six scales between crests (100%, $n = 4$) dorsally; below caudal crests, scales subequal, keeled; scales above cloaca and immediately behind thigh small except for two or three (both sides with two except for three on right side only of MZB 14993) [2/2] distinctly enlarged scales and more heavily keeled scales.

Scales on limbs much larger than those on body, imbricate, heavily keeled, and pointed distally; in center of antebrachium, two or three noticeably much larger scales with high keels and pointed tips on postaxial edge; scales of palm keeled, imbricate, mucronate, often with three mucrons (largest mucron at end of central keel and a single small mucron on either side of it); Finger IV 71.4–73.7% (72.9 ± 1.1, $n = 4$) [71.4%] as long as Toe IV, slightly shorter than Finger III (length of Finger III 85.7–90.0%, 87.5 ± 2.2, $n = 4$ [90.0%] of length of Finger IV); lamellae under fingers bicarinate (some multicarinate or divided at base), 18 or 19 [18/18] under Finger IV; scales on dorsal surfaces of legs heterogeneous in size; 4–6 [5/5] enlarged scales postaxial to dorsal midline with noticeably higher, keels with prominent points directed more postaxial than adjacent scales; shank 21.4–24.3% (22.7 ± 1.1, $n = 4$) [22.5%] as long as SVL; scales on dorsal surface of shank somewhat heterogeneous: enlarged scales with higher keels in center of shank; scales of sole keeled with mucron directed distally and downward; Toe V relatively short (1–4 [1/2] fourth-toe lamellae within span of fifth toe), 53.7–61.1% (58.0 ± 3.1, $n = 4$) [58.6%] as long as Toe IV; 18–24 (21 ± 2, $n = 4$) [18/20] lamellae under Toe IV; subdigital lamellae of toes bicarinate, including those at base of Toe III; lamellae unicarinate under proximal phalanx of Toe IV (100%, $n = 4$).

Bristled sense organs (Scortecci 1937; Ananjeva et al. 1991) widespread on dorsal and ventral surfaces; single bristled sense organs usually positioned just below apex of keels and projecting beyond apex; callous glands absent; femoral and precloacal pores absent.

Coloration.—We base our description on photos of the type series including photos of live paratypes and the holotype immediately after being euthanized. In life, *Pelturagonia anolophium* is green with contrasting pale saffron tubercles and reddish brown to brick red markings. In dorsal aspect, five (UTA 65255, 65256) or six (MZB 14992, 14993) wide W-shaped bands cross the body, the most prominent overlapping the scapulae. These bands narrow on the flanks and have somewhat paler centers. The paratypes had green pigment in interspaces vertebrally; however, the entire area above the dorsolateral series of tubercles was brown (dark brown bands, lighter brown interspaces) in the holotype. Across the mostly green flanks (mostly brown in the male specimen), the large tubercular scales are much paler than the interspaces and are arrayed along the borders between the bands and interspaces.

Dorsally, *Pelturagonia anolophium* has a green head with brown bands, mostly edged in black. Each of the four specimens has an immaculate green blotch edged in black and occupying the depressed area between the transverse parietal ridge and circumorbitals. Viewed in dorsal aspect, the nuchal crest has a distinctive banded appearance because of alternating dark brown and saffron scales. The banding of the nuchal crest is somewhat striking, because it contrasts with a wide field of lime green paravertebrals flanking it. The sides of the head are mostly green with 11–13 brown or black lines radiating out from the eye (the lines are poorly differentiated and not countable in the holotype). Below and in front of the eye, the black lines continue across sutures of the labials. Somewhat strikingly, the first row of palpebrals is an immaculate bright green, so that the eye appears ringed. Two particularly distinct black lines extend behind the orbit to edge the otherwise green scales of the orbito-tympanic series. Abutting these black lines, *Pe. anolophium* has distinctive postocular and subocular pale saffron brands, each 2–4 scales wide. The subocular saffron band extends from the first row of palpebrals to cross the rictal fold and enclose the last sublabial tubercular scale. The postocular saffron band is shorter, extending onto the first two rows of scales behind the ocular margin.

Behind the postocular saffron band, the sides of the head and neck are green with thin black lines and sharply contrasting cream to very pale saffron tubercular scales. The scapular band is widest at the level of the dorsolateral series of tubercular scales. Ventrally it narrows to a wide line

edging the antehumeral fold posteriorly. In line with the corner of the mouth, each specimen has a prominent pale saffron blotch abutting the front edge of the scapular blotch. This saffron blotch follows the scapular band to overlap the anterior edge of the antehumeral fold. Finally, we note that in the holotype only, the scapular band is incomplete medially so that, when viewed in dorsal aspect, this specimen appears to have a pair of triangular scapular markings separated by a medial band of light brown scales.

Pigmentation of the throat varies among the type specimens. Except for some white to pale saffron tubercles, ventral surfaces of head of the holotype were dull orange and the gular pouch of the male specimen was bright pale orange. The remaining two juvenile females had reticulated throats with about equal numbers of orange and black gulars anteriorly grading to much fewer black scales on the pouch. The chin shields and sublabial tubercular scales are very pale saffron or cream with almost white keels, contrasting with the orange gular pigment. On the venter, this species has extensive charcoal mottling ventrolaterally on the body and under the limbs; otherwise, the venter is light grayish brown but with no trace of the orange gular pigment. The tail has 12–14 [13] dark brown bands, all much wider than the light brown interspaces. Distally, the bands lengthen and tend to fuse near the tip; they could not be counted on UTA 65255 because of fusion near the tip. On the ventral surface, the caudal bands are incomplete proximally, but complete for the distal two-thirds of the tail. Scales of the dorsolateral caudal crests are the same color as adjacent scales; however, the supracloacal tubercular scales are white to pale saffron.

In *Pelturagonia anolophium*, three or four [3/3] bands cross the brachium, four cross the antebrachium, 4–6 [4/4] cross the fourth finger, three or four cross the thigh [4/4], four or five cross the shank [4/4], and five or six cross the fourth toe [not visible on left/6]. On both the hand and foot, a dark brown band crosses the bases of the digits and another dark brown band crosses the middle of each foot. Scales of the brachial, antebrachial, and femoral armor have pale, contrasting keels. Above the leg, all four type specimens have a distinctive, pale saffron stripe edged in front and in back by black stripes. These stripes are associated with the ilial armor: the enlarged, heavily keeled scales are each entirely pale saffron, whereas scales immediately in front and behind them are black.

Pelturagonia anolophium has round pupil, pale yellow ciliary ring, bright orange iris, and pale blue buccal epithelium. The parietal and visceral peritonea in the abdominal cavity are unpigmented.

Measurements (in millimeters).—We provide measurements of the holotype followed by UTA 21846 then UTA 21844 and MZB 14993 in parentheses: SVL 79.5 (39.2, 44.5, 42.8), body length 38.8 (19.0, 21.0, 19.8), pectoral width 15.4 (7.2, 8.3, 7.7), length of tail 113 (63, 66, 65), head length 17.9 (10.7, 11.6, 10.9), head width 17.0 (9.3, 10.0, 9.5), diameter of orbit 8.2 (5.4, 5.7, 5.3), width of snout 5.4 (3.4, 3.9, 3.7), width of medial rostral 1.1 (not measured for paratypes), length of shank 17.9 (8.8, 10.8, 9.2), height of longest nuchal crest scale 1.4 (not measured for paratypes), height of longest dorsal crest scale 1.2 (not measured for paratypes), length of Finger III 9 (5.5, 6, 6), length of Finger IV 10 (6.2, 7, 7), length of Toe IV 14 (8.5, 9.5, 9.5), length of Toe V 8.2 (5, 5.8, 5.1), mass 10 g (2.1, 2.1, 2.6 g).

Dermatocranial roofing bones.—Nasals paired, smooth, each 43% as wide as long, not diverging widely, contacting one another for 27% of their length (Fig. 16); each nasal with short lateral process overlapping maxilla; small foramen behind each lateral process of nasal; frontal 42% of skull length, 57% as wide as long at its suture with prefrontal, mostly smooth anteriorly, rugosely sculptured behind posterior third of orbit and in parietal region; postorbital process of frontal extending to base of rounded postciliary ornament of postorbital bone; parietal 41% as long as wide, 17% of head length; rugosely sculptured dorsally with transverse ridge of rugosities along frontoparietal suture (dorsally, high rugosities make the bone somewhat convex in its anterior half. The bone is concave in its posterior half between ridges bordering the supratemporal fossae and a transverse ridge between the origins of the supratemporal processes); supratemporal processes of parietal forming angle of 76° with one another and curving downward at 36° to horizontal [14.2 of Moody]; in dorsal aspect, posterior side of parietal between bases of supratemporal processes deeply excavated and shelf-like on either side of fossa for processus ascendens; fossa for processus ascendens roofed by short occipital projection of parietal extending posteriorly below level of transverse ridge between supratemporal processes; supratemporal process ventrally with broad and pointed epipterygoid process [15.0 of Moody]; pineal foramen absent [16.1 of Moody], nonetheless, its position earlier in ontogeny marked by dip between otherwise high sculpturing behind straight line formed between lateral margins of frontoparietal suture [10.2 of Stilson et al.].

Circumorbital bones and temporal arcade.—Prefrontal in point contact with nasal, laterally rounded at canthus, with low rounded knob continuing canthus into orbit [32.1. In lateral aspect, the prefrontal curves downward to the lacrimal foramen below the canthus, and a short groove separates this bend of the prefrontal from the maxilla]; orbitonasal flange of prefrontal extending medial to orbital margin, overlapped dorsally by frontal and excluded from middle of dorsal orbital border by this bone; in orbital view, prefrontal surrounding most of lacrimal foramen, excluded from suborbital fenestra by palatine [33.1 of Moody]; lacrimal foramen oval, its area 16% of area of suborbital fenestra [35.0 of Moody]; lacrimal foramen visible in lateral aspect due to loss of lacrimal bone [34.2 of Moody]; ventral margin of lacrimal foramen eroded across prefrontal–palatine suture so that canal extends to palatal shelf of maxilla.

Jugal contributing about 70% of lower orbital rim, excluded from suborbital fenestra by maxilla and pterygoid [30.1 of Moody]; in lateral view, jugal and maxilla contributing about equally to infraorbital region [29.1 of Moody]; postfrontal absent; postorbital oriented nearly vertical [20.1 of Moody] with substantial dorso-medial expansion to support parietal; postciliary ornament [21.2 of Moody] continuous with ridge of bone bridging short gap between ornament and margin of supratemporal fossa; laterally, postorbital concave both above and below postciliary ornament and ridge; ventromedial process of postorbital narrow, bracing jugal medially and ventrally to

approximate pterygoid closely (the narrow gap between the postorbital and pterygoid is medial to a foramen in the medial side of the jugal; presumably this is a foramen for the maxillary division of cranial Nerve 5, see Evans 2008:Fig. 1.5); postorbital bracing squamosal dorsally for about one-third its length; area of contact between squamosal and postorbital somewhat greater than its contact with jugal [28.0 of Moody]; anterior process of squamosal with substantial antero-ventral extension bracing jugal ventrally but not curving downward to brace against vertical portion of jugal; squamosal not articulating with anterior lamina of quadrate, instead firmly seated in dorsal groove of quadrate pillar; squamosal with ventro-lateral margin notched at articulation with lateral condylar head of quadrate and with low, rounded ventral projection fitting between lateral and medial heads of dorsal condyle of quadrate [23.0 of Moody]; squamosal with short process along medial wall of supratemporal fossa [22.1 of Moody]; supratemporal inconspicuous, rounded under squamosal, with short process extending 22% of length of supratemporal fossa along ventro-lateral margin of supratemporal process of parietal [17.0, 18.2 of Moody; this supratemporal process forms a suture for the length of the somewhat shorter process of the squamosal along the medial wall of the supratemporal fossa]; supratemporal fossa 55.3% as wide as long [19.0 of Moody].

Palatoquadrate derivatives.—Quadrate relatively short and robust, 57% as wide at ventral condyle as high; dorsal condyle of quadrate with rounded knob at anteromedial corner partially filling gap between squamosal and supratemporal; conch of quadrate triangular, widest dorsally, 73% as wide as ventral condyle, with oval concavity near pillar of quadrate, with thickened triangular portion occupying antero-dorsal corner, with small rounded knob atop triangular antero-dorsal corner; lateral edge of conch smooth, thickened slightly [24.2 of Moody]; medial lamina of quadrate 40% as wide as conch, extending from dorsal condyle as bony flange to quadrate–pterygoid articulation, where it terminates at excavated articular surface for pterygoid; anterior face of quadrate concave between conch and medial lamina with rectangular patch of thickened bony reinforcement demarcating merger of medial lamina and column of quadrate; lateral portion of medial condyle much smaller than medial portion [25.0 of Moody], its width 66% of width of medial condyle.

Epipterygoid a long narrow rod, ending dorsally in point, projecting into soft tissue of skull in line with pointed ventral process of supratemporal process of parietal [i.e., incomplete, 26.1 of Moody]; length of epipterygoid 64% of distance from fossa columella of pterygoid to pointed ventral process of supratemporal process of parietal; epipterygoid not articulating with alar process of prootic [27.1 of Moody; nonetheless, the alar process of the prootic bears an anterior concavity medial to the crista alaris and dorsal to the incisura prootica that is the same size and shape as the epipterygoid. This depression closely approximates the epipterygoid and may be a point of articulation during certain types of cranial kinesis]; fossa columella near medial margin of pterygoid, not separated from pterygoid–basisphenoid joint by dorsal bony flange; nonetheless, epipterygoid immediately behind basipterygoid process and likely not ever articulating with this process [21.0 of Stilson et al.].

Otoccipital region of braincase.—Supraoccipital hexagonal, 80% as wide as long, with middorsal crest continuing antero-dorsally as short processus ascendens; ossified portion of processus ascendens separated from parietal by short gap [connection between processus ascendens and lateral parietal processes membranous, 13.0 of Moody]; anterior margin of supraoccipital lacking notches on either side of processus ascendens and sloping smoothly downward to bone's articulation with alar process of prootic; distinct dorsal constriction of supraoccipital in anterior half of this bone positioned at level of common crus of anterior and posterior semicircular ducts, its position 58% of bone's length from foramen magnum; posterior half of supraoccipital deeply concave between semicircular canals; posterior semicircular canals extending into exoccipitals [8.2 of Moody]; sphenoccipital foramen large [11.2 of Moody].

Supratemporal process of parietal seated in shallow groove formed by slight upturn in anterior margin of supraoccipital and short antero-dorsal expansion of alar process of prootic [9.0 of Moody]; medial surface of alar process with short projecting supratrigeminal process [10.1 of Moody] positioned medial to anterior ampulla; low ridge of bone extending postero-ventral from crista alaris to approach supratrigeminal process, but separated from it by narrow groove; anterior tip of inferior process of prootic and dorso-anterior tip of alar process of sphenoid forming small dorsal process [39.1 of Stilson et al.; this process and the supratrigeminal process form a semicircular notch in the dorsal margin of the inferior process of the prootic]; dorsum sella low and concave; crista prootica narrow at level of crista alaris and with prominent, rounded expansion (i.e., flaring) both above and below crista alaris.

Fenestra ovalis 9.64 times larger than shaft of stapes [7.2 of Moody], 1.55 times larger than recessus scali tympani; stapedial rod narrowing to 12% of diameter of relatively large stapedial footplate, extending laterally to attach to triangular intercalary element braced against medial side of quadrate and distal paroccipital process of otoccipital; extrastapes (likely cartilaginous) relatively long, curving antero-ventrally under skin covering conch of quadrate; recessus scali tympani ovoid, bordered by high cristae interfenestralis and tuberalis; fenestra cochleae large, oval, visible within recessus [5.0 of Moody]; area of medial opening of recessus 26% of lateral opening; crista interfenestralis excavated above tuber of basioccipital but not forming recess on tuber itself; crista tuberalis extending onto tuber, where lateral expansion of crista increases somewhat.

Trabeculae communis ossified but hypophyseal floor and cultriform process of parasphenoid membranous; basipterygoid process relatively short, its narrowest diameter 67% of its length and its articular surface 1.06 × larger than its length, articulating with pterygoid but not with base of epipterygoid [21.0 of Stilson et al.]; basisphenoid–basioccipital suture positioned just in front of tubera [12.1 of Moody], 32% of distance between distal tip of tuber and medial midpoint of facet of basipterygoid process; tuber of basioccipital relatively short, its length 40% of diameter of foramen magnum [1.1 of Moody], projecting backward 123° to anterior when viewed laterally [3.1 of Moody]; tubera forming angle of 132° with one another [2.1 of Moody], their distal separation 23% of skull width.

Paroccipital processes of otoccipitals extending upward 39° to their base [4.0 of Moody], separation of their distal tips 64% of skull width; each paroccipital process thickened along its long axis, slightly excavated both above and below its long axis.

Palatal bones.—Premaxilla very narrow, 8% as wide as skull, 27% as wide as long; nasal process of premaxilla 95% as wide as alveolar portion [36.0 of Moody], widest immediately above maxilla, overlapped by nasals posteriorly [37.0 of Moody], tapering posteriorly to point; medial suture of nasals separating posterior tip of premaxilla from frontal [2.0 of Stilson et al.]; nasal process broad and flat dorsally, not vertically compressed, incisive flange of nasal process about half as tall as width of nasal process [38.1 of Moody]; anterior margin of premaxilla continuous with that of maxilla in dorsal aspect [39.0 of Moody]; premaxillary processes of maxilla completely overlapping premaxilla dorsally [43.2 of Moody]; paired lappets of premaxillary processes of maxilla fused behind premaxilla [40.0 of Moody]; maxilla relatively short, 73% of skull length; facial process of maxilla supporting most of canthus, contacting nasals [41.0 of Moody], ventrally pierced by 3/3 foramina [62.3 of Stilson et al.] arrayed in line above bases of maxillary teeth between anterior border of orbit and middle of nares; maxilla contributing anterior quarter of ventral orbital margin; maxilla–palatine suture extending anteriorly and dorsally 26° to maxillary teeth row [42.1 of Moody].

In dorsal aspect, vomers and palatines upturned medially to form thickened medial ridge; this ridge mostly rounded where vomer sutures with its contralateral element, however, medial suturing of palatines and posterior ends of vomers interrupted dorsally by longitudinal groove (bottom of this groove formed by suturing of palatines); vomers paired, in palatal view separated by medial groove, flat, and sloping slightly upward laterally; vomers in dorsal view concave with upturned lateral edges [55.0 of Moody], in medial contact for about two-thirds their length [11.1 of Stilson et al.]; each vomer relatively short and broad, 15% of head length, 71% as wide as long; palatines shortened by anterior elongation of pterygoids, medially sutured to one another throughout their length [i.e., not separated from one another by process of pterygoid, 45.0 of Moody]; dorsal process of palatine relatively broad, edging prefrontal medially to suture with frontal firmly [54.2 of Moody]; maxillary process of palatine edging choana for about half length of choana, posteriorly attenuated along medial side of maxilla, though still widely separated from ectopterygoid; palatine contributing about half of medial border of infraorbital fenestra in both palatal and dorsal view [53.0 of Moody].

Interpterygoid vacuity ventrally bordered by thickened palatal ridge at medial edge of each pterygoid; palatal ridge restricted to pterygoid, not extending onto palatine; pterygoids very long, 65% as long as skull, moderately separated from one another anteriorly [46.0 of Moody; separation between palatal ridges 14% of head length at palatine–pterygoid suture], diverging posteriorly to articular surface for basisphenoid [44.0 of Moody, but see Discussion. Gap at inflection point 21% of head length]; each pterygoid relatively narrow, 10% as wide as long at palatine–pterygoid suture, with dorsal flange bordering interpterygoid vacuity but not suturing with contralateral element [47.2 of Moody]; palatal ridge of pterygoid low, broad, and rounded anteriorly, gradually becoming more pronounced at pterygoid–basisphenoid joint; pterygoid–basisphenoid joint relatively shallow, bound ventrally by medial thickening of palatal ridge at inflection point and slight ventro-medial bend in ridge below basipterygoid process of basisphenoid, but palatal ridge not folding over basipterygoid process [50.0 of Moody]; posteriorly process of pterygoid barely decreasing in height before its bony articulation with quadrate [49.0 of Moody], lacking ventral flange [new character state for Character 14 of Stilson et al.]; posterior tip of pterygoid longer medially with shallow vertical groove to articulate with antero-medial edge of quadrate; lateral process of ectopterygoid expanded horizontally along medial side of jugal and dorso-medial side of posterior process of maxilla, forming postero-lateral and posterior border of infraorbital fenestra, extending backward along jugal to closely approximate postorbital where separated by narrow groove adjacent to foramen in orbital margin of jugal; pterygoid-ectopterygoid vertical flange positioned just anterior to posterior border of orbit [48.0 of Moody]; medial process of ectopterygoid contributing majority of pterygoid-ectopterygoid vertical flange [18.2 of Stilson et al.], braced firmly against lateral process of pterygoid; lateral process of pterygoid closely approximating coronoid process of mandible when jaw closed, completely overlapping the ectopterygoid in posterior aspect [19.0 of Stilson et al.]; in dorsal view, ectopterygoid extending about half distance from infraorbital fenestra to medial margin of pterygoid [52.0 of Moody].

Mandible.—Precoronoid portion of mandible 57%, coronoid–articular length 29%, and length of retroarticular process 20% of total length of mandible; dentary not overlapping coronoid in labial view, pierced by 3/3 mental foramina all in front of orbit; posterior margin of dentary extending for short distance onto surangular as pointed process dorsal to anterior surangular foramen, lacking process below foramen, instead being broadly concave in front of and below surangular foramen; Meckelian groove low on lingual side, approaching ventral side of dentary near symphysis but lateral margin of dentary obscuring groove in labial aspect; approaching coronoid, dentary gradually increasing in depth but not "very deep" sensu Moody (1980) [58.0]; dorsal process of coronoid cylindrical, tilted somewhat medially, curving slightly posteriorly, lacking labial process [59.1 of Moody], its height in labial view 39% of height of coronoid in lingual view; posterolateral processes of coronoid accounting for 35% of coronoid–articular distance; posterolateral process of coronoid atop surangular along dorsal margin of mandible, contributing about half of mandible's dorsal surface for this section; coronoid overlapping dentary and triangular in lingual aspect, its anterior process wide, sloping, and flat; posteromedial process of coronoid robust, strongly ridged medially [60.0 of Moody], overlapping most of prearticular and approaching its ventral edge but not extending to ventral surface of mandible [61.1 of Moody]; ventromedial notch between anterior and posteromedial processes of coronoid exposing triangular anterior section of prearticular; posteriorly concave sheet of bone connecting posterolateral and posteromedial process of coronoid, in front of adductor fossa; adductor fossa large, 63% of coronoid–articular length; angular relatively deep in labial view, compressed to narrow sliver between splenial and dentary, anteriorly just reaching posterior edge of

Meckelian groove; angular foramen on medial side [65.1 of Moody] short distance in front of prearticular–splenial suture; splenial narrow, 20% of precoronoid length [66.0 of Moody]; retroarticular process 35% as long as precoronoid length, curving upward [62.0 and 63.1 of Moody], dorsal surface with distinct, elongate concavity lateral to and behind articular, lacking glenoid fossa; angular process ("medial process of prearticular" sensu Moody 1980) prominent, developed vertically, extending posteromedially (about 78° to long axis of retroarticular process) then curving anteriorly at its medial tip [64.0 of Moody]; ventrally, thin shelf of bone between angular process and retroarticular process and somewhat narrower shelf in front of angular process, giving impression of webbing.

Teeth.—Premaxilla bearing one medial pleurodont tooth [69.4 of Moody], 74% as long as largest maxillary pleurodont tooth [68.0 of Moody], fitting between first pair of dental pleurodont teeth and symphysis of jaw when mouth closed; maxillae bearing 2/2 pleurodont teeth; second pleurodont tooth of maxilla largest but nonetheless relatively small compared to other agamids, 1.09 × as long as largest dental pleurodont tooth and 1.33 × as long as sheering surface of penultimate maxillary acrodont tooth; dentary with 2/2 pleurodont teeth, first of these at symphysis [total number of pleurodont teeth = 9; 67.3 of Moody]; maxilla with 12/12 and dentary with 13/13 acrodont teeth; acrodont teeth abutting one another, compressed laterally, their labial surfaces more flattened than their lingual surfaces, gradually increasing in size posteriorly with last tooth on both maxilla and dentary being slightly smaller than penultimate tooth (second maxillary acrodont tooth 46% as high as penultimate tooth; second dental acrodont tooth 56% as high as penultimate tooth); sheering portion of acrodont teeth triangular, with single cusps anteriorly; posterior acrodont teeth weakly tricuspid; maxillary acrodont teeth larger than those on dentary (penultimate maxillary tooth 120% as high as penultimate dental tooth); last tooth of maxilla positioned below posterior quarter of orbit, at about level of postorbital–frontal suture; last tooth of dentary separated from coronoid by short diastema somewhat longer than adjacent teeth.

Etymology.—The new name *anolophium* is a neuter noun used in apposition to *Pelturagonia* and derived from the Greek prefix *ano-* meaning above and noun *lophos* meaning crest. The new name refers to the diagnostic projecting, enlarged scales positioned above the dorsolateral caudal crests in *Pelturagonia anolophium*.

Distribution and natural history.—With few specimens obtained during a single night of collecting, we can say little about the natural history of *Pelturagonia anolophium*. The type specimens were sleeping in low vegetation within a narrow elevational range of 823–1,090 m in montane rainforest. The holotype was on a thorny bush, 1.5 m aboveground, and the paratypes were sleeping on leaves 20–50 cm aboveground. The holotype contains few (perhaps two or four) oviductal eggs. Through the small ventrolateral incision used to sex the specimen, we could measure the smallest diameter of one of these eggs at 10 mm. Further study would have caused unnecessary damage to the holotype. At least 10 specimens of an unidentified nematode infected the body cavity of the holotype. We removed specimens of this nematode for further study and will report on its identity elsewhere.

Pelturagonia anolophium is known only from the type locality on Mount Lumut in East Kalimantan (Fig. 15). Mount Lumut lies at the northern end of the Meratus Range, a chain of low mountains extending approximately 200 km NNE and straddling the border between East and South Kalimantan. The Meratus Range is relatively narrow (approximately 10–30 km wide) throughout its length and parallels the coast, being separated from it by 45–60 km. Seemingly inhospitable lowlands isolate the Meratus Range from mountainous areas to the west and north. The tallest mountain of the Meratus Range is Gunung Besar (also known as Gunung Halau Halau) in South Kalimantan, which reaches 1,901 m in elevation.

Figure 16 shows the known distributions of *Phoxophrys* and *Pelturagonia*. A few localities on our map require further comment. We trace the type locality of *Pe. nigrilabris* "Pulo Matjan auf Borneo" (Peters 1864) to Pulau Majang, Kapuas Hulu Regency, West Kalimantan near the border with Sarawak (0.9428°N, 111.9914°E). Manthey (2010) illustrates a *Pe. nigrilabris* from "Ranchan Pool, Sarawak." We suspect this locality is at the Taman Rekreasi Ranchan, Serian, Sarawak (1.1434619°N, 110.5805242°E). We assumed that "Santubong (ca. 200 meters)" was within Santubong National Park, Kuching, Sarawak (1.7434202°N, 110.3153616°E). On the Indonesian side of Borneo, we found three recent records for *Pe. nigrilabris:* (1) Taman Nasional Bukit Baka Bukit Raya, Kabupaten Sintang, Kalimantan (Sardi and Siahaan 2014; traced to 0.7833°S, 112.6167°E; Manthey 2010 published a photo of a specimen of *Pe. nigrilabris* photographed by U. Arifin in this park), (2) Semahung Mountain, Landak District, Kalimantan (Amri et al. 2015; traced to 0.2873°N, 109.7620°E), and (3) "Kalimantan Barat, not far from the Malaysian border of Sarawak" 178–197 m elevation (Langner 2017; not traced).

To our knowledge, *Pelturagonia anolophium*, *Pe. nigrilabris*, and *Pe. spiniceps* are the only species of *Pelturagonia* known to occur in Kalimantan. Although we found three specimens from Kalimantan in the MZB labeled as *Pe. borneensis*, each is misidentified: MZB 2147 and MZB 10734 are specimens of *Pe. nigrilabris*, and MZB 2945 from "Maruwai" is not a specimen of *Pelturagonia*. Iskandar (2004) reported *Pe. borneensis* from Maruwai based on MZB 2945. He mentions Maruwai in passing (Iskander 2004:18), saying that it is "not far from the present site" (by "present site," he is referring to an unspecified locality in Malinau Regency, North Kalimantan). Then, in a note appended to his Table 4, he indicates that data from the site comes from unpublished personal communications. R. Stuebing collected MZB 2945 in 2000 while surveying lowland forest in the Maruwai region of the Kerangas forest biome, East Kalimantan. Stuebing (in litt., August 2019) clarified that he collected MZB 2945 at "NE Lampunut, 114°55.34′E, 00°03.92′S, 260 m."

Our study includes a female specimen of *Pelturagonia spiniceps* collected on Gunung Buduk Rakik, North Kalimantan, Indonesia, 10 August 1981. Approximately 23 km separate this locality from Mount Murud, the type locality of *P. spiniceps*. Interestingly, Gunung Buduk Rakik is the type locality of the snake gourd *Trichosanthes fusca*

W.J.de Wilde and Duyfjes (family Cucurbitaceae), whose holotype was collected by the same person (E.B. Walujo) that found this rare *Pelturagonia*.

DICHOTOMOUS KEY TO SPECIES OF PELTURAGONIA

1. A. Prominent spinose scale in center of supraciliary series, subequal to diameter of eye; posttemporal modified scales and some middorsal scales also long spines (northern Borneo) ..... *Pelturagonia spiniceps* (Smith)
   B. Long spinose scales absent from supraciliary series 2
2. A. Small lorilabial scale usually separating nasal from supralabials; middorsal scales on neck pointing anteriorly, undergoing 180° reorientation across pectoral gap; continuous dorsal crest in both sexes (Borneo) ..... *Pelturagonia nigrilabris* (Peters)
   B. Nasal usually contacting first supralabial; middorsal scales pointing posteriorly on neck, not undergoing abrupt reorientation across pectoral gap; dorsal crest of widely separated enlarged scales 3
3. A. Two rows of enlarged subcaudals near base of tail; single large tubercular scale below rictus without row of tubercular scales in front of it; gulars with rounded low keels, 23–30 down midline from mental or chin shields to chest; enlarged suprarictal scale usually in broad contact with first scale of rictal fold (northern Borneo); ..... *Pelturagonia cephalum* Moquard
   B. Four rows of enlarged subcaudals near base of tail or subcaudals similar in size to scales on sides of tail; short row of 2–7 tubercular to heavily keeled sublabials in addition to large subrictal tubercle; gulars with sharp keels and prominent mucrons, 26–36 (usually more than 30) from mental or chin shields to chest; lorilabial usually separating enlarged suprarictal scale from first scale of rictal fold 4
4. A. Area between caudal dorsolateral crests not flat (base of tail with large, projecting tubercular scales above dorsolateral crests, Fig. 6); nuchal crest consisting of 10–12 triangular scales in continuous series (rarely two crest scales separated by single small vertebral or medial contact between single pair of paravertebrals); continuous series of lorilabials separating enlarged infraorbitals from supralabials; chin and gular region mostly immaculate to mottled but lacking sharp lines extending postero-medially from labials (southern Kalimantan) .... *Pelturagonia anolophium* Harvey et al.
   B. Area between caudal dorsolateral crests flat (no enlarged, projecting tubercular scales between crests); nuchal crest consisting of 3–8 triangular scales often separated from one another by small vertebrals or pairs of paravertebrals in medial contact; one or more enlarged infraorbitals usually interrupting lorilabial series to contact supralabials; chin and gular region with black lines extending postero-medially (northern Borneo) .... *Pelturagonia borneensis* (Inger)

DISCUSSION

Although we certainly agree with Hillis (2019) that subgenera can be used to avoid prematurely overturning long established taxonomy, this remedy would be inappropriate here. No systematist considered the Bornean and Sumatran species to be congeneric until Inger (1960) began the process of partitioning *Japalura*. Smith (1925) simply assigned *Pelturagonia spiniceps* to the wrong genus (i.e., *Phoxophrys*) and did not comment on *Pe. cephalum* or *Pe. nigrilabris*. We base our revised taxonomy on two independent data sets: one morphological, the other molecular. Both sets of data reveal considerable divergence between *Ph. tuberculata* and the species of *Pelturagonia*. The molecular data unequivocally reveal *Phoxophrys* to be paraphyletic as previously defined. Although we did not use morphological data to test monophyly explicitly, we found multiple differences between *Phoxophrys* and *Pelturagonia* and two potential synapomorphies of *Phoxophrys* and *Dendragama*.

Before the advent of computed tomography, we could not have assessed our new osteological characters for this group of rare lizards. This major technological advance has energized the field of comparative osteology and overcome a dearth of skeletal preparations in museum collections (Bell and Mead 2014).

Prior to our study, the skull of *Pelturagonia* was virtually unknown. In his unpublished dissertation, Moody (1980) provided the only osteological data for this genus. His research remains the most comprehensive survey of agamid morphology and has informed broader surveys of squamate relationships (e.g., Estes et al. 1988; Gauthier et al. 2012).

Moody (1980:Appendix B) examined the skeleton of only one species of *Pelturagonia*, identified as *Pe. cephalum* (NMW 867). When M.B. Harvey visited the NMW in the summer of 2018, all of the *Pelturagonia* in the collection were correctly assigned to genus, but misidentified at the species level. Thus, the single skeleton (NMW 867) examined by Moody may have been prepared from a misidentified specimen. Harvey did not examine this specimen while at the NMW, and we cannot comment further upon its identity.

In our study, we scored each species of *Pelturagonia* for most of the first 70 of Moody's (1980) characters. We excluded characters 31 (presence of the nasal foramen) and 56 (count of scleral ossicles), because neither character could be evaluated on our scans. Stilson et al. (2017) redefined Moody's Character 51 and we followed their description. Of the remaining 67 characters, we confirm Moody's coding for 43 (67%) of them. For his characters 1, 2, 4, 7, 11, 12, 14, 18, 36, and 44, we may have measured various structures in a manner different than Moody or the characters may be more variable than he realized. For example, when trying to replicate his methods for Character 36, we first measured alveolar premaxillary width and greatest width of the premaxilla above the premaxillary process of the maxilla. A ratio of these measurements should capture Moody's character states: "denticulate portion of premaxilla broader than the internarial process (0), equal to or narrower than the internarial process (1)." However, our ratios ranged from 0.74 to 1.44, with the female *Pe. cephalum* and male *Pe. nigrilabris* having narrower processes (36.1) and the other specimens having broader processes (36.0).

Some discrepancies between our coding and Moody's reflect interspecific variation. Moody reported 9.1 and 21.1 for *Pelturagonia*, but we found these characters only in *Pe. nigrilabris*. For *Pelturagonia*, Moody (1980) reported that the ventral edge of the pterygoid folds over the articulating

head of the basisphenoid (his 50.1). We also observed this character state in all specimens of this genus except for the holotype of *Pe. anolophium*. Although Moody (1980) reports that the ectopterygoid extends dorsally over the pterygoid "to the midline" (52.1), we observed this trait in the male specimen of *Phoxophrys tuberculata*, but not in the holotype of *Japalura robinsoni* or in any of the specimens of *Pelturagonia*. If the tiny teeth on either side of the large premaxillary pleurodont teeth are included in the count, then only the holotypes of *Pe. spiniceps* and *Japalura robinsoni* have Character 67.2, whereas the remaining *Pelturagonia* have 8–10 total pleurodont teeth on the premaxilla, maxilla, and dentaries (67.3 of Moody).

For nine characters, our samples of *Pelturagonia* and *Phoxophrys* do not have the states reported by Moody (1980). *Pelturagonia*, *Phoxophrys*, and other draconines we examined have parasaggital ridges formed by enlargement of the postero-vertical semicircular canal in both the supraoccipital and exoccipital (8.2 of Moody). Most draconines and all *Pelturagonia* have a process on the cranial wall of the supratemporal process of the parietal (Fig. 9). This process bears a membranous connection to the dorsal end of the epipterygoid. Moody (1980:Character 15) coded *Phoxophrys* as having the cranial wall of the supratemporal as being "straight or with only a slightly rounded process" (1), whereas our description of this character matches his State 0 (i.e., *Phoxophrys* and *Pelturagonia* have "sharp downward" processes). In scans of some ingroup species, we could not score Moody's characters 10 and 23, but, as detailed in our description, *Pe. analophium* has a short projecting supratrigeminal process (10.1 of Moody) and a rounded ventral projection of the squamosal fitting between the lateral and medial heads of the dorsal condyle of the quadrate (23.0 of Moody). The ventral edge of the pterygoid does not fold over the basipterygoid process of the basisphenoid in any *Pelturagonia* or *Phoxophrys* (50.0 of Moody; Fig. 12). In *Pelturagonia*, *Phoxophrys*, and most draconines examined by us, the palatine contributes about half of the medial border of the infraorbital fenestra in both palatal and dorsal view (53.0 of Moody). For Moody's Character 54, we found each of his character states in one or more draconines; however, the ascending process of the palatine strongly contacts the ventral side of the frontal in *Pelturagonia*, *Phoxophrys*, and some near outgroups (54.2). The large median premaxillary tooth is substantially smaller than pleurodont teeth on the maxilla and dentary (68.0 of Moody). Moody (1980) coded *Phoxophrys* as having four pleurodont teeth on the premaxilla (his Character 69.1); however, *Pelturagonia* and *Phoxophrys* have greatly reduced premaxillae with a single large pleurodont tooth (69.4) or a large medial pleurodont tooth flanked on either side by single much smaller teeth (i.e., three premaxillary teeth, 69.2).

Moody's (1980) list of characters should be the starting point for future studies of the cranium in draconine agamids. By our count, Stilson et al. (2017) and our study of *Pelturagonia* and *Phoxophrys* add 30 new cranial characters to Moody's set of 70. Our survey of outgroups revealed considerable variation for many of these 100 characters, both within and among genera. With the advent of CT data, these characters can be used to resolve many other problems that continue to plague draconine systematics. Although molecular data can be used to generate well-supported phylogenies rapidly, tissue samples are not available for many species, and future collecting efforts are unlikely to ameliorate this problem substantially. Cranial characters proved more useful for resolving deep relationships in our phylogeny. Thus, they show particular promise for resolving intergeneric relationships with rare genera such as *Harpesaurus*, *Pseudocophotis*, and *Thaumatorhynchus*. They will also allow researchers to investigate phylogeny within genera suspected or known to be polyphyletic, such as *Gonocephalus* and *Pseudocalotes* (Denzer and Manthey 2009; Harvey et al. 2017b). Cranial morphology will also prove valuable in at least two other ways. As in our study, data sets of cranial and other morphological characters can be used to test phylogenetic hypotheses generated by the various molecular data sets that are being rapidly assembled for draconine agamids (Grismer et al. 2016; Shaney et al. 2016; Harvey et al. 2017a,b; Wang et al. 2018). Morphological data sets will remain the only way to place extinct species in phylogenetic hypotheses.

Acknowledgments.—For loan of specimens under their care, we thank L. Scheinberg (CAS), A. Resetar (FMNH), J. Rosado (MCZ), C. Spencer and J. McGuire (MVZ), and F. Tillack (ZMB). A. Ohler, M. Cugnet, and J. Courtois (MNHN), G. Gassner (NMW), E. Dondorp (RMNH), and F. Tillack and M.O. Rödel (ZMB) kindly hosted Harvey's research at their respective institutions. K. Lim Kok Peng (Lee Kong Chian Natural History Museum; National University of Singapore) kindly sent us six voucher photos of the *Pelturagonia* reported by Asad et al. (2015). We thank C.C. Lee, A. Masonzravky, and E. Wostl for kindly sending photos of various *Pelturagonia* and for giving us permission to publish some of their photos in our Fig. 1. For use and access to InspeXio SMX-100CT CT system we thank M. Loocke at the Shumadzu Center for Environmental Forensics and Material Science, UTA. We thank V. Fernandez, M. Wilkinson, and D. Gower for assistance with CT scanning at BMNH. Our manuscript benefited from thoughtful discussion with U. Manthey about difficulties with identifying *Pelturagonia*. R. Steubing kindly clarified collection data for MZB 2945. To fund his research in Kalimantan Timur, T. Larson received a 2015–2016 Fulbright Student Researcher Fellowship and award from the Fulbright American Indonesian Exchange Foundation. For their kind assistance with fieldwork in Kalimantan, we thank I. Hadiyana of ECOSITRUP, Huriel of PADI-Indonesia, M. Munir (MZB), and the Muluy people of Swan Slotung, Paser, Kalimantan Timur, Indonesia. We thank the Ministry of Research and Technology of the Republic of Indonesia, RISTEK, for coordinating and granting research permission. S. Wahyono (RISTEK) provided valuable assistance throughout the permit approval process. We thank past and present representatives of LIPI at the Museum Zoologicum Bogoriense for facilitating in-house study of specimens and export and field research permits, namely Boeadi, I. Sidik, R. Ubaidillah, R.M. Marwoto, and H. Sutrisno. RISTEK and LIPI reviewed and approved our fieldwork in Indonesia and provided export permits for specimens to the United States for study and deposition at UTA. W. Tri Laksono kindly provided laboratory assistance at the MZB, and N. Widodo and Mr. Marwoto (Faculty of Mathematics and Natural Sciences, UB) kindly provided logistical support. All specimens were collected, euthanized, and preserved following guidelines detailed in the ASIH pamphlet: *Guidelines for Use of Live Amphibians and Reptiles in Field and Laboratory Research*, second edition, available at http://www.asih.org/publications. A National Science Foundation grant (DEB-1146324) to E.N. Smith and M.B. Harvey funded some of this research.

Supplemental Material

Supplemental material associated with this article can be found online at https://doi.org/10.1655/HERPMONOGRAPHS-D-19-00006.S1.

Literature Cited

Amarasinghe, A.A.T., I. Ineich, D.M.S. Suranjan Karunarathna, W. Madhava, S. Botejue, and P.D. Campbell. 2015. Two new species of the genus *Sitana* Cuvier, 1829 (Reptilia: Agamidae) from Sri Lanka,

including a taxonomic revision of the Indian *Sitana* species. Zootaxa 3915:67–98.
Amri, S., B. Nurdjali, and S. Siahaan. 2015. The diversity of Squamates in Semahung Mountain protected forest in Sebatih village of Sengah Temila Sub-District in Landak District. Jurnal Hutan Lestari 3:30–34.
Ananjeva, N.B., and B.L. Stuart. 2001. The agamid lizard *Ptyctolaemus phuwuanensis* Manthey and Nabhitabhata, 1991 from Thailand and Laos represents a new genus. Russian Journal of Herpetology 8:165–170.
Ananjeva, N.B., M.E. Dilmuchamedov, and T.N. Matveyeva. 1991. The skin organs of some iguanian lizards. Journal of Herpetology 25:186–199.
Asad, S., J. Mathai, D. Laird, N. Ong and L. Buckingham. 2015. Preliminary herpetofaunal inventory of a logging concession in the Upper Baram, Sarawak, Borneo. Herpetological Review 46:64–68.
Avise, J.C., and R.M. Ball, Jr. 1990. Principles of genealogical concordance in species concepts and biological taxonomy. Oxford Survey in Evolutionary Biology 7:45–67.
Bell, C.J., and J.I. Mead. 2014. Not enough skeletons in the closet: Collections-based anatomical research in an age of conservation conscience. The Anatomical Record 297:344–348.
Boulenger, G.A. 1885. Catalogue of the Lizards in the British Museum (Natural History). Volume 1. Geckonidae, Eublepharidae, Uroplatidae, Pygopodidae, Agamidae. British Museum of Natural History, UK.
Boulenger, G.A. 1891. Remarks on the herpetological fauna of Mount Kina Baloo, North Borneo. The Annals and Magazine of Natural History 6:341–345.
Cadle, J.E. 1991. Systematics of lizards of the genus *Stenocercus* (Iguania: Tropiduridae) from northern Perú: New species and comments on relationships and distribution patterns. Proceedings of the Academy of Natural Sciences of Philadelphia 143:1–96.
Cherche, M.A. 1958. Note su Agama robecchi Blgr. Atti della Società italiana di scienze naturali e del Museo civico di storia naturale di Milano 97:233–238, pls. 9–11.
Darriba, D., G.L Taboada, R. Doallo, and D. Posada. 2012. jModelTest 2: More models, new heuristics and parallel computing. Nature Methods 9:772.
Das, I. 2010. A Field Guide to the Reptiles of South-East Asia. New Holland Ltd., UK.
David, P., and G. Vogel. 1996. The Snakes of Sumatra: An Annotated Checklist and Key with Natural History Notes. Edition Chimaira, Germany.
De Queiroz, K. 1998. The general lineage concept of species, species criteria, and the process of speciation: a conceptual unification and terminological recommendations. Pp. 57–75 in Endless Forms: Species and Speciation (D.J. Howard and S.H. Berlocher, eds). Oxford University Press, USA.
De Rooij, N. 1915 The Reptiles of the Indo-Australian Archipelago. I. Lacertilia, Chelonia, Emydosauria. E.J. Brill, The Netherlands.
Deepak, V., V.B. Giri, M. Asif, S.K. Dutta, R. Vyas, A.M. Zambre1, H. Bhosale, and K.P Karanth. 2016. Systematics and phylogeny of *Sitana* (Reptilia: Agamidae) of Peninsular India, with the description of one new genus and five new species. Contributions to Zoology 85:67–111.
Denzer, W., and U. Manthey. 2009. Remarks on the type specimen of *Gonocephalus mjobergi* Smith, 1925 (Sauria: Agamidae). Bonner zoologische Beiträge 56:255–258.
Estes, R., K. de Queiroz, and J.A. Gauthier. 1988. Phylogenetic relationships within Squamata. Pp. 119–281 in Phylogenetic Relationships of the Lizard Families (R. Estes and G. Pregil, eds.). Stanford University, USA.
Evans, S.E. 2008. The skull of lizards and Tuatara. Pp. 1–347 in Biology of the Reptilia, Volume 20 (C. Gans, A.S. Gaunt, and K. Adler, eds.). Society for the Study of Amphibians and Reptiles, USA.
Gauthier, J.A., M. Kearney, J.A. Maisano, O. Rieppel, and D.B. Behlke. 2012. Assembling the squamate tree of life: Perspectives from the phenotype and the fossil record. Bulletin of the Peabody Museum of Natural History 53:3–308.
Goloboff, P.A., J.S. Farris, and K.C. Nixon. 2008. TNT, a free program for phylogenetic analysis. Cladistics 24:1–13.
Grismer, J.L., J.A. Schulte, II, A. Alexander, P. Wagner, S.L. Travers, M.D. Buehler, L.J. Welton, and R.M. Brown. 2016. The Eurasian invasion: Phylogenomic data reveal multiple Southeast Asian origins for Indian dragon lizards. BMC Evolutionary Biology 16:1–11. DOI: http://doi.org/10.1186/s12862-016-0611-6.
Hammer, Ø., D.A.T. Harper, and P.D. Ryan. 2001. PAST: Paleontological statistics software package for education and data analysis. Palaeontologia Electronica 4:1–9.
Harvey, M.B. 2008. New and poorly known *Dipsas* (Serpentes: Colubridae) from northern South America. Herpetologica 64:422–451.
Harvey, M.B., A. Hamidy, N. Kurniawan, K. Shaney, and E.N. Smith. 2014. Three new species of *Pseudocalotes* (Squamata: Agamidae) from southern Sumatra, Indonesia. Zootaxa 3841:211–238. DOI: http://doi.org/10.11646/zootaxa.3841.2.3.
Harvey, M.B., K. Shaney, I. Sidik, N. Kurniawan, and E.N. Smith. 2017a. Endemic dragons of Sumatra's volcanoes: new species of *Dendragama* (Squamata: Agamidae) and status of *Salea rosaceum* Thominot. Herpetological Monographs 31:69–97.
Harvey, M.B., K. Shaney, A. Hamidy, N. Kurniawan, and E.N. Smith. 2017b. A new species of *Pseudocalotes* (Squamata: Agamidae) from the Bukit Barisan Range of Sumatra with an estimation of its phylogeny. Zootaxa 4276:215–232. DOI: https://doi.org/10.11646/zootaxa.4276.2.4.
Harvey, M.B., J. Scrivani, K. Shaney, A. Hamidy, N. Kurniawan, and E.N. Smith. 2018. Sumatra's endemic crested dragons (Agamidae: *Lophocalotes*): A new species from the Bukit Barisan Range, comments on *Lophocalotes ludekingi*, and ecology. Herpetologica 74:73–88.
Hillis, D.M. 2019. Species delimitation in herpetology. Journal of Herpetology 53:3–12.
Hubrecht, A.A.W. 1881. On a new genus and species of Agamidae from Sumatra. Notes from the Leyden Museum 3:51–52.
Inger, R.F. 1960. A review of the agamid lizards of the genus *Phoxophrys* Hubrecht. Copeia 1960:221–225.
Iskandar, D.T. 2004. The Amphibians and Reptiles of Malinau Region, Bulungan Research Forest, East Kalimantan: Annotated Checklist with notes on Ecological Preferences of the Species and Local Utilization. Center for International Forestry Research, Indonesia.
Katoh, K., and D.M. Standley. 2013. MAFFT multiple sequence alignment software Version 7: Improvements in performance and usability. Molecular Biology and Evolution 30:772–780.
Katoh, K., K. Misawa, K. Kuma, and T. Miyata. 2002. MAFFT: A novel method for rapid multiple sequence alignment based on fast Fourier transform. Nucleic Acids Research 30:3059–3066.
Kearse, M., R. Moir, A. Wilson, ... A. Drummond. 2012. Geneious Basic: An integrated and extendable desktop software platform for the organization and analysis of sequence data. Bioinformatics 28:1647–1649. DOI: http://dx.doi.org/10.1093/bioinformatics/bts199.
Langner, C. 2017. Hidden in the heart of Borneo—shedding light on some mysteries of an enigmatic lizard: first records of habitat use, behavior, and food items of *Lanthanotus borneensis* Steindachner, 1878, in its natural habitat. Russian Journal of Herpetology 24:1–10.
Lawing, M.A., J.M. Meik, and W.E. Schargel. 2008. Coding meristic characters for phylogenetic analysis: A comparison of step-matrix gap-weighting and generalized frequency coding. Systematic Biology 57:167–173.
Leaché, A.D., R.A. Chong, T.J. Papenfuss, ... S. Baha El Din. 2009. Phylogeny of the genus *Agama* based on mitochondrial DNA sequence data. Bonner zoologische Beiträge 56:273–278.
Lloyd, M., R.F. Inger, and F.W. King. 1968. On the diversity of reptile and amphibian species in a Bornean rain forest. The American Naturalist 102:497–515.
Maddison, W.P., M.J. Donoghue, and D.R. Maddison. 1984. Outgroup analysis and parsimony. Systematic Zoology 33:83–103.
Mahony, S. 2010. Systematic and taxonomic reevaluation of four little known Asian agamid species, *Calotes kingdonwardi* Smith, 1935, *Japalura kaulbacki* Smith, 1937, *Salea kakhienensis* Anderson, 1879 and the monotypic genus *Mictopholis* Smith, 1935 (Reptilia: Agamidae). Zootaxa 2514:1–23.
Malkmus, R., U. Manthey, G. Vogel, P. Hoffmann, and J. Kosuch. 2002. Amphibians and Reptiles of Mount Kinabalu (North Borneo). Koeltz Scientific Books, Germany.
Manthey, U. 2010. Agamid Lizards of Southern Asia—Draconinae 2. Edition Chimaira, Germany.
Manthey, U., and W. Denzer. 2019. Seltene Bergagamen des kinabalu-parks (Sabah, Nordborneo) oberhalb von 900 m ü.d.M. Sauria, Berlin 41:1–12.
Miller, M.A., W. Pfeiffer, and T. Schwartz. 2010. Creating the CIPRES Science Gateway for inference of large phylogenetic trees. Proceedings of the Gateway Computing Environments Workshop (GCE) 2010:1–8.
Mocquard, M.F. 1890. Recherches sur la fauna herpétologique des iles de Bornéo et de Palawan. Nouvelles archives du Muséum d'histoire naturelle 3:115–168 + unpaginated plates 7–11 at end of volume.

Moody, S.M. 1980. Phylogenetic and Historical Biogeographical Relationships of the Genera in the Family Agamidae (Reptilia: Lacertilia). Ph.D. dissertation, The University of Michigan, USA.

Murphy, J.B., and J. Hanken. 2018. Why are there not more agamid lizards in zoo collections? Herpetological Review 49:588–593.

Oelrich, T.M. 1956. The anatomy of the head of *Ctenosaura pectinata* (Iguanidae). Miscellaneous Publications Museum of Zoology, University of Michigan 94:9–122, Figs. 1–59.

Peters, W. 1864. Über einige neue Säugethiere (*Mormops*, *Macrotus*, *Vesperus*, *Molossus*, *Capromys*), Amphibien (*Platydactylus*, *Otocryptis*, *Euprepes*, *Ungalia*, *Dromicus*, *Tropidonotus*, *Xenodon*, *Hylodes*) und Fische (*Sillago*, *Sebastes*, *Channa*, *Myctophum*, *Carassius*, *Barbus*, *Capoëta*, *Poecilia*, *Saurenchelys*, *Leptocephalus*). Monatsberichte der königlich Akademie der Wissenschaften zu Berlin 1864:381–399.

Pethiyagoda, R., and K. Manamendra-Arachchi. 1998. A revision of the endemic Sri Lankan agamid lizard genus *Ceratophora* Gray, 1835, with description of two new species. Journal of South Asian Natural History 3:1–50.

Rohland, N., and D. Reich. 2012. Cost-effective, high throughput DNA sequencing libraries for multiplex target capture. Genome Research 22:939–946.

Ronquist, F., J.P. Huelsenbeck, and M. Teslenko. 2011. MrBayes Version 3.2 Manual: Tutorials and Model Summaries. Available at http://mrbayes.sourceforge.net/mb3.2_manual.pdf. Accessed on 10 September 2019.

Sabaj, M.H. 2016. Standard Symbolic Codes for Institutional Resource Collections in Herpetology and Ichthyology: An Online Reference. Version 6.5 (16 August 2016). Available at http://www.asih.org/. Accessed on 10 September 2019. American Society of Ichthyologists and Herpetologists, USA.

Sardi, M., and S. Siahaan. 2014. The diversity of herpetofauna at the resort Lekawai in Bukit Baka Bukit Raya National Park Sintang Regency in West Kalimantan. Jurnal Hutan Lestari 2:126–133.

Scortecci, G. 1937. Gli organi di senso della pelle degli Agamidi. Memorie della Società Italiana di Scienze Naturali e del Museo Civico di Storia Naturale di Milano 10:159–206.

Shaney, K.J. 2017. Biogeography and Conservation of Reptilian Diversity in Indonesia. Ph.D. dissertation, University of Texas at Arlington, USA.

Shaney, K.J., E. Wostl, A. Hamidy, N. Kurniawan, M.B. Harvey, and E.N. Smith. 2016. Conservation challenges regarding species status assessments in biogeographically complex regions: Examples from overexploited reptiles of Indonesia. Oryx 2016:1–12. DOI: http://dx.doi.org/10.1017/S0030605316000351.

Siebenrock, F. 1895. Das skelet der Agamidae. Sitzungsberichte der Mathematisch-Naturwissenschaftlichen Classe der Kaiserlichen Akademie der Wissenschaften 104:1089–1196, 6 plates.

Smith, E.N., and R.L. Gutberlet, Jr. 2001. Generalized frequency coding: A method of preparing polymorphic multistate characters for phylogenetic analysis. Systematic Biology 50:156–169.

Smith, M.A. 1925. On a collection of reptiles and amphibians from Mt. Murud, Borneo. The Sarawak Museum Journal 3:5–14, plate 1.

Stamatakis A. 2006. RAx/ML-VI-HPC: Maximum likelihood–based phylogenetic analyses with thousands of taxa and mixed models. Bioinformatics 22:2688–2690.

Stilson, K.T., C.J. Bell, and J.I. Mead. 2017. Patterns of variation in the cranial osteology of three species of endemic Australian lizards (*Ctenophorus*: Squamata: Agamidae): Implications for the fossil record and morphological analyses made with limited sample sizes. Journal of Herpetology 51:316–329.

Wang, K., J. Che, S. Lin, V. Deepak, D.-R. Aniruddha, K. Jiang, J. Jin, H. Chen, and C.D. Siler. 2018. Multilocus phylogeny and revised classification for mountain dragons of the genus *Japalura s.l.* (Reptilia: Agamidae: Draconinae) from Asia. Zoological Journal of the Linnean Society 185:246–267. DOI: https://doi.org/10.1093/zoolinnean/zly034.

Wiens, J.J., and T.A. Penkrot. 2002. Delimiting species using DNA and morphological variation and discordant species limits in spiny lizards (*Sceloporus*). Systematic Biology 51:69–91.

Wood, P.L., Jr., J.L. Grismer, L.L. Grismer, N. Ahmad, C.K. Onn, and A.M. Bauer. 2009. Two new montane species of *Acanthosaura* Gray, 1831 (Squamata: Agamidae) from Peninsular Malaysia. Zootaxa 2012:28–46.

Zug, G.R., H.H.K. Brown, J.A. Schulte, II, and J.V. Vindum. 2006. Systematics of the garden lizards, *Calotes versicolor* group (Reptilia, Squamata, Agamidae), in Myanmar: central dry zone populations. Proceedings of the California Academy of Sciences 57:35–68.

Accepted on 4 November 2019
Guest Editor: Bryan Stuart
ZooBank.org registration LSID: AA66B0D3-3F05-4A65-832A-70FBFE8D7ED2
Published on 13 March 2020

Appendix

Specimens Examined

We place an asterisk after specimen numbers that we scanned for osteological study.

Acanthosaura armata.—MALAYSIA. Penang: Perak, Buntar, Parit (UTA 6985). Unknown: no other data (UTA 9614, 9615, 18108, 18109*, 18110).

Acanthosaura crucigera.—THAILAND. Unknown: no other data (UTA 25080*, 25081, 25136–25138, 25139*).

Aphaniotis acutirostris.—INDONESIA. Bengkulu: highway from Bengkulu to Kepahiang, 610 m (MZB 6629*).

Bronchocoela hayeki.—INDONESIA. Sumatera Barat: Humbang Hasundutan (UTA 64391), vicinity of Berastagi geothermal plant (UTA 64392*).

Calotes mystaceus.—THAILAND. Unknown: no other data (UTA 25140*).

Ceratophora stoddartii.—SRI LANKA. Unknown: no other data (UTA 7669*, 7670, 7671*, 7672).

Cophotis ceylanica.—SRI LANKA. Unknown: no other data (UTA 7673*, 7674*, 7675).

Cristidorsa planidorsata.—MYANMAR. Chin: Falam Township, Liava village (CAS 233296), Kanpetlet Township (CAS 234703).

Dendragama australis.—INDONESIA. Sumatera Selatan: trail up Gunung Dempo above Kampung Empat (MZB 13786*, holotype; 13787*).

Dendragama boulengeri.—INDONESIA. Sumatera Barat: Aie Angek, Sepuluh Koto, Gunung Marapi (MZB 13821*).

Dendragama dioidema.—INDONESIA. Aceh: Bukit Sama, Kampung Telege Atu, Kebayakan (MZB 13814*, holotype; UTA 63438*).

Dendragama schneideri.—INDONESIA. Sumatera Utara: Mount Sibuatan, 1595–1883 m (UTA 62872*, 62873*).

Diploderma polygonatum.—JAPAN. Kagoshima: Naze, Amami O. Shima, Loo Choo Islands (CAS 21340, 21344).

Diploderma slowinskii.—CHINA. Yunnan: Nujiang District, E side of Salween River (CAS 214906, 228178).

Diploderma spendidum.—CHINA. Unknown: no other data (UTA 31943*).

Diploderma swinhonis.—TAIWAN. Chiayi: Tenshiko Formosa (CAS 18157, 18166).

Diploderma varcoae.—CHINA. Yunnan: Yunan-fu (CAS 63926).

Diploderma yunnanense.—CHINA. Yunnan: GuChenShan (Mountain) Nature Reserve (CAS 242242).

Draco sumatranus.—INDONESIA. Lampung: Krui, Kecamatan Psisir (UTA 64503*).

Gonocephalus grandis.—INDONESIA. Sumatera Utara: Road from Medan to Berastagi (UTA 64573*).

Lophocalotes achlios.—INDONESIA. Bengkulu: along main trail up Gunung Kaba (MZB 14038, holotype).

Lophocalotes ludekingi.—INDONESIA. Jambi: trail to Danau Tujuh (UTA 62848, 62850).

Lyriocephalus scutatus.—SRI LANKA. Central: near Kandy (UTA 35611*, 35612*).

Pelturagonia borneensis (5).—MALAYSIA. Sarawak: Upper Baram, 1,129 m, 3.24682°N, 115.1198°E [photos only, ZRC(IMG).2.187a–f]; "Trusan River" Fifth Division, Lawas District, 610 m (traced to Trusan River, Limbang, a road crosses the river at 4.779797°N, 115.272119°E, and is likely close to the collection locality of this specimen. FMNH 67326, paratype). Sabah: Mahubayon, Mt. Kinabalu (MCZ 43486); Ludidan River, Mt. Kinabalu (MCZ 43487). "Bundu Tuhan," Mt. Kinabalu, 1,371 m (FMNH 71856, paratype). Unknown. "N Borneo" no other data (NMW 20854-1, 20854-2, 20854-3, 20854-5, 20854-7. Specimens donated by Steindachner in 1902), "Borneo" no other data (NMW 20945-2. Specimen purchased by F. Werner from collector "Rolle" in 1905, acquired by NMW in 1918).

Pelturagonia cephalum (14).—MALAYSIA: Sabah: Mt. Kinabalu (MNHN 1889-170, 1889-171, syntypes); "Ranau" Mt. Kinabalu (FMNH 71861), Mesilau Base Camp, Mt. Kinabalu, 1524 m, 6.0667°N, 116.5667°E (FMNH 152165, 152166), Liwagu Trail, near Power Station, Mt. Kinabalu (ZMB 67191), Sunsuron Camp, Crocker Range National Park, 5.8000°N,

116.3667°E (FMNH 239329, 239331, 239332, 251005, 251006); Gunung Emas, Crocker Range National Park, 5.9167°N, 116.2167°E (FMNH 251007); "Sungai Liwago," Mt. Kinabalu, 1,450 m (ZMB 57237, 57238). UNKNOWN. "N Borneo" no other data (NMW 20854-4. Specimens donated by Steindachner in 1902).

Pelturagonia nigrilabris (36).—MALAYSIA: SARAWAK: Kuching, (FMNH 76259); Nanga Tekalit Camp, Mengiong River, Kapit District, 1.633°N, 113.5667°E (FMNH 138475–138484, 145672, 145674, 145676 145677, 151537, 188578, 188580, 188582, 188583, 221688); Labang Camp on Sungai Seran, Bintulu District, 3.500°N, 113.4500°E (FMNH 147654, 147656, 147657, 148985, 148986); Tubau Camp on Sungai Pesu, Bintulu District, 3.100°N, 113.6333°E (FMNH 158727); Samarakan Nursery, Bintulu Division, 2.9333°N, 113.0833°E (FMNH 267959, 269084, 273323, 273324); Bintulu, Bintulu Division, 3.1667°N, 113.0333°E (FMNH 273327); Sungai Segaham Camp, Belaga District, 2.7167°N, 113.9000°E (FMNH 221683–221685); "across S Tekalit," 2.43333°N, 112.51667°E (MVZ 111840). UNKNOWN. "Borneo" no other data (NMW 20945-1. Specimen purchased by the NMW in 1897 from collector "Prič.").

Pelturagonia spiniceps (2).—MALAYSIA: SARAWAK: Mount Murud (likely from lower slopes, peak located at 3.9064546°N, 115.4800667°E, BMNH 1946.8.27.45). INDONESIA. KALIMANTAN UTARA: Gunung Buduk Rakik, north of Long Bawan, Krayan District, Nunukan Regency, 1,675 m (MZB 1869; traced to 3.943991°N, 115.685510°E).

Phoxophrys tuberculata (4).—INDONESIA. SUMATERA UTARA: Batang Gadis, Kecematan Rau, 0.70866°N, 99.51953°E, 1,223 m (UTA 65254); "Batang Singalang" (Batang Singgalang, 0.0800°N, 100.1667°E [traced by David and Vogel 1996], holotype of *Phoxophrys tuberculata* Hubrecht, RMNH 4104). JAMBI: "Sungei Kumbang, Korinchi, Sumatra, Alt. 4700 ft." (presumably on the slopes of Mount Kerinci, peak of which is at 1.6967°S, 101.2467°E, BMNH 1946.8.13.92, holotype of *Japalura robinsoni* Boulenger); DS Dunian Rambun Kab." Merangin Regency (MZB 9454).

Pseudocalotes floweri.—THAILAND. No other data (FMNH 114514*).

Pseudocalotes kingdonwardi.—CHINA. YUNNAN: Dulong Valley, Kongdang (CAS 242674).

Ptyctolaemus collicristatus.—MYANMAR. CHIN: Between old Kanpetlet township and New Kanpetlet township (CAS 234779*).

Salea anamallayana.—INDIA. KARNATAKA: Palni Hills, Kodaikanal, at Bear Shola (CAS 104246*).

Sitana ponticeriana.—INDIA. MADHYA PRADESH: 5 mi SW of Manpur (CAS 94355*).